A Thesis for the Degree of Ph.D. in Engineering

Data Rate Adaptation and Cooperative Diversity for Future Wireless Communications

March 2011

Graduate School of Science and Technology
Keio University

Nandar Lynn

Contents

List of Figures

List of Tables

List of Acronyms

ACK	(positive) acknowledgment
AF	amplify and forward
AMC	adaptive modulation and coding
ARQ	automatic repeat request
AWGN	additive white Gaussian noise
BER	bit error rate
BLER	block error rate
BPSK	binary phase shift keying
CDMA	code-division multiple-access
CRC	cyclic redundancy check
CSMA	carrier sense multiple-access
CTS	clear to send
DF	decode and forward
DVB	digital video broadcasting
EGC	equal gain combining
FDD	frequency division duplex
FFT	fast Fourier transform
GMSK	Gaussian minimum shift keying
GSM	global system for mobile communications
HARQ	hybrid automatic repeat request
IFFT	inverse fast Fourier transform
LDPC	low density parity check
MAC	medium access control
MC-CDMA	multicarrier code-division multiple-access
MCS	modulation and coding scheme
MIMO	multiple-input-multiple-output
MRRC	maximum ratio received combining
NACK	negative acknowledgment
OFDM	orthogonal frequency division multiplexing
OL	opportunistic listening
PER	packet error rate
QAM	quadrature amplitude modulation
QPSK	quadrature phase shift keying
RTS	ready to send
SDMA	space-division multiple-access
SF	space frequency
SNR	signal to noise power ratio
STC	space time code
STTD	space time transmit diversity
TDD	time division duplex

TDMA	time division multiple access
TD-SCDMA	time-division synchronous code-division multiple-access
VSF-OFCDM	variable spreading factor orthogonal frequency code-division multiplexing
W-CDMA	wideband code-division multiple-access
WiBro	wireless broadband
WiMAX	worldwide interoperability for microwave access
WLAN	wireless local area network
WMAN	wireless metropolitan area network

Abstract

The future wireless communication systems are anticipated to be able to fulfill requirements of higher data rate, larger coverage, low power consumption, generic architecture, high scalability and re-configurability. This dissertation mainly focuses on three issues related to the mentioned requirements: rate adaptation, coverage extension and low power consumption.

As wireless communication has been integral part in our daily lives, a multitude of mobile applications, multimedia, data access and sharing, streaming video and many other services have been emerging day by day. As a result, demands for higher data rate, larger capacity and broader radio coverage to deliver mobile services to as large area as possible have been constantly increasing. To meet those demands, inevitable challenging task is to cope with wireless mobile channel. In particular, propagation channels in most metropolitan areas such as city centers where there are densely scattering large obstacles are dynamic in nature and do not have line of sight paths between local base stations and end users. Thus, means to adapt with dynamic behavior of channels, mitigate propagation loss and shadowed fading effect, and reduce dynamic range of received signal power at end users are essential.

Key solutions to cope with wireless mobile channels are: controlling transmission rate with channel; compensating pathloss by using power control and signal repeaters (relays); diversity techniques to mitigate fast fluctuation of channel; avoiding shadowed channel path by providing diverse paths. Transmission rate can be controlled by means of adaptive modulation and coding (AMC) to adapt with instantaneous channel condition. Multihop cooperative relays can mitigate pathloss as well as shadowing while reducing dynamic range of channel fluctuation given the relays are able to cooperate with each other to exploit spatial diversity. Automatic repeat request (ARQ) can add reliability to the rate adapted relay cooperated links.

With regard to data rate adaptation and link reliability, this study investigated control delays in AMC and HARQ in asymmetric time division duplex (TDD). Owing to variation in wireless mobile channels, AMC may select inappropriate modulation and coding scheme (MCS) at some instants. Such erroneous selection results in packet errors. The analysis in this study formulates a theoretical expression to calculate erroneous MCS selection probability for different TDD time slot allocations. Next, throughput degradation and corresponding delay in HARQ are evaluated in relation with the calculated probability. Regarding the issues related to coverage extension and diversity gain, this study focuses on a relay selection based cooperation strategy called selective cooperative ARQ. A novel cooperative ARQ protocol is proposed for multihop relay system to enhance selection diversity gain in retransmission process of ARQ.

Specifically, the topics in this dissertation are contributed by the following two main research studies.

- Evaluation of asymmetric TDD systems with AMC and HARQ
- Cooperative relay communication: cooperative ARQ protocols for multihop relay systems

Chapter 1 gives a general introduction of the thesis. Firstly, recent remarkable evolution of wireless communications and major requirements for future systems are discussed. A comprehensive description of wireless mobile channel is also described. Moreover, highlighting the key technologies for future systems, motivation of the study is laid out. Finally, overviews and scopes of each chapter are summarized, followed by position and contributions of the studies.

Chapter 2 introduces fundamentals of the key technologies used in the topics in this dissertation. Firstly, it describes data rate adaptation using multilevel modulations and variable coding. Secondly, it gives the principle of multicarrier transmission for future wireless systems in downlink. Thirdly, a brief description on asymmetric TDD system is introduced. Finally, relay cooperation strategies and topologies are discussed highlighting achievable diversity order and bandwidth efficiencies.

Chapter 3 evaluates asymmetric TDD systems by taking control delays in AMC and HARQ into account. Flexibility in assigning different bandwidth in TDD systems enables flexible traffic control in uplink and downlink according to the demands. AMC further enhances instantaneous rate adaption for each user on the assigned traffic volume or bandwidth. However, in asymmetric TDD systems with a significant larger traffic in downlink than that in uplink, performance of AMC may degrade owing to erroneous selection of modulation and channel coding rate as a result of channel fluctuation during downlink slots. To investigate this, MCS selection error probability in asymmetric TDD systems is evaluated by both theoretical calculation and computer simulations. Based on computed selection error probability, the corresponding performance degradation in terms of throughput and average delay to successfully receive packet is evaluated.

In Chapter 4, a novel selective cooperative ARQ scheme is proposed for a multihop relay system. The proposed relay system employs a distributed relay selection scheme that enables cooperating relays to independently decide whether to transmit or not based on their channel conditions and self-error checking results. The proposed system can overcome influence of source-relay channel and achieve higher diversity gain in subsequent transmissions. Theoretical expressions for packet error rate performance of the proposed system are also derived. Performance evaluations are carried out extensively by means of theoretical approach and simulations.

Finally, Chapter 5 draws overall conclusions for the main topics presented in this dissertation.

Chapter 1

General Introduction

1.1 *Recent Evolution in Wireless Communications*

Current wireless communication systems support a variety of services in various forms as switched traffic, internet protocol (IP) packet, and broadband streaming. Nomadicity, mobility, and computing are what mainly characterizing the current and future wireless communications. In general, the public wireless communication systems widely deployed throughout the world are classified as

- cellular mobile telecommunications: GSM[1], CDMA 2000, W-CDMA[2], TD-SCDMA[3]
- wireless local area networks (WLAN): Wi-Fi, Wireless local loop (WLL), Bluetooth
- wireless wide area networks (WWAN): HiperMAN, WiMAX[4], WiBro[5]
- broadcast: Digital audio broadcast (DAB), Digital video broadcast (DVB)

Looking back to nearly three decades of developments in wireless communications, the first generation (1G) public cellular system that used analog frequency modulation (FM) was started in 1983. The first generation analog mobile networks were replaced by the 2nd generation (2G) systems (GSM, IS-95, digital advanced mobile phone service (D-AMPS) and personal digital cellular (PDC)) in the beginning of 1990s. 2G networks are accredited as transition from analog to wireless digital networks. With further advancement in wireless technologies, 2G systems evolved to nowadays' 3G systems (universal mobile telephone system

1. Global system for mobile communications 2.Wideband code division multiple access 3. Time-division synchronous CDMA 4.Worldwide interoperability for microwave access 5.Wireless broadband

(UMTS)/international mobile telecommunication systems (IMT-2000), CDMA 2000). Currently deployed 3G networks are capable of supporting a wide range of multimedia services that include, speech, audio, image, video and data with a speed of 2 Mbps.

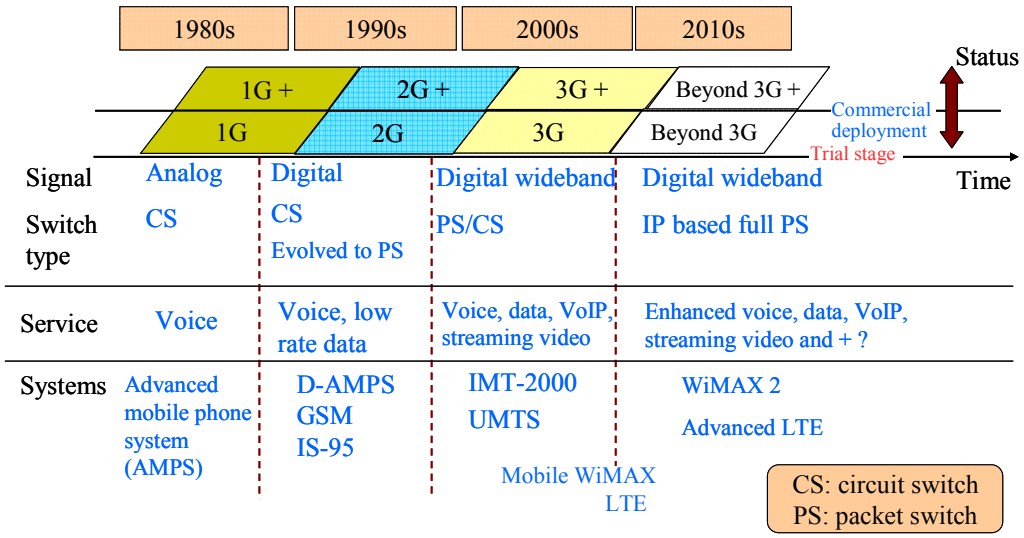

Fig.1.1 Evolution of wireless communications

On the other hand, following public commercialization of internet in 1993, potential of demands for wireless internet access was a major driving force of the emergence of broadband wireless internet access technologies [1.1]. In 1997, standardization efforts for Wireless Local Area Network (WLAN) technology known as Wi-Fi began and finally approved IEEE 802.11a and 802.11b in 1999 [1.2]. Meanwhile, as 1G wireless broadband system, the very first fixed wireless access service was provided by AT&T in 1997. 1G broadband system relied on line of sight (LOS) technology that requires installation of outdoor antennas at subscriber premises. The 2G broadband systems relaxed the requirement of LOS and started using cellular architecture, employing orthogonal frequency division multiplexing (OFDM) and CDMA as wireless access technologies. Remarkably, wireless broadband evolved into standard based technologies with a formation of standardization organization called IEEE 802.16 [1.3] for wireless metropolitan area networks (Wireless MAN) in 1998. Initial specifications of IEEE 802.16 include very

broad range of standards and technologies. To develop interoperable solutions based on 802.16 families of standards, WiMAX forum was established in 2001. Later on, a series of WiMAX standards were approved/amended/revised to emerge as 802.16a in 2003, 802.16-2004 and 802.16e in 2005, respectively. Such wireless broadband solutions as WiMAX are now being considered and implemented as backhaul networks for Wi-Fi serving at hotspots. The following Tables summarize key features of 2G and 3G mobile radio systems and WLAN/WMAN systems.

Table 1.1 Key features of 2G and 3G wireless communication systems

	2G systems		3G systems
	GSM	IS-95	IMT-2000/UMTS
Carrier frequencies	900 MHz 1800 MHz	850 MHz 1900 MHz	1900-1980 MHz 2010-2025 MHz 2110-2170 MHz
Peak data rate	64 kbps	64 kbps	2 Mbps
Modulation	GMSK[1]	QPSK[2]	QPSK
Channel coding	Convolutional code	Convolutional code	Convolutional code, Turbo code
Multiple access	TDMA[3]	CDMA	CDMA
Services	Voice, low rate data	Voice, low rate data	Voice, data, video

Table 1.2 Key features of widely deployed wireless broadband systems

Parameter	Wi-Fi IEEE 802.11a	HIPERLAN/2	Mobile WiMAX IEEE 802.16e-2005
Carrier freq.	5 GHz	5 GHz	2.3, 2.5, 3.5 GHz initially
Peak data rate (downlink)	54 Mbps	54 Mbps	46 Mbps with 3:1DL-to-UL TDD ratio; 32 Mbps with 1:1
Modulation	BPSK,QPSK,16 QAM, 64QAM[4]	BPSK,QPSK,16 QAM, 64QAM	QPSK,16QAM, 64QAM
Channel coding	Convolutional code	Convolutional code	Convolutional code (mandatory)/Turbo, LDPC[5] code (optional)
Multiple access	CSMA[6]-TDMA	CSMA-TDMA	TDM/OFDMA
Duplexing	TDD	TDD	TDD/FDD (TDD initially)

In addition to real time voice and low rate data services, mobile operators around the world also deliver broadband applications to their mobile subscribers by means of different broadband solutions. For instance, 3G systems as WCDMA and

1. Gaussian minimum shift keying 2. Quadrature phase shift keying 3. Time-division multiple-access
4. Quadrature amplitude modulation 5. Low density parity check 6. Carrier sense multiple-access

GSM operators deploy UMTS and high speed downlink packet access (HSDPA) that supports a typical data rate about 3.6 Mbps~7.2 Mbps [1.4]. Under the initiative of third generation partnership project (3GPP), as a solution for wireless broadband beyond 3G, a broadband technology called long term evolution (LTE) [1.5] which is parallel to the mobile WiMAX has recently emerged. LTE is expected to deliver a maximum data speed of 100 Mbps in downlink and 50 Mbps in uplink. Fig. 1.1 summarizes evolution of wireless communications in each generation highlighting type of the signals, services supported and major systems in each generation.

1.2 *Requirements for Next Generation systems*

A major requirement in next generation systems is to provide high bit rate with high reliability in larger coverage areas than the 3G systems. High data rate and capacity enhancement in future generation systems will be realized by means of advanced transmission rate adaptation, multiple antennas processing and multihop relay techniques. More specifically, the key technologies for high data rate and capacity enhancement will be: adaptive modulation and coding (AMC) [1.6], space-time/frequency code transmission (ST/FC) [1.7], multiple-input-multiple-output (MIMO) technology with space division multiple-access (SDMA) [1.8] using multiple antennas and multihop cooperative relay systems. Hybrid automatic repeat request (HARQ) [1.9] has been incorporated in some broadband systems such as HSDPA and will be an integral part in future generation wireless systems to realize reliable communications. As for wireless multiple access schemes, OFDM based spread spectrum multicarrier transmissions are being considered as promising candidates for downlink in systems beyond 3G owing to their high spectral efficiency and low receiver complexity [1.10][1.11]. Furthermore, future portable mobile terminals should consume low power to prolong battery life. On the other hand, multihop cooperative relay systems can be deployed to extend the radio coverage. At the same time, multihop cooperative relaying can provide spatial diversity gain that can reduce required signal to noise power ratio (SNR) to maintain a target bit error rate (BER). Such SNR gain can be interpreted as less required power.

The significant requirement or feature of 4G systems distinguishing from 3G and systems beyond 3G is interoperability with which mobile users from one system can roam to another with different air interface by means of reconfigurable software defined radio [1.11]. Although deployments of 3G networks are still under progress currently even in developed countries, the general aspects of 4G systems have already been laid out. In most aspects, 4G systems may be regarded as super enhanced version of a mixture of 3G wireless mobile radio and broadband systems. Witnessing convergence of technologies in 3G mobile systems and wireless broadband, there is a tendency to agree that 4G will integrate mobile radio communications as specified by IMT standards and WLAN or general broadband radio access networks (BRAN) [1.11]. The concept of convergence as claimed in [1.11] is depicted in Fig. 1.2. The core network will be based on Public Switched Telecommunications Network (PSTN) and Public Land Mobile Networks (PLMN) based on Internet Protocol (IP).

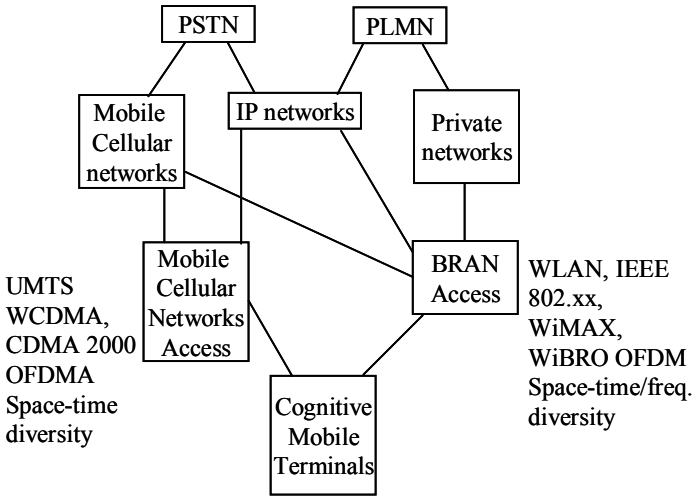

Fig.1.2 Convergence of wireless technologies

1.3 *Wireless Mobile Channel*

In each generation of wireless mobile communications, an inevitable challenging task is to cope with wireless mobile channel. Wireless mobile channels can be generally classified into line of sight and none line of sight channels. When there are no obstructions in propagation path, i.e., channel between transmitter and

receiver is line of sight, the signal power attenuation is categorized as path loss or free space loss which can be shown as

$$L_s(d) = \left(\frac{4\pi d}{\lambda}\right)^2 \tag{1.1}$$

where, d is distance between transmitter and receiver and λ is wavelength. However, practical propagation channel in terrestrial communications usually travels through multiple reflective paths due to the presence of hilly terrains, trees, buildings, mobile objects and other obstructions.

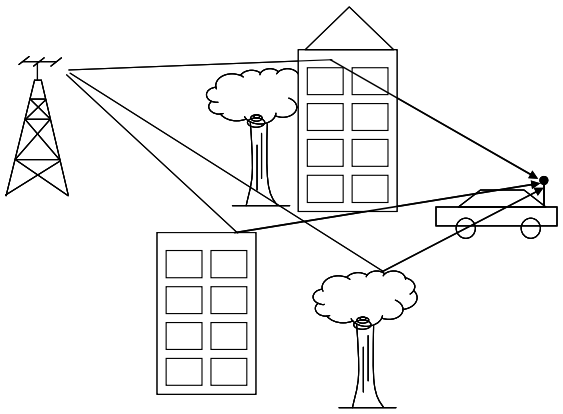

Fig. 1.3 Multipath propagation

Figure 1.3 depicts a typical mobile channel with multipath propagation. The signal transmitted from the base station scatters into multiple paths, reflect from the obstructions and arrive at the mobile receiver with different delays. The signals through different paths arrive with different amplitudes, phases and angles. The actual received signal at the mobile terminal is the summation of the signals from different paths. Since the receiver is in motion, signal amplitude, phase and angle through each path are also changing with time. Thus, arriving signal's envelope rapidly fluctuates with mobility. Such phenomenon is known as multipath fading. Fading of wireless mobile channel is characterized by two main fading effects called, large scale fading and small scale fading.

1.3.1 Large Scale Fading

Large scale fading is average signal power attenuation due to motion of either transmitter or receiver or both over large areas. It is often called as path loss. Path loss with transmitter and receiver separation distance d relative to a reference distance d_0 can be expressed as

$$\bar{L}_p(d)\,(\text{dB}) = L_s(d_0) + 10n\log\left(\frac{d}{d_0}\right) \tag{1.2}$$

where, $L_s(d_0)$ is the path loss in dB at reference distance d_0 and n is path loss exponent whose value differs in different channel environment. For instance, free space propagation has $n = 2$, and heavily obstructed channels have $n > 2$. Table 1.3 represents commonly used n values for different propagation environments. Usually, $L_s(d_0)$ is estimated by either measurements or by approximation using Eq. (1.1). It should be noted that Eq. (1.2) gives an average value. Actual received signal at the same distance d may vary depending on the surroundings. For instance, at distance d, the receiver may be travelling through tunnels, hills, large buildings and trees, etc. Then, the received signal largely varies about the average path-loss. This is called shadowed fading. In other word, it is known as medium scale fading. The variation of channel in such case follows log-normal distribution characterized by zero mean Gaussian random variable. The path loss variation can then be expressed as

$$L_p(d)\,(\text{dB}) = \bar{L}_p(d) + X_\sigma . \tag{1.3}$$

X_σ is a zero mean Gaussian random variable with standard deviation σ in dB as given by

$$X_\sigma = 10^{\frac{\zeta_\sigma}{10}}, \tag{1.4}$$

where ζ_σ is a Gaussian random variable. Typically, standard deviation σ can vary from 4 to 10 dB depending on the degree of shadowing.

Table 1.3 Path loss exponent values in different environments

Environments	Path loss exponent (n)
Free space	2
Urban cellular radio	2.7-3.5
Shadowed Urban cellular radio	3-5
In door line-of-sight	1.6-1.8
In door non line-of -sight	4-6

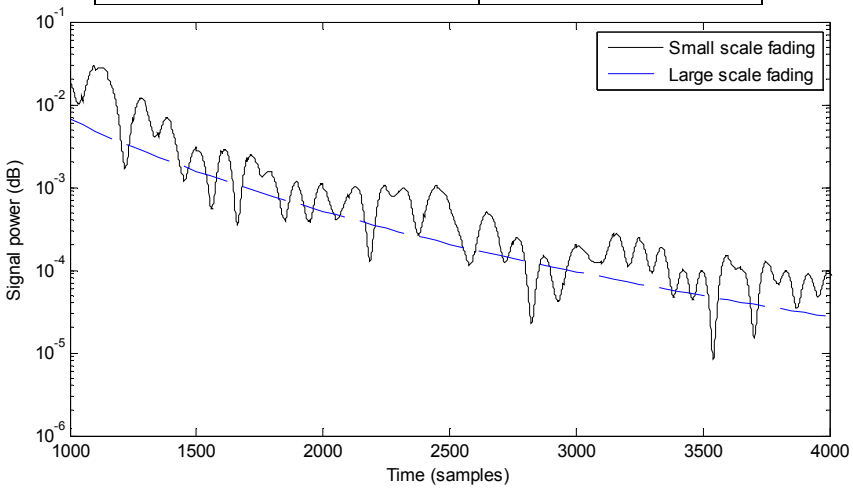

Fig. 1.4 Small scale fading superimposed on large scale fading

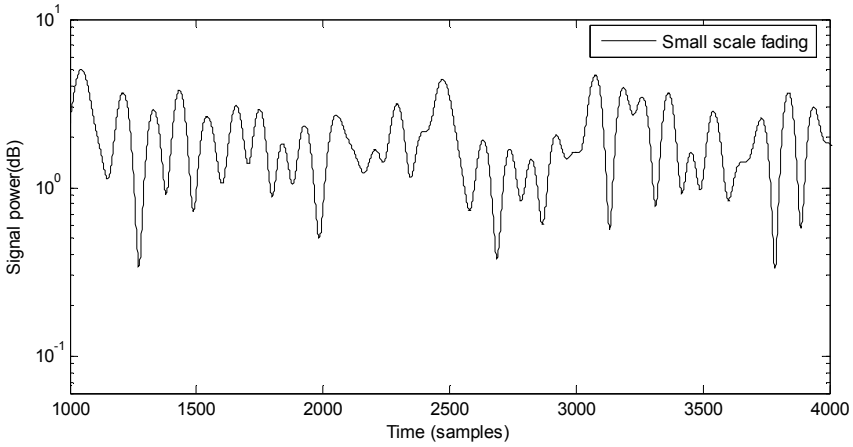

Fig. 1.5 Small scale fading in multipath channel

1.3.2 Small Scale Fading

Small scale fading happens due to microscopic change of distance in order of wavelengths in a multipath propagation channel depicted in Fig. 1.3. Signal arriving

through each path is impaired by different attenuation and delay. The attenuation factor and delay associated with each path are time variant due to motion of transmitter or receiver or both. The amplitudes and delays of different paths are summed up at the receiver. Thus, the resultant amplitude and phase of the received signal is also time variant, which allows mobile channel to be modeled as linear filter with time varying impulse response. The variations of resultant amplitude and phase causes received signal power fluctuations about the average received signal or large scale fading. The speed of fluctuations is a function of relative mobility between the transmitter and the receiver. Fig. 1.4 shows small scale fading variation superimposed on large scale fading for demonstration purpose. In practice, a large distance relative to that needed for small scale fading must be covered to experience significant change in large scale fading. Having removed the large scale fading effect, a typical small fading is depicted in Fig. 1.5. Time variant channel response of multipath channel with L paths is given by,

$$h(\tau,t)=\sum_{l=0}^{L-1} a_l e^{j\phi_l}\delta(\tau-\tau_l) \tag{1.5}$$

where, $\delta(\tau-\tau_l)=\begin{cases}1, & \text{if } \tau=\tau_l\\ 0, & \text{otherwise}\end{cases}$,

and a_l, ϕ_l and τ_l are Rayleigh distributed complex amplitude, resultant phase given by $\phi_l = 2\pi f_{d,l} t + \varphi_l$ and propagation delay of l^{th} path. Again, $f_{d,l}$ and φ_l are Doppler frequency due to motion and the phase associated with propagation delay of l^{th} path, respectively. f_d depends on the velocity of the mobile terminal, the operating carrier frequency and the angle of arrival of each path. Although multipath channels are time variant, they are observed as not varying significantly within a certain period of time called coherent time. The coherent time T_c is a function of Doppler frequency. The most common expression for T_c in relation to maximum Doppler frequency $f_{d,max}$ is given by $T_c = \frac{0.423}{f_{d,\max}}$.

Time variant channel response of the multipath channel can be expressed in terms of frequency transfer function given by

$$H(f,t)=\sum_{l=0}^{L-1}a_l e^{j2\pi f_{d,l}t}e^{-j2\pi f\tau_l} \quad . \tag{1.6}$$

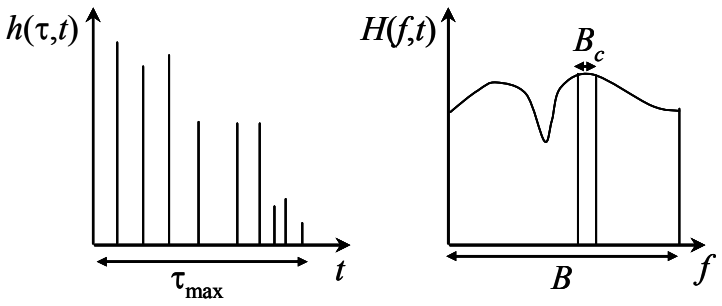

Fig. 1.6 Time variant channel response and equivalent channel frequency transfer function

Fig. 1.6 illustrates channel time response and equivalent frequency response. τ_{max} is the delay of the last path with the weakest signal strength. The delays of the paths with weaker signal strength than a predetermined value are not taken into account since their contributions to the channel impulse response is negligibly small. Channel frequency response is different with f and is known as channel frequency selectivity. Channel frequency selectivity is a function of delay τ_l and power a_l of each path, which is characterized by mean delay $\overline{\tau}$ and root mean square (RMS) delay spread τ_{RMS}.

$$\overline{\tau}=\frac{\sum_{l=0}^{L-1}\tau_l\left|a_l\right|^2}{\sum_{l=0}^{L-1}\left|a_l\right|^2} \tag{1.7}$$

$$\tau_{RMS}=\sqrt{\frac{\sum_{l=0}^{L-1}\tau_l^{\,2}\left|a_l\right|^2}{\sum_{l=0}^{L-1}\left|a_l\right|^2}-\overline{\tau}} \tag{1.8}$$

In Fig. 1.6, B represents overall bandwidth of the signal and B_c represents a frequency range known as coherent bandwidth over which channel frequency responses are essentially the same. The definition of B_c is different depending on the correlation of frequency responses. For instance, the bandwidth over which the frequency response has correlation larger than 0.9 is given by $B_c = 1/50\tau_{RMS}$ while the bandwidth with correlation over 0.5 is given by $B_c = 1/5\tau_{RMS}$.

Based on the time delay spread of the multipath channel, small scale fading can be further classified into flat fading and frequency selective fading. When channel delay spread is smaller than transmitted symbol time duration, the channel frequency response is flat across the signal bandwidth which is smaller than B_c. When channel delay spread is larger than transmitted symbol time duration, channel frequency response is selective since signal bandwidth is larger than B_c. Fig. 1.7 illustrates flat fading in a narrow bandwidth system and frequency selective fading in broad bandwidth system.

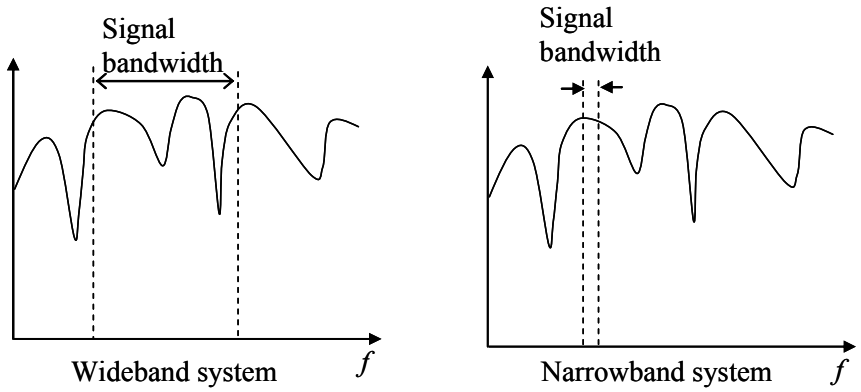

Fig. 1.7 Frequency selective fading and flat fading

1.3.3 Modeling Frequency Selective Fading

The statistical characteristic of amplitude of complex channel coefficients in flat fading follows Rayleigh distribution. In multipath fading channel, each component path can be viewed as impaired by independent flat fading with different path delay.

Thus, a frequency selective fading can be modeled as the summation of several independent flat fading channels with different relays as shown in Fig. 1.8.

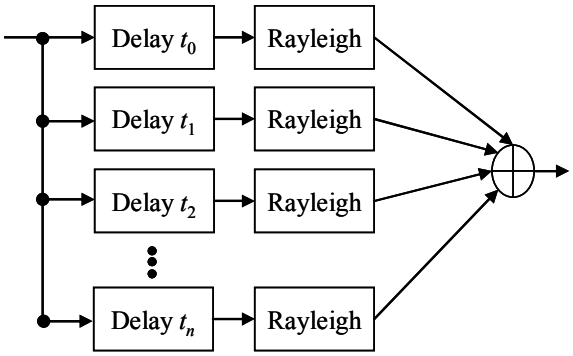

Fig.1.8 Model of frequency selective fading from n+1 flat fading

1.4 *Motivation of the Study*

In Section 1.2, major requirements for next generation wireless systems have been described. Among them, requirements such as high data rate, high reliability, larger coverage and low power consumption demand higher priority for the systems to be deployed in near future since these requirements are pragmatic for the systems beyond 3G. Thus, the studies in this dissertation focus on these requirements. Moreover, future systems should be flexible to support asymmetric traffic demand since most of the mobile applications are data-centric unlike voice that exhibits symmetric traffic volume. As seen in Section 1.1, TDD is major duplex scheme for WLAN and WMAN since it can support flexible bandwidth assignment. Thus, this study focuses on TDD. In order to fulfill the requirements mentioned above, firstly, we need to cope with wireless mobile channel. In urban mobile channel environment where there are densely scattered obstructions, adaptation of transmission rate and mitigation of rapidly fluctuating mobile channel become indispensible. There are four ways in this study to cope with wireless mobile channel:

1. Channel estimation to track instantaneous channel variation
2. Transmission rate adaptation with channel variation
3. Compensating large scale fading by employing relay stations

4. Compensating small scale fading by means of diversity techniques.

In TDD, channel reciprocity allows the use of open loop channel estimation that does not require feedback from receiver to report channel state information (CSI) to transmitter. CSI from open loop estimation provides faster link adaptation with fluctuation of small scale fading. Transmission rate adaptation can be realized by means of AMC based on measured CSI. On the other hand, to extend coverage by reducing pathloss and shadowed fading, relaying is cost-effective solution, which is already in use in existing WiMAX systems. Current WiMAX systems use fixed relays. Future WiMAX, IEEE 802.16j [1.13], includes the use of multihop mobile relays in its standard. The role of relays will be not only simple signal repeater, but also cooperative distributed antennas or virtual antenna arrays to provide spatial diversity gain. Multihop cooperative relays can reduce power consumption in mobile terminals by exploiting cooperative diversity gain [1.14]. Based on these facts, the studies in this dissertation address issues related to data rate adaptation, reliable packet reception and cooperative relay communications.

1.5 *Overview of Each Chapter and Position of the Study*

In the following, overview and motivation of each chapter are described. Finally, with respective to previous literatures and related works, the position and contribution of the studies in this dissertation are highlighted.

Table 1.4 Key technologies in this study

Requirements/goals	Solutions
Transmission rate adaptation	AMC
High reliability	FEC, HARQ
Spectrally efficient high speed downlink access scheme	Multicarrier based wireless access
Flexible bandwidth allocation	Asymmetric TDD
➢ Reduce pathloss, shadowing ➢ Mitigate dynamic fluctuation ➢ Low power consumption	Multihop cooperative relaying o Cooperative ARQ

Overview of Chapter 2: Chapter 2 introduces key technologies related to the topics in this study. Firstly, it describes adaptive modulation and variable coding rate for transmission rate adaptation with fading channel. Then, it addresses principle of multicarrier transmission as a promising wireless access for downlink in current and future systems. Next, a brief description of asymmetric TDD is given. Finally, as a solution to mitigate path loss and channel fluctuation, a concept called cooperative relay communication is introduced. Different relay cooperation strategies, topologies and achievable performance of each cooperation scheme are discussed.

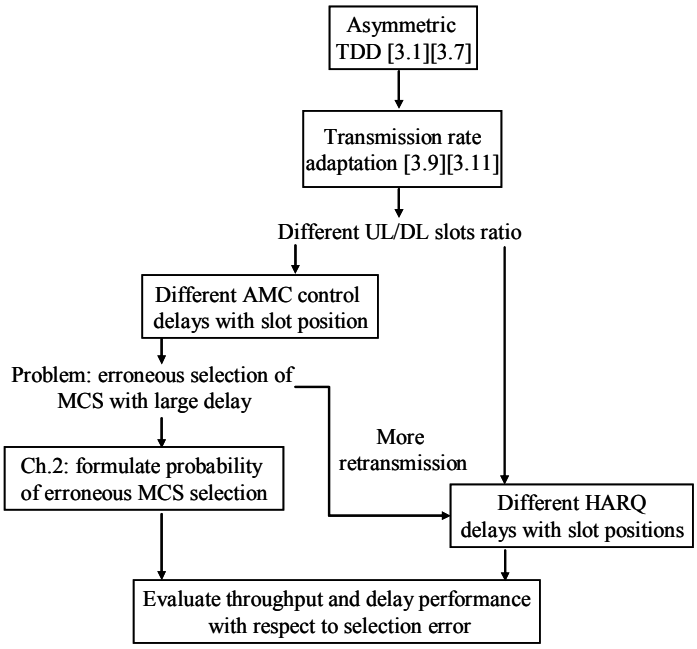

Fig. 1.9 The scope of Chapter 3

Overview of Chapter 3: Fig. 1.9 illustrates the scope of Chapter 3. This chapter presents a study on control delays of AMC and HARQ in TDD systems. Since traffic demand in downlink significantly outweigh than that in uplink, TDD systems are likely to assign more downlink slots than uplink slots. In TDD, the channel state information (CSI) measured from uplink can be used to adapt transmission rate in downlink. When channel varies significantly at actual transmission time from what measured, the modulation and coding rate employed may not match with the actual channel condition. Such mismatch causes performance

degradation in terms of throughput, and delay to receive error free packet. This study formulates calculation of probability of erroneous selection of transmission rate and investigates corresponding performances in asymmetric TDD systems.

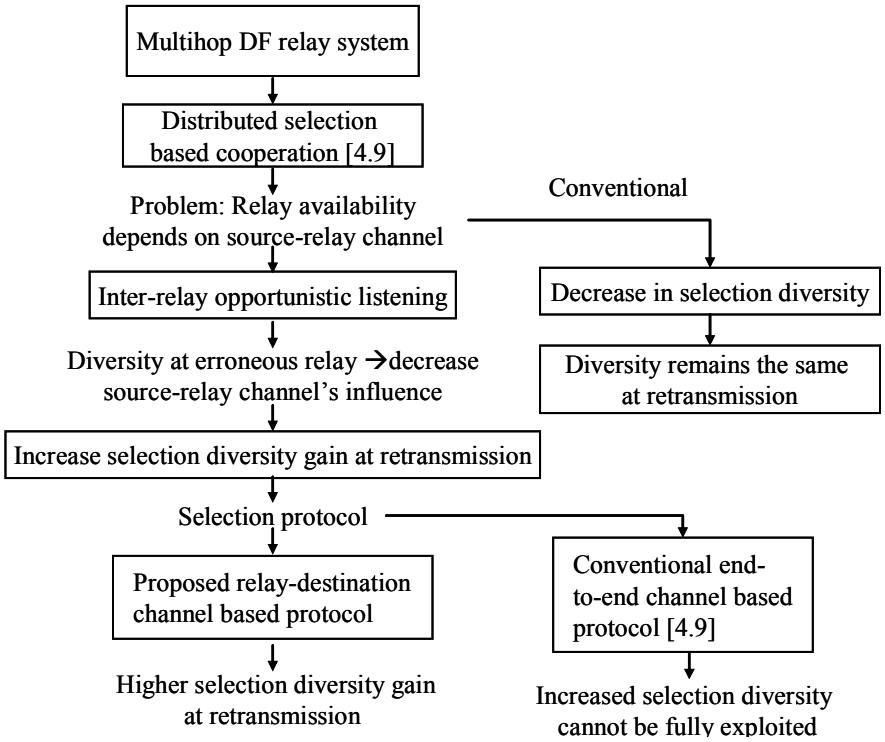

Fig. 1.10 The scope of Chapter 4

Overview of Chapter 4: This chapter presents a new relay cooperation scheme designed to increase selection diversity gain in ARQ for a relay communication that has no direct link between the source terminal and the destination station. The relays employ decode and forward (DF) to establish link between the source and the destination. The relays in the system under consideration have complete freedom in deciding whether to transmit or not based on whether they have received the signal correctly or not. Such freedom is realized by the use of a distributed relay selection method. Upon reception from the source, the number of relays available to be selected, i.e., error free relays, depends on the conditions of source-relay channels. To reduce relay availability dependency over the source-relay channels, providing diversity path to the erroneous relays is considered. In this approach, erroneous relays

exploit inter-relay channels to opportunistically listen (OL) to the transmissions of a relay without errors whose channel to the destination is the best. By combining their erroneous signals with the same signal overheard from the error-free relay of the best channel and decoding again, the erroneous relay nodes may be able to decode the signals successfully thanks to the obtained spatial diversity. This results in an increase in relay availability for selection in subsequent retransmissions. Thus, limitation of source-relay channels over the number of relays available to be selected is overcome by exploiting inter-relay channels. The performance of the proposed cooperative ARQ is verified by both theoretical analysis and simulations. Fig. 1.4 illustrates the scope of Chapter 4.

Finally **Chapter 5** gives overall conclusions for the topics presented in this dissertation.

Table 1.3 Position and contribution of this study

<table>
<tr><th colspan="2">Evaluation of asymmetric TDD systems employing AMC and HARQ</th></tr>
<tr><th>Related previous researches</th><th>Contribution of my research</th></tr>
<tr><td>- Feasibility of open-loop channel estimation and power control in TDD systems [3.2][3.3][3.7][3.8]
- What were not addressed in previous studies?
o Did not take into account asymmetric time slot assignment in TDD
o Did not consider control delays in asymmetric TDD
- Problems with the issues left open in previous studies
o Asymmetric time slot assignment in TDD causes errors in open loop channel estimation and power control
o Different control delays occur according to time slot assignment in asymmetric TDD</td><td>1. Considered control delays in asymmetric TDD systems

2. Clarified that control delays in AMC and HARQ depend on time slot assignment</td></tr>
<tr><td>- Investigated throughputs of spread spectrum and multicarrier systems employing key technologies such as AMC and HARQ [3.10][3.11][3.12][3.13]
- What were not addressed?
o Throughputs evaluated were mainly for FDD where control delays are fixed, not for TDD
o Did not take effect of erroneous MCS selection into account
- Problems with the issues left open in previous studies
o Erroneous MCS selection causes degradation in throughput and increases packet arrival latency</td><td>1. Investigated effect of erroneous MCS selection over throughput and delay in HARQ
2. Formulated analytical framework to calculate probability of erroneous MCS selection for different asymmetric TDD time slot assignments
3. Evaluated throughput degradation and delay incurred in HARQ affected by erroneous MCS selection</td></tr>
<tr><th colspan="2">Cooperative ARQ protocols for multihop relay systems</th></tr>
<tr><th>Related previous researches</th><th>Contribution of my research</th></tr>
<tr><td>- Cooperative ARQ protocols proposed so far: 1) distributed space-time code (STC) cooperation [4.2][4.5]; 2) distributed beamforming [4.4]; 3) selective cooperation [4.6][4.7][4.8]
- What are the problems with conventional protocols?
1) No guarantee for full rate, full diversity for an arbitrary number of relays other than two; strict synchronization
2) Only applicable to fixed relays where channel information of each relay can be shared each other via wired link; strict synchronization
3) Conventional selective protocols: the number of relays available to be selected depends on source-relay channel</td><td>-Distributed relay selection based on transmit timing control is considered
1) The proposed cooperative ARQ overcomes the influence of source-relay channel by exploiting diversity from inter-relay channel
2) Selection diversity gain increases in subsequent retransmissions
3) Provides autonomy to relays in deciding whether they will attempt to transmit or not based on their channel condition and CRC results of their received signals.</td></tr>
</table>

References

[1.1] J.G.Andrews, A.Ghosh, and R.Muhamed, *Fundamentals of Wimax: Understanding broadband wireless networking*, Prentice Hall, Oct. 2007.

[1.2] IEEE 802.11a-1999 (R2003), Wireless LAN medium access control (MAC) and physical layer specifications- high speed physical layer in the 5 GHz band, June 2003.

[1.3] IEEE 802.16-2004, Part 16: Air interface for fixed and mobile broadband wireless access systems, Oct. 2004.

[1.4] 3GPP, 3G TR25.858, Physical Layer Aspects of UTRA High Speed Downlink Packet Access.

[1.5] H. Ekstrom, A.Furuskar, J.Karlsson, M.Meyer, S.Parkvall, J.Torsner, and M.Wahlqvist, "Technical solutions for the 3G long-term evolution," IEEE Commun. Mag., vol. 44, no. 3, pp.38-45, March 2006.

[1.6] 3GPP, R1-060076, Samsung, Adaptive modulation and channel coding rate, Jan. 2006.

[1.7] A. F. Molisch, M. Z. Win, and J. H. Winters, "Space–time–frequency (STF) coding for MIMO-OFDM systems," IEEE Commun. Lett., vol. 6, no. 9, pp. 370-372, Sept. 2002.

[1.8] V. T. Ermolayev, A. G. Flaksman, I. M. Averin, and D. V. Gribov, "Effectiveness of space-division multiple-access in MIMO communication systems with parallel data transmission," Journal of Radiophysics and Quantum Elect., vol. 47, no. 2, pp. 129-138, Feb. 2004.

[1.9] M. Raitola and H. Holma, "Wideband CDMA with packet data with hybrid ARQ," Proc. ISSSTA'98, vol. 1, pp. 318-321, Sept. 1998.

[1.10] K. Fazel and S. Kaiser, *Multi-carrier and spread spectrum systems*, John Wiley & Sons Ltd, 2003.

[1.11] S.G. Glisic, *Advanced wireless communications 2nd Edt-4G cognitive and cooperative broadband technology*, Wiley, 2007.

[1.12] G. Kramer, I. Maric, and R. D. Yates, *Cooperative communications: foundations and trends in networking*, Now Publisher, June 2007.

[1.13] IEEE 802. 16j-2007, IEEE standard for Local and Metropolitan area networks. Part 16: Air Interface for Fixed and Mobile Broadband Wireless Access Systems- multihop relay specification.

[1.14] A. Sendonaris, E. Erkip, and, B. Aazhang, "User cooperation diversity: Part I. System description," IEEE Trans. on Commun., vol. 51, no. 11, pp. 1927-1938, Nov. 2003.

Chapter 2

Transmission Rate Adaptation and Multihop Cooperative Relaying

In this chapter, techniques to cope with small scale and large scale fading effects are introduced. Firstly, adaptive modulation and coding (**AMC**) is explained. Secondly, principle of ***multicarrier transmission*** is described as a robust wireless access against multipath channel delay spread for future wireless systems in downlink. Thirdly, ***asymmetric TDD system*** is introduced, highlighting its major advantage of flexibility to cope with asymmetric traffic demand in most of the broadband wireless systems. Finally, fundamentals of ***multihop cooperative relay*** systems are discussed highlighting achievable diversity order and bandwidth efficiencies.

2.1 *Rate Adaptation with Channel Condition*

The capacity of the channel as a function of average received signal to noise power ratio is given by $R\ (\text{bits/s/Hz}) = \log_2\left(1+\frac{S}{N}\right)$ [2.1], where S and N represents signal power and noise power, respectively. It shows that increasing either bandwidth or S/N can increase capacity logarithmically. Fig. 2.1 plots channel capacity as a function of SNR. As seen in the previous section, channel is fluctuated by both large scale and small scale fading. Usually, the effect of large scale fading is mitigated by power control. Even with a perfect power control mitigating large scale fading, the received signal may still fluctuate several dBs as large as 20~30 dB due to small scale fading. Thus, it is required that instantaneous small scale fading is tracked and the

amount of data to be transmitted is adapted according to channel SNR fluctuation. When channel condition is good, i.e. large channel SNR, the number of transmit data bits (data rate) can be increased. Otherwise, the data rate must be decreased. Data rate adaptation is realized by using multilevel modulations and variable channel coding rate.

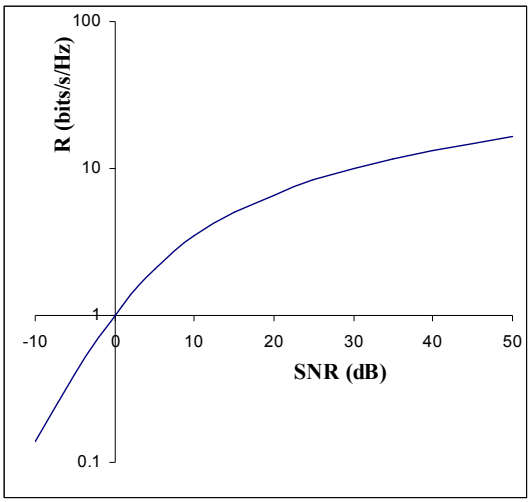

Fig. 2.1 Channel capacity versus SNR

2.1.1 Multilevel Modulations

Multilevel symbol modulations map data bits into symbol points in two dimensional signal constellations. For instance, quadrature phase shift keying (QPSK) maps each group of two binary bits into one of the four constellation points as shown in Fig. 2.2. Thus, each QPSK data symbol represents two binary bits. Similarly, 8PSK maps each group of three binary bits into one of the eight PSK symbols. Thus, modulation level of a data symbol mapping scheme is normally represented by the number of data bits each modulated symbol represents. For instance, modulation levels (m) of QPSK and 8PSK, are $m = 2$ and $m = 3$, respectively.

Fig. 2.2 also depicts constellations of quadrature amplitude modulations (QAM). Unlike PSK based modulation, QAM symbols vary not only phase, but also amplitude. Each symbol of 16QAM and 64QAM represents 4 and 6 binary bits and

thus, with the modulation levels *m* being 4 and 6, respectively. It should be noted that amplitudes of data symbols in each modulation are normalized so that the average signal power of symbols in constellation of each modulation scheme is unit power. More SNR is needed to be able to use higher level modulations. Normally, when the distance between transmitter and receiver is small, average received SNR is large, allowing the use of higher level modulation. Even so, as the receiver moves, small scale fading effect may cause severe attenuation instantaneously. Under such circumstances, lower level modulations such as QPSK may be temporarily used in order to maintain a required Quality of Service (QoS) such as, bit error rate (BER).

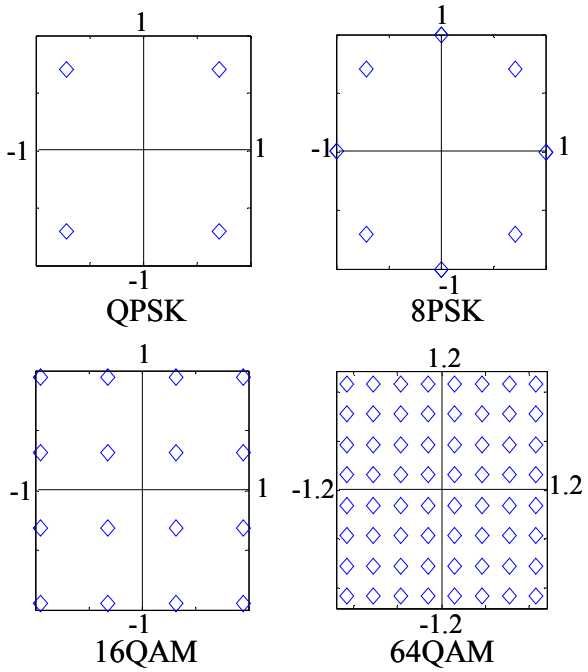

Fig.2.2 Signal constellations of QPSK, 8PSK, 16QAM, and 64QAM

A simple criterion for switching modulation level is target bit error rate (BER). For instance, Fig. 2.3 plots BER versus average bit energy to noise power ratio (E_b/N_0) in multipath Rayleigh fading. Suppose target BER is 10^{-2}, QPSK requires at least about 14 dB to achieve the target BER. As channel SNR becomes larger than 17 dB, the modulation may be switched from QPSK to 16QAM as the later can also meet the target BER at SNRs > 17 dB while increasing the number of bits per

modulated symbol. By employing such adaptation, the channel is utilized more efficiently.

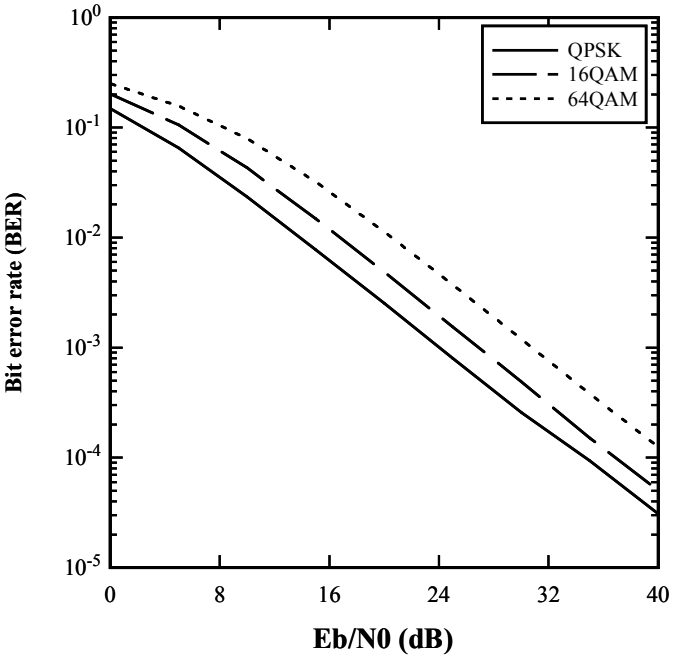

Fig. 2.3 BER of different modulations in multipath Rayleigh fading

2.1.2 Variable Rate Channel Coding

Application of error control/correction coding in wireless communication can improve performance significantly. The basic concept of error control/correction coding is transmission of data using a set of code words with deliberately added structured redundancy by an encoder and decoder to detect and/or correct errors in the received sequence [2.2] [2.3]. We can control channel coding rate by means of rate compatible punctured code (RCPC) [2.4]. Turbo code is the most well known RCPC at present and, this section briefs some basics of Turbo code.

Fig. 2.4 illustrates a block diagram showing a communication system with channel coding. An encoder transforms a sequence of k data bits into a code word of length n, where $n > k$. The code rate r is defined as the ratio of k/n, thus $r = k/n$. r must be such that $r < R$ to establish reliable communications. Turbo code is a powerful and popular error correction codes which has been a part of the 3G wireless

standards. The basic building block of Turbo code is concatenated recursive convolutional code. Before introducing Turbo code, a brief description of convolutional code will be presented. A detailed description with an example encoding/decoding procedure can be found in [2.2].

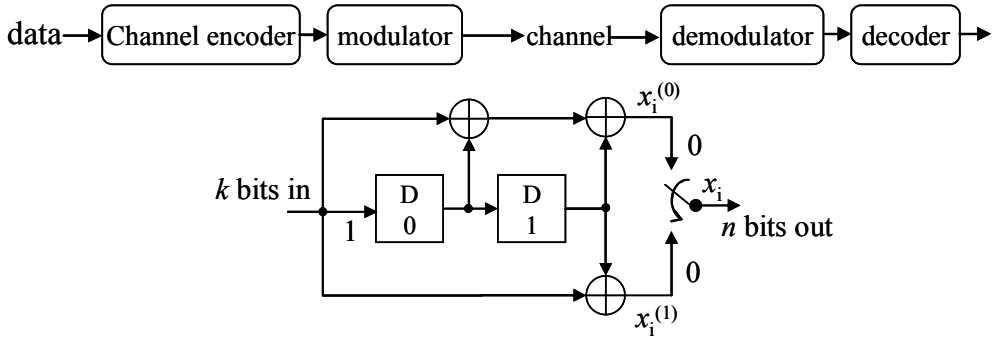

Fig. 2.4 Transmission model with channel coding; convolutional encoder with K=1/3, r = 1/2

Figure 2.4 depicts a typical convolutional encoder with D representing shift register. Each input bit undergoes XOR operation with the previous input bits stored in D. For each input bit, the output code word has two encoded bits, making the code rate r =½. For instance, with input bit 1 and the stored bits 0 and 1 in each D, the output code word is 00. The total number of bits involved for each output code bit is called constraint length K. The encoder in Fig. 2.4 has K = 3. The contents of the shift registers represent state of the encoder. For the example encoder, there can be 4 states (00, 01, 10, and 11). As a new bit comes in, the state changes and the resulting code word also changes. The code generator is usually represented by generator matrix G for each output. The upper code word is generated using G = [1 1 1], and the lower code word by G = [1 0 1], with 1 representing D having connectivity to the XOR operation and 0 otherwise. The pattern of changes in state with incoming bit and the associated output code word is known to both encoder and decoder. Thus, for any size of block of data, a diagram called trellis [2.2] can be used to represent possible state changes and associated output code word with each input bit. Using trellis, receiver can predict which of 0 and 1 was transmitted from the received code words by comparing them with each code word corresponding to state changes at each

instant. The comparison process uses a correlation metric which represents how similar the received code word is to each of the possible code words in the trellis at each time. For example, given the received code word is 11 and the codeword resulted from certain state change is 00, their correlation metric is 2, meaning both bits are different. Such comparison is carried out throughout the whole block of received code words. Finally, the path representing the code word sequence with the smallest metric value is what with the maximum likelihood (ML) to be the transmitted code words. The decoder decides that the sequence of data bits associated with the path of most possible transmit code words is the transmitted data bits.

Recursive systematic convolutional (RSC) code differs from simple convolutional code in that the output of the encoder is fed back to the input of the encoder. Such arrangement is known to have better error rate performance than non recursive codes [2.5]. An example of RSC encoder is shown in Fig. 2.5. Unlike non recursive code, RSC encoder outputs unmodified data bit called systematic bit and structured redundant bit. Free distance [2.6] of non recursive code in Fig.2.4 is the same as that of RSC in Fig. 2.5. Also, state transitions and trellis structure corresponding to output code words are the same except for the input bit being modified by XOR operation with previous input bits in the shift registers.

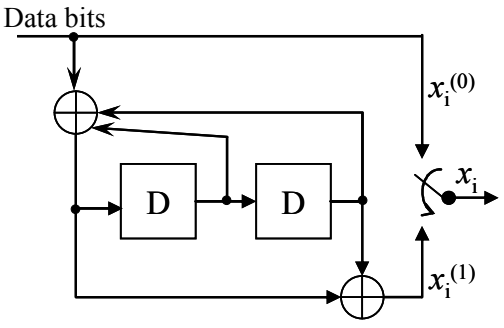

Fig. 2.5 Recursive systematic convolutional encoder

Turbo code is usually generated by parallel concatenation of two RSC codes as shown in Fig. 2.6. The number of component RSC encoders to be concatenated is not limited. The upper encoder is fed by the serial data bits as it is while randomly

reshuffled version of data sequence is fed to the 2nd encoder. Reshuffling of the data is done by the block interleaver at the input of the 2nd encoder. As a result of interleaving, the input sequences to each encoder seem to be independent from one another and so are the output sequences of two encoders. With the systematic output bit $x_i^{(0)}$ and two independent redundant bits $x_i^{(1)}, x_i^{(2)}$ for each input d_i, the overall code rate of the encoder in Fig. 2.4 is r = 1/3. The coding rate can be adapted by deleting out or puncturing the redundant bits. For instance, rate 1/2 code can be achieved by alternately deleting out the output bits of each encoder to result in one systematic bit and one parity bit output for each input bit. A typical puncturing pattern for a rate 1/2 code from mother code rate 1/3 is given by,

$$P = \begin{bmatrix} 11 \\ 10 \\ 01 \end{bmatrix}$$

where puncturing period, represented by the number of columns, is two. '1' in each column represents the connectivity of each of three taps to the multiplexing switch at the output of the encoder in Fig. 2.4. Different puncturing patterns are used for different coding rates > 1/3. Higher rate Turbo codes can be generated by the use of higher rate convolutional codes [2.7]. With the different code rates in combined with multi-level modulations, degree of freedom in selection of most suitable modulation and code-rate scheme (MCS) increases. Thus, data rate adaptation to the channel becomes more flexible.

Turbo decoder at the receiver is fed with soft decision bit output from the demodulator. Fig. 2.7 shows the iterative Turbo decoder that consists of two component decoders for the Turbo code in Fig.2.6. Such iterative decoder receives soft input sequences as a priori information from the demodulator and produces soft output sequence as a posteriori information to be fed to the partner decoder as a priori information for it [2.2][2.5][2.7].

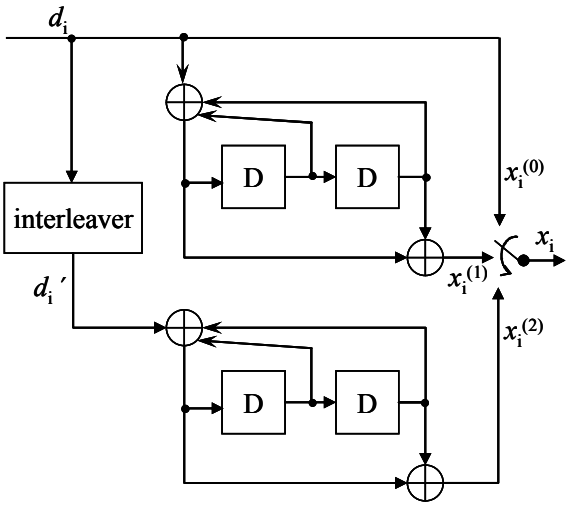

Fig.2.6 Turbo encoder with two RSC codes

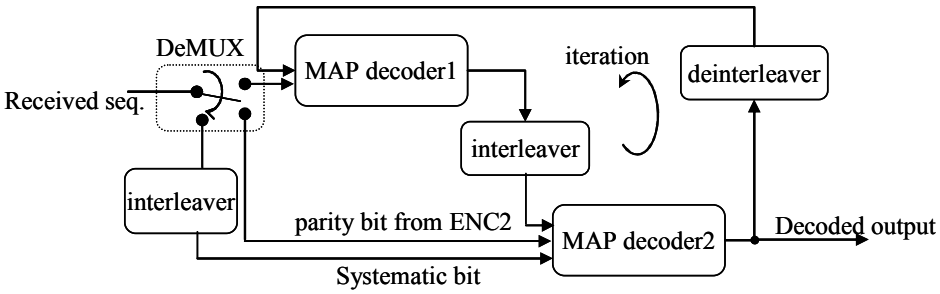

Fig.2.7 Turbo decoder

At the input of the decoder, the received soft sequence is de-multiplexed to feed systematic bit and parity bit associated with each encoder to decoder 1 and decoder 2, respectively. The soft values of systematic bit and the parity bit associated with encoder 1 are directly fed to the decoder 1. On the other hand, the systematic bits for decoder 2 are reshuffled by the same interleaver used at the encoder. The decoders use maximum a posteriori probability (MAP) algorithm [2.5][2.7] to produce soft outputs based on received soft input. The decoding process is repeated iteratively according to the pre-determined iteration number and the final outputs are hard decision bits.

2.2 *Fundamentals of Multicarrier Transmission*

The motivation of multicarrier transmission is establishing radio links that can facilitate high data rate communication over inter-symbol interference (ISI) free channels. ISI happens due to mutual interference of the symbols in multiple paths with different delays. In a wide band system having very short symbol duration T_s, effect of ISI is severe. Multicarrier systems combat ISI by converting short duration serial data symbols into a longer duration parallel symbols. Intuitively, a certain amount of interference over a relatively long symbol will have small impact. Thus, multicarrier modulation first transforms the serial symbols with duration T_d into N_c parallel symbols, resulting in the effective duration of parallel symbols $T_s = N_c T_d$. Then, N_c parallel symbols are modulated on each sub-carrier, summed up the modulated symbols and sampled to make time samples of multicarrier modulated symbols as shown in Fig. 2.8.

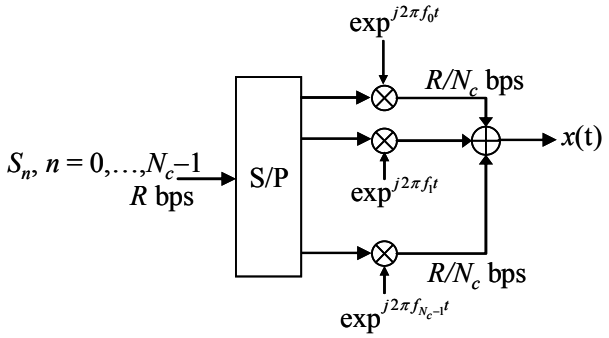

Fig. 2.8 Multicarrier modulation

Orthogonal frequency division multiplex (OFDM) is a low complexity multicarrier modulation scheme that uses digital signal processing; multicarrier modulation is efficiently carried out by an operation called inverse fast Fourier transform (IFFT) [2.9]. In OFDM, sub-carriers are spaced by $F_s = 1/T_s$ and the over all bandwidth B is given by $B = N_c/T_s$. Thus, each sub-carrier is located at $f_n = n/T_s$, $n = 0, 1,\ldots, N_c-1$. If data symbols S_n, $n = 0, 1,\ldots, N_c-1$, are multicarrier modulated and the envelope of multicarrier symbol is time sampled with a rate $1/T_d$, the sampled envelope is given by

$$x_k = \frac{1}{N_c}\sum_{n=0}^{N_c-1} S_n e^{j2\pi n k/N_c - 1}, \; k = 0, 1, \ldots, N_c - 1. \tag{2.1}$$

Serial symbols S_n may be the symbols resulted from modulation of output bits from channel encoder or interleaver. As the number of carriers, N_c, is increased, the symbol duration T_s on each carrier increases, making each symbol more robust against ISI. In frequency domain, each sub-carrier has bandwidth $B_{sc} = B/N_c$. Thus, channel frequency response of each sub-carrier is essentially flat if $B_{sc} << B$.

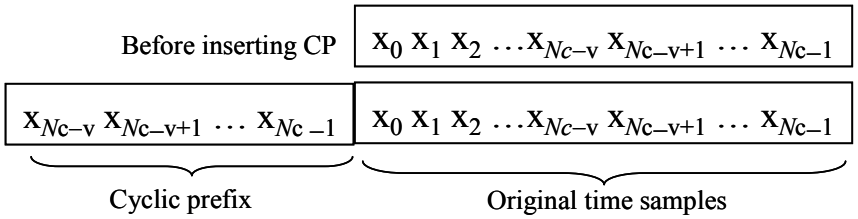

Fig. 2.9 GI or cyclic prefix of OFDM

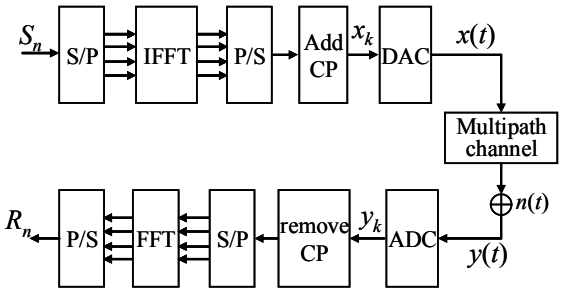

Fig.2.10 OFDM transmitter and receiver

To completely remove ISI, a guard interval (GI), T_g, is inserted before the first sample x_0 as shown in Fig. 2.9. GI is the cyclic extension of v samples of own OFDM envelop in Eq. (2.1) ensuring T_g to be longer than the maximum delay spread of the channel. GI is often called as cyclic prefix. Due to cyclic prefix (CP), the time samples of OFDM symbol appear to be periodic over N_c samples. CP also ensures that delayed copies of OFDM symbols always have integer number of cycles within sampling interval of effective data symbols as long as the delay is smaller than CP length, maintaining orthogonality among sub-carriers [2.9]. The resultant OFDM symbol with CP is also the form given by Eq. (2.1) but with longer duration and

sample index k, $k = N_c - v, N_c - v+1, \ldots, 0, \ldots N_c - 1$. After inserting CP, OFDM symbol is transmitted into the channel. In the channel, the transmitted signal circularly convolves with the channel of L paths, which in discrete form can be expressed as

$$y[n] = \sum_{l=0}^{L-1} h[l]\left(x[n-l] \bmod N_c\right). \tag{2.2}$$

Through a multipath channel, interference from the delayed preceding OFDM symbol falls in the CP. By removing the interfered CP from y_k, an ISI free OFDM symbol is received.

After CP removal, y_k, $k = 0,1,\ldots N_c - 1$, is transformed into frequency domain by means of FFT as

$$R_n = \sum_{k=0}^{N_c-1} y_k e^{-j2\pi nk/N_c}, \; n = 0, 1, \ldots, N_c - 1. \tag{2.3}$$

The frequency domain representation of circularly convolved received signal R_n is

$$R_n = H_n S_n + N_n, \; n = 0, 1, \ldots, N_c - 1 \tag{2.4}$$

where, H_n and N_n are channel frequency response and noise of n^{th} sub-carrier. Given receiver has knowledge on H_n, the detection of R_n is simply $\tilde{S}_n = \frac{R_n}{H_n}$. In order to make channel frequency response H_n of each sub-carrier flat, the number of sub-carriers N_c must be carefully chosen such that $B_{sc} << B_c$ (coherent bandwidth).

Channel frequency diversity of multicarrier systems causes deep fading for some sub-carriers. Overall error rate performance of an OFDM system is dominated by deeply faded sub-carriers [2.9]. With application of error correction codes in OFDM, errors in the symbols on deeply faded sub-carrier can be effectively corrected.

Furthermore, application of interleaver to best exploit channel frequency diversity of multicarrier systems increases error correction capability of channel

coding. Fig.2.11 shows BER performance of OFDM with and without channel coding. The same modulation was employed at all the sub-carriers. Table 2.1 lists the system parameters of the simulated OFDM system. One of the main advantages of OFDM is feasibility of using different modulation schemes with respect to frequency response of individual sub-carrier. It makes OFDM systems flexible to adapt data rate efficiently. The main drawback of OFDM is high peak to average power ratio (PAPR) due to summation of multicarrier modulated symbols across all the sub-carriers. High PAPR is the primary cause of non-linear distortion of the transmit signal and poor power efficiency at RF amplifier. However, application of OFDM in point to multipoint transmissions such as broadcast and wireless LAN where transmit power back-off does not impose a large challenge has been witnessed as very efficient nowadays. Some well-known transmission systems employing OFDM includes digital audio broadcasting (DAB), terrestrial digital video broadcast (DVB-T) [2.10], wireless LAN standards as IEEE 802.11a/b and HIPERLAN/2 and broadband wireless standards as WiMAX [2.11].

Table 2.1 Coded OFDM parameters

Number of carriers (N_c)	64
Guard interval length (samples)	16
Modulations	QPSK, 16QAM, 64QAM
Channel coding, decoding algorithm Constraint length (k) of component codes Coding rates	Turbo, SOVA 3 1/2, 1/3
Channel model	12 paths Rayleigh fading
Channel estimation	Ideal

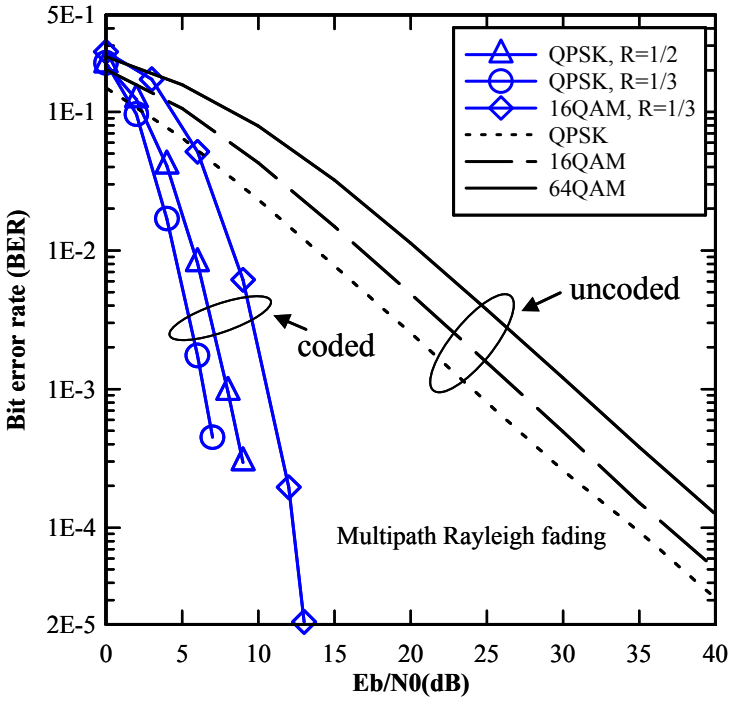

Fig. 2.11 BER Performance of OFDM with and without channel coding

2.3 *Asymmetric TDD Systems*

With the emergence of many multimedia applications and services, in addition to data rate adaption for individual user, capability of providing flexible bandwidth allocation to a desired link direction in a whole service area has become mandatory. The amount of downlink traffic is generally expected to dominate because of applications such as data downloading [2.12]. For this requirement, TDD mode of operation can support asymmetric traffic by simply assigning more transmission slots in the direction of higher traffic demand. Fig. 2.12 shows TDD systems with different number of downlink to uplink slot ratio. As the demands for traffic in downlink increases, more downlink slots can be assigned in TDD. Since transmissions in downlink and uplink are operating on same frequency band, channel responses in both links are highly correlated allowing the use of open loop control and channel estimation. In contrast to FDD systems, which generally employ an uplink feedback channel to provide the base station (BS) transmitter with downlink CSI collected by

mobile station (MS) measurements, TDD systems can exploit channel reciprocity to estimate CSI from the most recently received signals without requiring feedback.

It is expected that future wireless mobile systems will provide unpaired bands using the TDD mode more extensively than is true with 3G systems due to the scarcity of the spectrum resources and possible integration with other existing or future wireless broadband networks [2.13] such as WiMAX. Mobile WiMAX, based on IEEE 802.16e air interface standard, initially adopted TDD as the key duplex scheme along with other key technologies such as scalable OFDMA, AMC, and HARQ. Moreover, TDD systems can be deployed in micro-cells, at places beyond frequency division duplex (FDD) coverage, and as a complement to FDD macro cell networks.

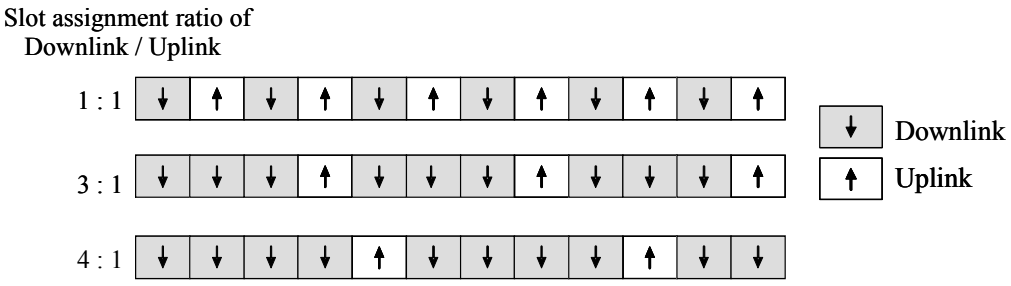

Fig. 2.12 Asymmetric assignment of time slots in TDD

2.4 *Multi-hop Relay Systems and Cooperative Diversity*

Having discussed the issues related to AMC, the fundamentals of multicarrier wireless access scheme and asymmetric TDD in the previous sections, this section provides a general aspect of relay communication and its necessity in present and future wireless communications. Relay stations can be incorporated in the existing wireless networks, such as public cellular networks, Wireless Metropolitan Area Networks (WMAN), and Wireless Local Area Networks (WLAN) networks [2.11][2.14], to extend communication coverage of a local base station in the same wireless air interface employing any wireless access scheme of interest. Thus, in the following, discussions focus mainly on the issues related with relay topologies, relay

cooperation procedures, protocols and achievable diversity rather than specific wireless access schemes.

The achievable capacity of the wireless channel is inherently limited by signal power attenuation in wireless channel [2.15]. Attenuation due to mobile channel fading is characterized by three main factors such as small scale fading, large scale fading called path loss and shadowing. From these three factors, large scale fading and shadowing contribute to the average received signal power variation, while small scale fading contributes to the instantaneous fast signal power fluctuation superimposed on the average signal power. In addition to transmission rate adaptation to cope with channel fluctuation, multihop cooperative relaying can further reduce dynamic range of channel fluctuation by means of cooperative diversity while extending radio coverage.

Path loss is mean signal power attenuation with distance in free space between transmitter and receiver. The amount of attenuation is inversely proportional to the square of the free space distance between transmitter and receiver. In an environment where there is no line of sight path between transmitter and receiver, amount of attenuation will become larger with the n^{th} power of the distance where $n > 2$ [2.16]. Shadowing is caused by obstacles such as hills, buildings and trees in the propagation channel and results in short-term average signal strength variation. It is often regarded as slow fading and characterized by log-normal distribution. Since shadowing varies slowly compared to the small scale fading, receiver needs to move longer distance to significantly change a shadowing effect compared to small scale fading. Both shadowing and large scale fading effect can be mitigated by power control. A base station transmitter may increase transmit power for mobile users suffering from a large signal attenuation due to either large scale fading or shadowing. However, increasing transmit power is not always a good solution since the transmit power budget is normally limited. In addition, increasing transmit power may result in increased interference power for other users either in the same or neighboring coverage areas. On the other hand, decreasing coverage area, i.e. cell size is also

another option. However, the need to deploy more infrastructures for a larger number of smaller power base stations is not cost effective.

Thus, as alternative to the above discussed options, deployment of relay stations has been considered as a cost effective option while meeting constrained power budget and desired data rate demand in a network. In present 3G wireless cellular networks such as GPRS and Wideband CDMA (WCDMA) [2.17], despite their relatively small cell size compared to 2G networks, there still exist coverage holes in densely obstructed urban wireless channel environments. That requires deployment of low cost relay stations to serve as signal booster or repeaters to deliver services to the users in the coverage holes. Thanks to the relay stations, mobile terminals at the cell edge which otherwise experience weak received signal power can also enjoy a better received signal strength that can fulfill target data rate demands. Likewise, IEEE 802.16e wireless broadband standards also includes relaying mode by the use of fixed relay stations. As further improvement, IEEE 802.16j [2.18] considers employment of not only fixed relays, but also nomadic and mobile relays. Relay access points installed on mobile vehicles can serve mobile terminals on board or nearby.

In addition to the coverage extension which is the primary goal, relaying lends itself to more efficient communication scheme called "***cooperative relaying***" [2.19] to realize diversity gain through multiple relays transmitting the same information to the same destination. By combining the multiple signal copies transmitted from the relays coherently at the receiver, effects of small scale fading can be significantly mitigated by virtues of obtained spatial diversity. As will be shown in the following sections, diversity gain can be interpreted into the smaller amount of required transmit power to achieve the same performance when there is no diversity. This is plausible since transmitters in a network would need to invest less power to meet required data rate. It has been known that Multiple-Input-Multiple-Output (MIMO) channel realized by the use of multiple antennas can linearly increase system capacity (or spectral efficiency) with the total number of transmit and receive antennas [2.20][2.21].

However, the attainable capacity of MIMO channel is limited by the channel correlation among the individual paths in the channel.

In order to realize an uncorrelated MIMO channel, the antennas must be sufficiently spaced in order of wavelengths which is of tens of centimeters (cm) for Giga hertz (GHz) bands on which current systems are operating. For instance, 2.5 GHz carrier frequency used by most of the nowadays' wireless standards use has a wavelength of 12 cm. It is not practically feasible for small mobile terminals to have multiple antennas. On the other hand, since distributed relay nodes are located at different positions, the antennas are sufficiently spaced. Thus, uncorrelated virtual MIMO channel may be readily achieved with single omnidirectional antenna on each cooperating terminal nodes.

2.4.1 Cooperative Relay Systems

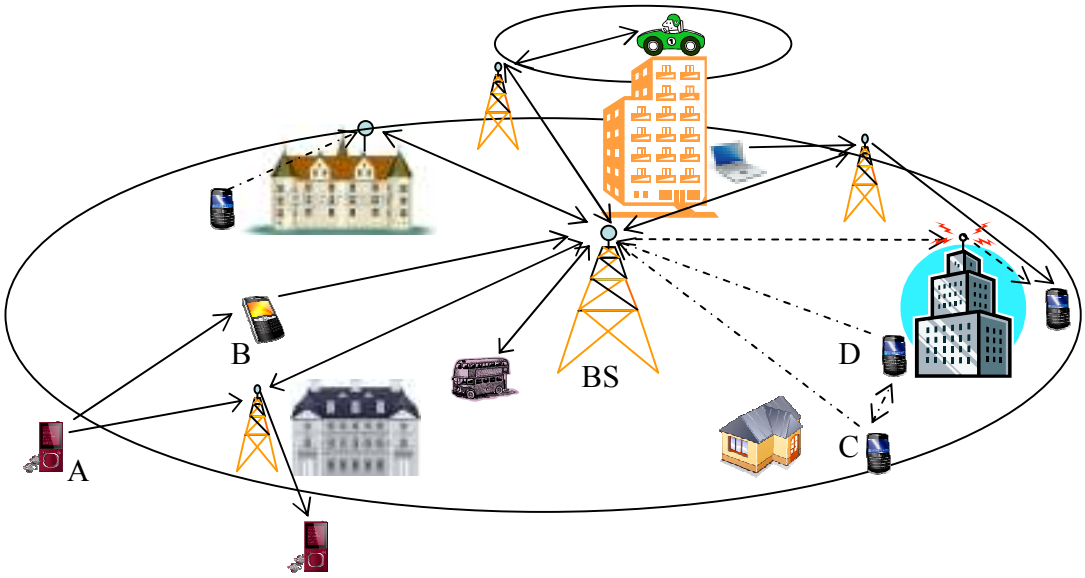

Fig. 2.13 Wireless fixed and mobile relay system model

Figure 2.13 depicts a generic relay system model. The relays include both fixed relays and mobile wireless stations. It has been envisioned that a future mobile terminal can not only serve as transceiver for a specific user but also as a relay node

for other user terminals in their radio signal coverage [2.22]. In Fig. 2.12, terminal A which is outside the coverage of base station (BS) establishes communication link through a fixed relay station as well as user terminal B. Thus, terminal A benefits additional diversity gain from terminal B through a mobile channel in addition to a line of sight wireless channel through fixed relay station. Such additional diversity may facilitate a high data rate which otherwise is impossible with a two hop fixed relay link. On the other hand, nodes D and C mutually serve as relay nodes for each other although both of them are located in the coverage range of the base station. Firstly, they form cooperation group by acknowledging each other as partners. Partner selection and decision may be carried out by means of some protocols in Medium Access Control (MAC) layer [2.23]. Secondly, each terminal either detects or simply scales the received signal from the partner and then relays the partner's signal to the destination, base-station. At first glance, since they also transmit partner's signal in addition to their own signals, one may tend to conclude that the cooperating terminals (C and D) might consume more transmit power. However, user cooperation diversity derived from spatial diversity provides significant SNR gain over the non-cooperation mode in which each terminal transmits its own signal alone [2.24].

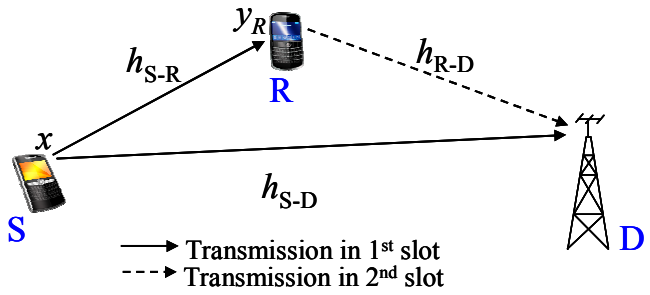

Fig. 2.14 A simplified cooperative relay system

2.4.2 Relaying Strategies

There are two main relaying strategies namely Amplify and Forward (AF) and Decode and Forward (DF). A simple relay system consisting of source (S), relay (R),

and destination (D) is depicted in Fig. 2.14. The model in Fig. 2.14 assumes that S and D can directly communicate each other and it uses two time slots to provide orthogonal time slots for S and R transmission. In such case, the main objective of employing R is to achieve cooperative diversity by assisting S rather than coverage extension.

(a) Amplify and Forward (AF)

Conventional signal booster or repeaters use strategy similar to AF. With AF, received signal is not detected. Thus, it does not incur delay of demodulation/detection process. Instead, the received signal is amplified or scaled by a factor and relay the signal forward. Suppose, S in Fig. 2.14 transmits signal x to both R and D. Assuming the transmit signal has a unit energy, the received signal at R is

$$y_R = h_{S-R}x + n \tag{2.5}$$

where $h_{\text{S-R}}$ and n represent complex channel coefficient source-relay (S-R) channel and zero mean complex AWGN additive noise of receiver front end. R scales the received signal y_R by a power normalization factor α_{AF} and retransmits it to D. The scaled transmit signal can be expressed as [2.25]

$$\begin{aligned} x_R &= \alpha_{AF} y_R \\ \alpha_{AF} &= \sqrt{\frac{1}{\left|h_{S-R}\right|^2 + N}}, \end{aligned} \tag{2.6}$$

where N is variance of n. The drawback of AF is noise signal amplification of received signal due to power scaling by the factor α_{AF}. On the other hand, AF allows simple receiver structure except for the need to have buffer to temporarily store the received signal since signal detection/demodulation is not carried out. Thus, it can be claimed that AF is advantageous when source-relay channel condition is good [2.26].

(b) Decode and Forward (DF)

With this relay strategy, relay node detects the received signal from the source, re-encode and modulate the signal and then relays it to the destination node. To prevent error propagation in the relayed signal, error detection codes are often used. S encodes the data bits by an error detection code before data modulation. The most well-known error detection code is cyclic redundancy check (CRC) code [2.27]. After signal detection and hard decision, R conducts CRC check on the hard decided bits. If CRC result shows no error, the hard decided bits are re-encoded and modulated in the same way as processed at the source transmitter. Thus, error propagation does not occur with DF at the expense of increased complexity and delay at relays. More advanced relaying scheme uses incremental code combining technique [2.28]. In that, error correction codes are also used along with CRC. With incremental code combining, R in Fig. 2.14 re-encodes the detected bits by using complementary puncturing pattern to make incremental redundant bits different from that transmitted by S. Hence, the redundancy bits transmitted from the S and R are complementary to each other and the combined signal at D can achieve higher coding gain in addition to inherent spatial diversity.

2.4.3 Relay Cooperation Topologies

Based on the two main relaying strategies, there can be three key relay cooperation topologies- (a) repetition based cooperation (b) space-time/frequency based cooperation and (c) selective cooperation.

(a) Repetition Based Cooperation

Fig. 2.15 illustrates repetition based cooperative relay system. There are n relays available to cooperate in between S and D. In the first phase, S broadcasts to all the nodes. In the second phase, each R relays the signal from S to D in their assigned orthogonal time slots. Since there are $n + 1$ copies of signal arriving at D, diversity order of $n + 1$ is achieved. However, the requirement of orthogonal channel for each cooperating R degrades the spectral efficiency with the number of cooperating relays.

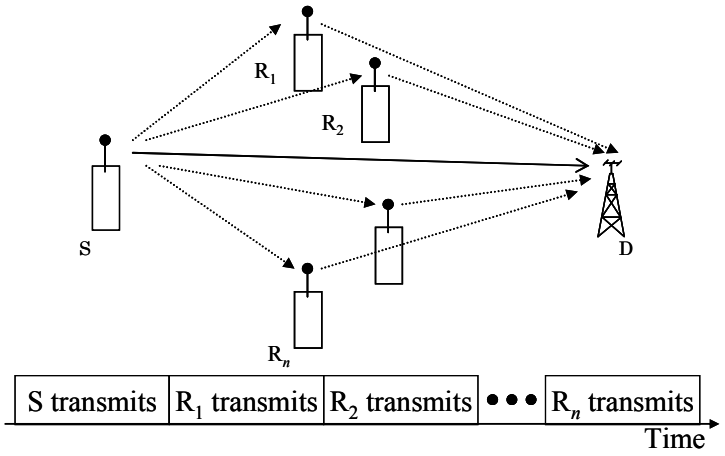

Fig. 2.15 Repetition based relay system

(b) Distributed Space Time/Frequency Code Cooperation

The transmit diversity using orthogonal space-time code (STC) can achieve the same diversity order as with the received diversity [2.29]. Conventional MIMO systems employ STC for a transmitter with co-located multiple antennas. STC can be applied for also a virtual MIMO transmission with distributed antennas as in cooperative relay systems. Eq. (2.7) describes space time/frequency code matrix.

$$A = \begin{pmatrix} a_1 & -a_2^* \\ a_2 & a_1^* \end{pmatrix} \tag{2.7}$$

where a_1 and a_2 are consecutive modulated symbols in time or frequency domain. In STC, rows of the matrix represent antenna entities and columns represent time. Table 2.2 shows transmit data sequence in space and time dimensions with STC. For simplicity, transmit data sequence is described in symbol by symbol. In practice, STC may be applied on a block of symbols. T_s in Table 2.2 represents symbol time duration.

Table 2.2 Space-time code sequence

Time	R_1's transmit sequence	R_2's transmit sequence
t	S_1	S_2
$t + T_s$	$-S_2^*$	S_1^*

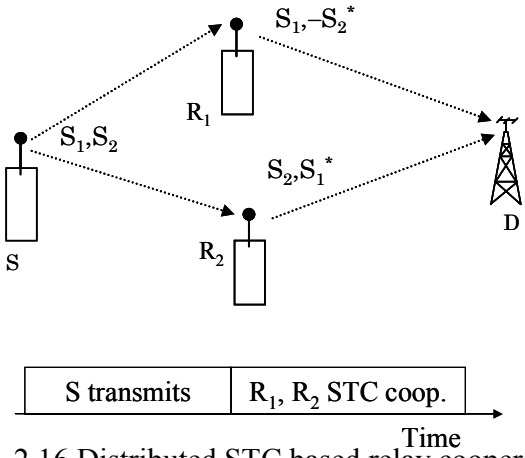

Fig. 2.16 Distributed STC based relay cooperation

Fig. 2.16 depicts a distributed STC relay cooperation. In the first phase, S transmits data symbol sequence to the relays. There may or may not be direct link between S and D. Then, each relay transmits STC coded data symbols according to the assigned space time code matrix. As seen in the Fig. 2.16, since no orthogonal time slots are required with the use of STC, superior spectral efficiency is achieved compared to the repetition based cooperation. However, the drawback of STC cooperation is that the number of cooperating relays cannot be an arbitrary number due to the STC code design issue. A conventional Almouti code [2.29] cannot achieve full rate and full diversity for an arbitrary number of transmit antennas since there is no rate one code for the number of antennas more than two. That imposes limitation on the number of cooperating relays.

Moreover, STC matrix entity must be assigned in advance to the cooperating relays. Again, the cooperating relays are required to employ DF strategy since STC encoding must be carried out after signal detection and re-modulation. Thus, D must have knowledge on which relays representing which assigned antenna code entities are cooperating so that D can decide decoding rule accordingly.

Multi-carrier systems can use STC like code in space-frequency (SF) dimension. Fig. 2.17 shows an example of distributed SF code transmission in two-relay system using OFDM. k represents OFDM sub-carrier index, with k =1,2,..N_c where N_c is the

number of sub-carriers. First, N_c data symbols are block interleaved such that SF encoded data symbols impaired by the highly correlated fading coefficients are not subsequent data symbols in the original serial data sequence [2.30]. Table 2.3 shows space frequency encoded sequence at each relay. The SF mapping is carried out such that R_1 transmits the original data symbols without being modified and R_2 transmits data symbols modified by SF encoder.

Table 2.3 Space-frequency code sequence at two relays

OFDM symbol time	R_1's transmit sequence ($x_{1,n}$)	R_2's transmit sequence ($x_{2,n}$)
k	S_k	$-S_{k+1}^*$
$k+1$	S_{k+1}	S_k^*

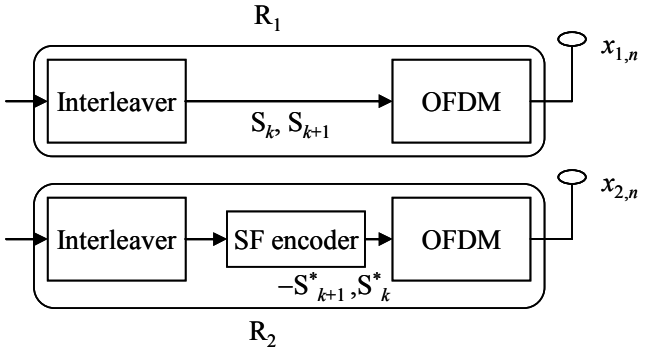

Fig. 2.17 Space-frequency coded transmission at two relays

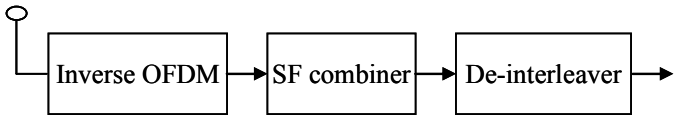

Fig. 2.18 Space-frequency decoding at destination receiver

The receiver structure of OFDM with SF decoder is depicted in Fig. 2.18. Systems with STC/SFC demand strict data symbol level synchronization to coherently combine signals from different antennas. For a MIMO system with co-located antennas, synchronization requirement is not a problem. However, for a virtual MIMO system formed by distributed antennas at different relays, offset in

transmit timing and difference in propagation delays through channel impose a very challenging task to achieve symbol level synchronization.

(c) Selective Cooperation

Transmit antenna selection diversity can achieve the same diversity order as space-time transmit diversity (STTD) and maximum ratio combined received diversity (MRRC) [2.31]. Cooperative relay networks also exploit transmit selection diversity derived from distributed antennas of relays. The advantage of selection diversity in relay communications is its simplicity since only one relay node is involved in relaying signal to the destination.

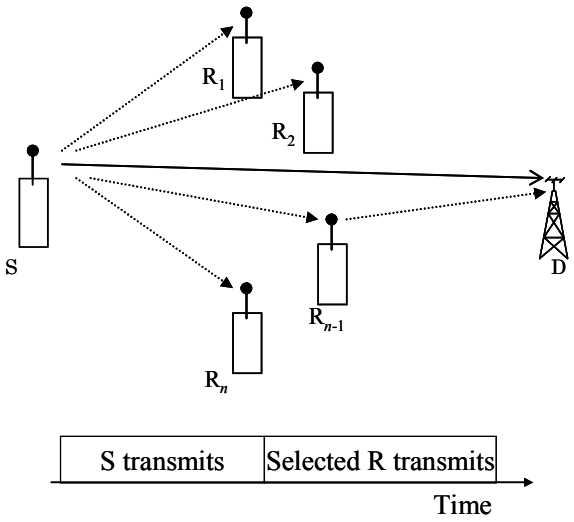

Fig. 2.19 Selection based relay cooperation

Fig. 2.19 plots a selection based relay cooperation. In the first phase, S broadcasts to all the nodes. The direct path between S and D may or may not exist. In the second phase, the relay with the best channel condition towards D is selected to allow relaying. In order to decide the best relay, the system must have knowledge on channel state information (CSI) of cooperating relays. In most cases, D serves as central decision maker in selecting the best relay since CSI of each relay may be available at D by using pilots. In such centralized selection, each R transmits pilots to D to provide CSI of their channels. D extracts CSI from the received pilots and then

broadcasts the best relay's ID. In systems that use AF, relay selection is carried out based on end-to-end channel quality of each relay. Typically, there are two main policies in deciding end-to-end channel.

Policy I: end-to-end channel quality a_i of each relay R_i is decided by taking harmonic mean of S-R and R-D channel gains as below

$$a_i = \frac{2\left|h_{SR_i}\right|^2 \left|h_{R_iD}\right|^2}{\left|h_{SR_i}\right|^2 + \left|h_{R_iD}\right|^2} \ . \tag{2.8}$$

Policy II: end-to-end channel quality a_i of each relay R_i is decided by taking minimum of S-R and R-D channel gains as below

$$a_i = \min\left\{\left|h_{SR_i}\right|^2, \left|h_{R_iD}\right|^2\right\}. \tag{2.9}$$

In both policies, the relay whose a_i is the largest is selected as the best relay. With DF, relay selection is carried out among a set of relays whose CRC results show correct reception. Since the quality of channels in the first link, S-R channel, has been explicitly decided by means of CRC in relay systems employing DF strategy, the selection policy needs to take into account R-D channels only in relay selection.

Performance metric called Diversity-multiplexing Tradeoff [2.32] has been defined to evaluate and compare the performances of different cooperation schemes. For a given cooperation scheme with an SNR=Γ, let the corresponding data rate and outage probability are $\Re(\Gamma)$ and $P_{out}(\Gamma)$. Then, the multiplexing gain r and the diversity order d are defined as

$$r = \Re(\Gamma)/\log(\Gamma)$$

$$d = \frac{\log P_{out}(\Gamma)}{\log \Gamma}. \tag{2.10}$$

For a selective relay network employing either AF or DF with M cooperating relays, assuming statistically identical channels, the outage probability $P_{\text{out}}(\Gamma)$ is

given by $\Gamma^{(M+1)(2r-1)}$ [2.33]. Fig. 2.20 plots diversity-multiplexing tradeoffs with different relay cooperation schemes. It shows that selective relaying can offer the same tradeoffs as more complicated STC cooperation. The multiplexing gain r is 0.5 in both selective cooperation and STC since both of them operates on two phases demanding two time slots. All schemes achieve diversity order of $M + 1$, i.e. M relays plus S, given that direct link between S and D exists.

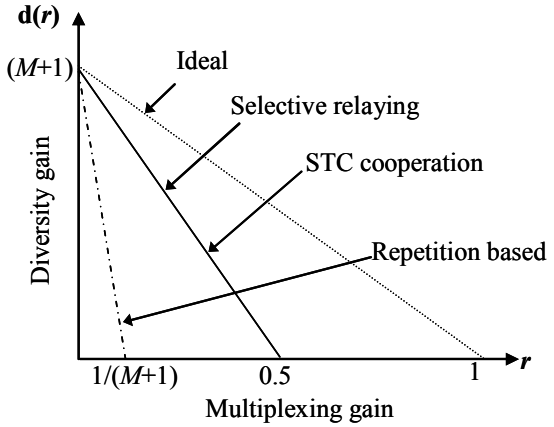

Fig. 2.20 Diversity-multiplexing tradeoff with different relay cooperation schemes

2.5 *Conclusion*

In this chapter, general overviews of transmission rate adaptation and cooperative relay systems were presented. Transmission rate adaptation with channel is realized by the use of adaptive modulation and variable coding rate. Principle of multicarrier modulation was also explained as a major wireless scheme robust against multipath channel delay spread. Asymmetric TDD was introduced as a major duplex scheme for present and future wireless broadband systems. Then, the needs and evolution of relay systems were highlighted. Relay topologies and achievable diversity were discussed. The advantages and drawbacks of different relay cooperation topologies were also outlined. Relay selection technique is a simpler alternative yet achieve comparable performance to space-time/frequency based relay cooperation.

In future wireless communications, mobile terminals have been expected to have capability to serve as relays. Future relay systems are likely to employ not only designated relays such as access points, but also portable mobile terminals. As a result, security related issues and criteria to form cooperation group are demanding more attention. More researches need to be done to solve such issues.

References

[2.1] C. E. Shannon, "Communication in the presence of noise," Proc. IRE, vol. 37, no. 1, pp. 10-21, Jan. 1949.

[2.2] B. Sklar, *Digital communications: Fundamentals and Applications*, Prentice Hall, 2001.

[2.3] M.C. Valenti, "Turbo codes and iterative processing," in Proc. IEEE Wireless Commun. Symp., pp. 216-219, Auckland, New Zealand, Nov. 1998.

[2.4] K. Hasung and G. L. Struber, "Rate compatible punctured turbo coding for W-CDMA," IEEE ICPWC, pp.143-147, Aug. 2000.

[2.5] C. Berrou, A. Glavieux, and P. Thitimajshima, "Near optimum error correction coding and decoding: Turbo codes," in Proc. IEEE ICC 93, pp. 1064-1070, Geneva, Switzarland, May 1993.

[2.6] S. Lin and D. J. Costello Jr., *Error control coding: fundamentals and applications*, Prentice Hall, Inc., Englewood Cliffs, New Jersey, 1983.

[2.7] M. R. Soleymani, Y. Gao, and U. Vilaipornsawai, *Turbo coding for satellite and wireless communications*, Kluwer Academic Publishers, 2002.

[2.8] L. Bahl, J. Cocke, F. Jelinek, and J. Raviv, "Optimal decoding of linear codes for minimizing symbol error rate," IEEE Trans. Inf. Theory, vol.IT-20, pp. 284-287, Mar. 1974.

[2.9] R. Van Nee and R. Prasad, *OFDM for wireless multimedia communications*, Boston, Artech House Publishers, 2002.

[2.10] ETSI DVB-T (EN 300 744), "Digital video broadcasting (DVB); frame structure, channel coding and modulation for digital terrestrial television," Sophia Antipolis, France, July 1999.

[2.11] Mobile WiMAX Part I: "A technical overview and performance evaluation", WiMAX Forum, Apr. 2006.

[2.12] R. Esmailzadeh and M. Nakagawa, *TDD-CDMA for wireless communications*, Artech House, 2003.

[2.13] K. Fazel and S. Kaiser, *Multi-carrier and spread spectrum systems*, John Wiley & Sons Ltd, 2003.

[2.14] IEEE 802. 16e-2005, IEEE Standard for Local and Metropolitan Area Networks. Part 16: Air Interface for Fixed and Mobile Broadband Wireless Access Systems.

[2.15] A. Sendonaris, E. Erkip, and B. Aazhang, "Increasing uplink capacity via user cooperation diversity," in Proc. IEEE Int. Symposium Inform. Theory (ISIT'98), Cambridge, MA, pp. 156, Aug. 1998.

[2.16] Parsons D., *The mobile radio propagation channel*, John Wiley & Sons, 1992.

[2.17] ETSI UMTS (TR-101 112), V 3.2.0, Sophia Antipolis, France, April 1988.

[2.18] IEEE 802. 14j-2007, IEEE standard for Local and Metropolitan area networks. Part 16: Air Interface for Fixed and Mobile Broadband Wireless Access Systems- multihop relay specification.

[2.19] P. Herhld, E. Zimmermann, and G. Fettweis, "Cooperative multi-hop transmission in wireless networks," Computer Networks, vol. 49, no. 4, pp. 299-324, Oct. 2005.

[2.20] A. Goldsmith, S. A. Jafar, N. Jindal, and S. Vishwanath, "Capacity limits of MIMO channels," IEEE JSAC, vol. 21, no. 5, pp. 684-701, June 2003.

[2.21] D. Gesbert, M. Shafi, D. Shiu, P.J. Smith, and A. Naguib, "From theory to practice: an overview of MIMO space-time coded wireless systems," IEEE JSAC, vol.21, no. 3, pp. 281-302, Apr. 2003.

[2.22] H. Nourizadeh, S. Nourizadeh, and R. Tafazolli, "Performance evaluation of cellular networks with mobile and fixed relay station," in Proc. 2006 IEEE 64th, VTC-fall, pp. 1-5, 25-28 Sept. 2006

[2.23] IEEE 802.11 WG, IEEE standard for wireless LAN Medium Access Control (MAC) and Physical Layer (PHY) specifications, ANSI/IEEE Std 802.11, 1999 Edition.

[2.24] A. Sendonaris, E. Erkip, and B. Aazhang, "User cooperation diversity-part II: Implementation aspect and performance analysis," IEEE Trans. on Commun., vol. 51, no. 11, pp. 1939-1948.

[2.25] M. R. Souryal and B. R. Vojcic, "Performance of amplify-and-forward and decode-and-forward relaying in Rayleigh fading with turbo codes," in Proc. ICAPSSP 2006, vol. 4, pp. 681-684, May 2006.

[2.26] Y. Meng and L. Jing, "Is amplify-and-forward practically better than decode-and-forward or vice versa?," in Proc. IEEE ICASSP 2005, vol.3, pp. iii/365-iii/368, March 2005.

[2.27] T.V.Ramabadran and S.S.Gaitonde, "A tutorial on CRC computations," IEEE Micro, vol. 8, no. 4, pp. 62-75, Aug. 1988.

[2.28] A. Nosratinia, T.E. Hunter, and A. Hedayat, "Cooperative communication in wireless networks," IEEE Communications Magazine, vol.42, no.10, pp. 74-80, Oct. 2004.

[2.29] S.M.Almouti, "A simple transmit diversity technique for wireless communications," IEEE JSAC, vol. 18, no. 8, pp. 1451-1458, Oct. 1998.

[2.30] M. Torabi, S. Aissa, and M.R. Soleymani, "On the BER performance of space-frequency block coded OFDM systems in fading MIMO channels," IEEE Trans. on Wireless Commun., vol.6, no.4, pp.1366-1373, April 2007.

[2.31] A. Abrardo and C. Maraffon, “Analytical evaluation of transmit selection diversity for wireless channels with multiple receive antennas,” in Proc. IEEE ICC 2003, vol. 5, pp. 3200-3204, May 2003.

[2.32] L. Zheng and D. Tse, “Diversity and multiplexing: A fundamental tradeoff in multiple antenna channels,” IEEE Trans. Inf. Theory, vol. 49, no. 5, pp. 1073-1096, May 2003.

[2.33] A. Bletsas, A. Khisti, D. P. Reed, and A. Lippman, “A simple cooperative diversity method based on network path selection,” IEEE JSAC, vol. 24, no. 3, pp. 659-672, Mar. 2006.

Chapter 3

Asymmetric TDD Systems with AMC and HARQ

3.1 *Background*

In present wireless mobile communication systems, as mobile users' demands for interactive multimedia applications and Internet-like data services increase, traffic becomes more bursty and asymmetric. For such data-centric services, time division duplex (TDD) has long been considered as the most appropriate choice owing to its flexibility in supporting asymmetric traffic [3.1][3.2]. Thus, standards for future wireless broadband systems such as mobile WiMAX (IEEE 802.16e) [3.3] and advanced LTE [3.4] have included TDD as a major duplex scheme. Moreover, these standards also include AMC, HARQ and OFDM based wireless access in downlink. In genral, the received signal to noise power ratio (SNR) is the common criterion in AMC to switch modulation and coding scheme (MCS) [3.5]. In [3.6] and [3.7] it was shown that open loop power control in TDD can achieve satisfactory performance with little control delay. In [3.6] [3.7], the authors investigated only symmetric slot assignment, i.e. transmit and receive slots alternate with 1:1 downlink to uplink slot ratio. In [3.8], the channel estimation error in MC-CDMA/TDD was investigated for symmetric slot allocation and a pre-equalization scheme was proposed to mitigate the error.

Fig. 3.1 depicts FDD and asymmetric TDD systems. In FDD mode, since continuous transmission and reception is possible in both link directions, the delay in feeding back CSI and performing link adaptation may be kept constant. Roughly

speaking, the control delay equals transmission delay plus some processing time. However, in asymmetric TDD, where BS and MS transmissions alternate according to the time slot format, the control delay can vary significantly. This is particularly true if one direction, either uplink or downlink outweighs the other. This control delay affects two important link adaptation functions: the selection of MCS in AMC; and delay in hybrid automatic repeat request (HARQ) [3.9]. This study examines the effect of TDD asymmetric slot allocation on the performance of AMC and HARQ.

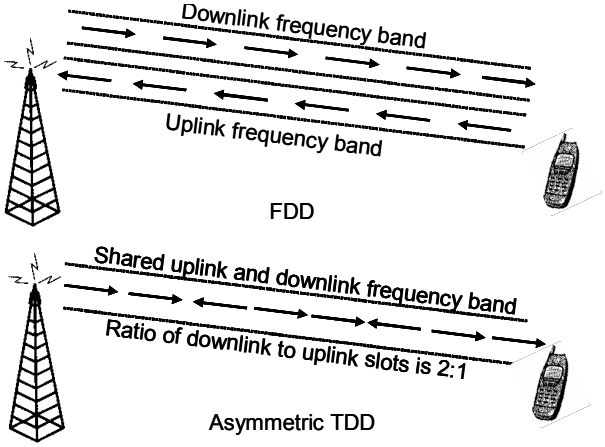

Fig. 3.1 FDD and Asymmetric TDD

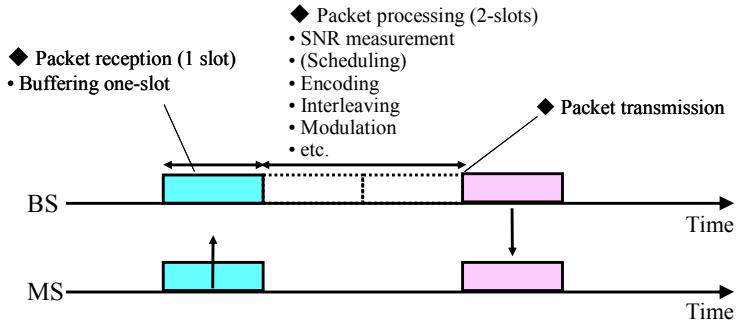

Fig. 3.2 Packet processing delay resulting in AMC control delay

Fig. 3.2 illustrates delay incurs in open loop control of TDD systems. In uplink, to buffer to the whole packet, BS takes one time slot. After buffering, BS measures the channel SNR from the pilot symbols distributed in time throughout the packet. Based on measured SNR, BS decides which MCS to be chosen for downlink transmission. Having chosen MCS, packet generation process that includes encoding,

interleaving and modulation can be started. These processes incur some delay. It is assumed that packet processing delay takes two time slots from the time when the received packet has been completely buffered to the time of transmitting the next packet on the opposite link with selected MCS based on the measured SNR. Therefore, a total of at least three time slots are required from the time of reception to the time of downlink transmission with selected MCS based on measured SNR. This assumption can be applied to both FDD and TDD. In case of FDD, owing to the requirement of feedback to report CSI at MS to BS, the round trip delay will be twice as large as open loop control delay in TDD. For instance, NTT DoCoMo assumes round trip control delay in AMC and HARQ using FDD to be 10 packets and 6 packets, respectively [3.10][3.12]. In TDD with open loop channel estimation, as shown in Fig. 3.2, correlation between the estimated channel state and the instantaneous channel state at the time of actual transmission decreases as the number of continuous downlink slots increases. Consequently, inappropriate MCS levels may be selected. This MCS level selection error will result in erroneous packet reception and degrade achievable system throughput.

Previous researches [3.7][3.8][3.13] have discussed MCS selection in FDD systems and the result of power control error in TDD systems. However, no report exists on the effect of MCS level selection error in TDD systems, with or without asymmetric downlink/uplink slot allocation. This study formulates an analytical expression to calculate the probability of erroneous MCS selection. Then, using this formula, the probability of erroneous MCS selection is calculated for different TDD time slot allocations. Computer simulations are conducted to validate the numerical results and to investigate the effect of asymmetric slot allocation, taking into account the effect of control delay on AMC and HARQ performance.

This chapter is organized as follows. Section 3.2 represents a system description of the TDD system under consideration. Section 3.3 discusses the control delay components in TDD, and Section 3.4 represents the analytical approach to the calculation of erroneous MCS selection probability. Simulation parameters and a

channel model are presented in Section 3.5, followed by numerical and simulation results in Section 3.6. Finally Section 3.7 concludes the chapter.

MCS_1	QPSK *r* 1/3
MCS_2	QPSK *r* 1/2
MCS_3	16QAM *r* 1/3
MCS_4	16QAM *r* 1/2
MCS_5	16QAM *r* 2/3
MCS_6	16QAM *r* 3/4

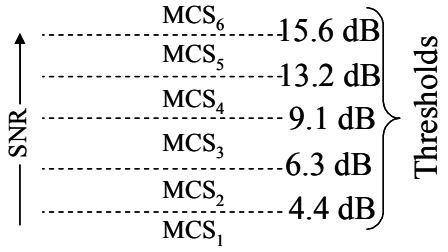

Fig. 3.3 Thresholds and MCS

3.2 *System Description*

AMC in our system utilizes open loop channel estimation based on uplink pilot symbols to select MCS for the downlink packets. A set of SNR thresholds are set as shown in Fig. 3.3 to decide which modulation and coding combination scheme (MCS) should be selected according to channel condition. The threshold levels were decided based on maximum throughput criteria [3.11]. The first step in this method is to obtain the throughput versus average symbol energy per noise power (SNR) curves of each MCS_i (i=1, 2,…, 6). The maximum throughput of MCS_i crosses the throughput curve of MCS_{i+1} at certain SNR value and that SNR can be chosen as the threshold to switch from MCS_i to MCS_{i+1} and so achieve the maximum throughput each MCS provides. For example, the maximum throughput of MCS_2 crosses the throughput curve of MCS_3 at the SNR of 6.3 dB.

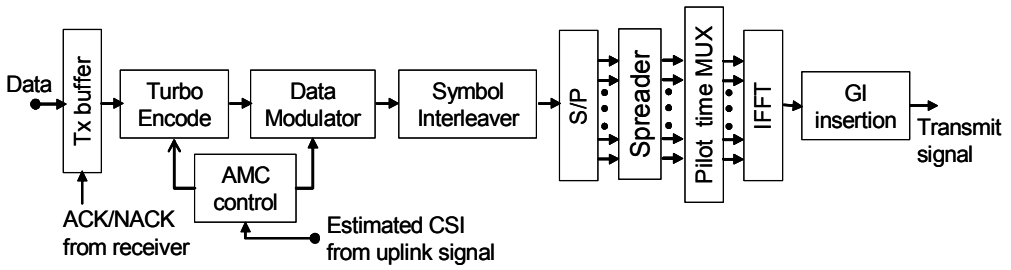

(a) Transmitter

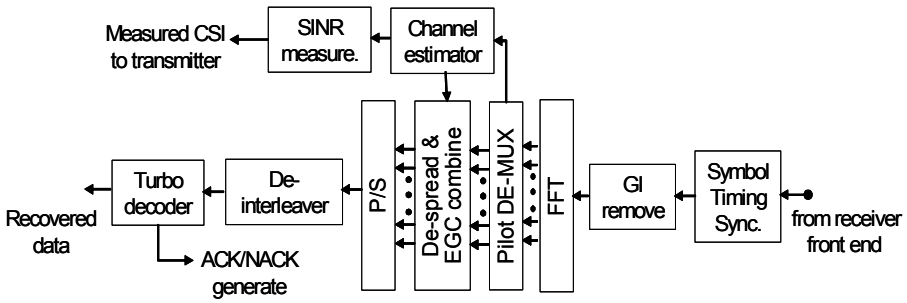

(b) Receiver

Fig. 3.4 Configuration of transmitter and receiver

The hybrid ARQ scheme in this study adopts the Type II Hybrid ARQ also known as incremental redundancy (IR) as it exhibits the best throughput performance [3.10][3.12]. In this scheme, the transmit packet is initially encoded with the designed initial coding rate and punctured to achieve the desired coding rate. When error is detected, the first retransmission is carried out using the complementary puncturing pattern of the initial transmission; subsequent combination with the stored erroneous packet achieves a highly effective initial coding rate. If error still exists, a second retransmission is carried out by transmitting the same packet as in the initial transmission and it is combined with the first and second erroneous packets stored in the receiver. Complementary puncturing patterns are used alternately for every odd and even transmission.

The configurations of the transmitter and receiver in our TDD system are shown in Fig. 3.4. The wireless access scheme is MC-CDMA with 768 sub-carriers. The wireless access scheme is based on the Variable Spreading Factor-OFCDM (VSF-OFCDM) proposed by NTT DoCoMo [3.13]. VSF-OFCDM, originally based on multi-carrier CDMA, can achieve a high throughput of more than 100 Mbps in 100 MHz bandwidth if used with multi-code transmission [3.10][3.13][3.14]. The number of sub-carriers is 768 since this number can satisfy the requirement that the sub-carrier spacing must be less than the coherence bandwidth in a 100 MHz broadband channel. This number also provides a sufficient guard-interval (GI) length in dispersive channels such that the packet energy loss due to GI is held under 20 % in typical suburban micro-cell environments. Note that the same transmitter/receiver

configuration is applicable to both FDD and TDD, except for the presence of transmit/receive switching unit at the transceiver front end in the latter case.

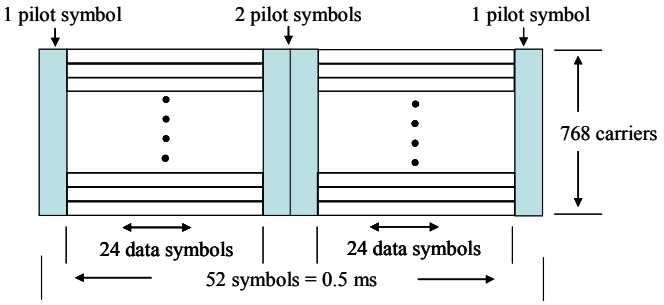

Fig. 3.5 Packet structure

In the transmitter, information bits are initially encoded with rate 1/3 Turbo code. Variable channel coding rates can be achieved by puncturing the mother code. Data modulation mapping is then carried out for AMC based on the measured SNR provided by the received signal; symbol level interleaving in the frequency domain over 768 sub-carriers is performed to randomize the burst errors caused by frequency-selective fading. The interleaved, modulated data is then spread by using orthogonal codes with spreading factor SF =16. The spread sequence is time multiplexed with pilot symbols, whose positions in the packet are as shown in Fig. 3.5. Packet length (or slot length) is 0.5 msec and each packet includes 52 OFDM symbols comprised of 48 data symbols and 4 pilot symbols multiplexed in time. The pilot multiplexed spread sequence is then multi-carrier modulated by IFFT and GI is inserted. Finally, a new packet is transmitted into the propagation channel after RF up-conversion. The transmit data is also stored in the buffer to allow retransmission if needed.

At the receiver, synchronization of the FFT window or OFDM symbol timing is carried out by using the auto-correlation of the received signal. Synchronization can be achieved by looking for the correlation peak caused by the effective symbol interval and the GI, i.e. cyclic prefix of OFDM symbol [3.13][3.14]. Once synchronization is achieved, the GI is removed. The parallel data on 768 sub-carriers are then de-multiplexed by FFT. Channel estimation is carried out after FFT. Channel

values at known pilot symbols on each carrier are calculated and the acquired channel SNRs from 4 pilot symbols on each sub-carrier are averaged throughout the whole packet. By employing the obtained channel estimate, the spread sequence at each sub-carrier is despread based on equal gain combining (EGC). The despread sequence is then symbol de-interleaved in the frequency domain and the output is sent to the decoder to recover the data. In our TDD system, to facilitate open loop channel estimation at the BS, dummy packets with the same packet structure are transmitted by the MS in uplink slots. After retrieving channel information from the uplink packets, they are discarded without proceeding further processing such as decoding.

3.3 *Control Delay of AMC and HARQ in TDD Systems*

Fig. 3.6 illustrates the control delay components in TDD systems. Fig. 3.6 (a) shows the control delay in AMC in two different TDD time slot allocation formats; the ratio of the number of downlink to uplink slots is either 1:1 or 3:1. BS receiver performs channel estimation from the uplink signal using the pilot symbols and that channel information is used to select MCS for the downlink packets. Since received packet buffering and packet processing takes some time, there exists a time difference between packet reception and the downlink transmission time with MCS based on uplink signal SNR measurement. We define this as the AMC control delay, D_{AMC}. As seen in Fig. 3.6 (a), asymmetric slot assignment with 3:1 downlink to uplink slot ratio causes larger AMC control delay. Furthermore, this delay D_{AMC} differs depending on the slot positions.

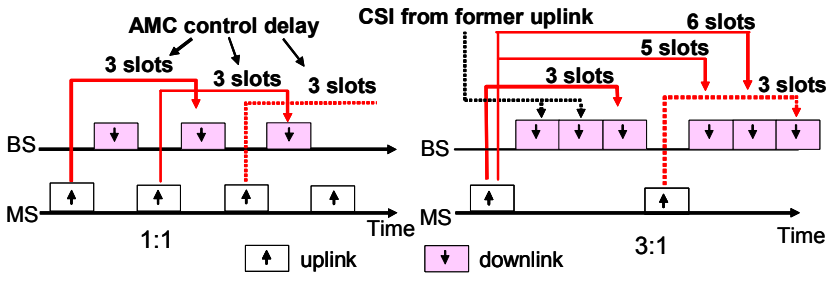

(a) AMC control delay

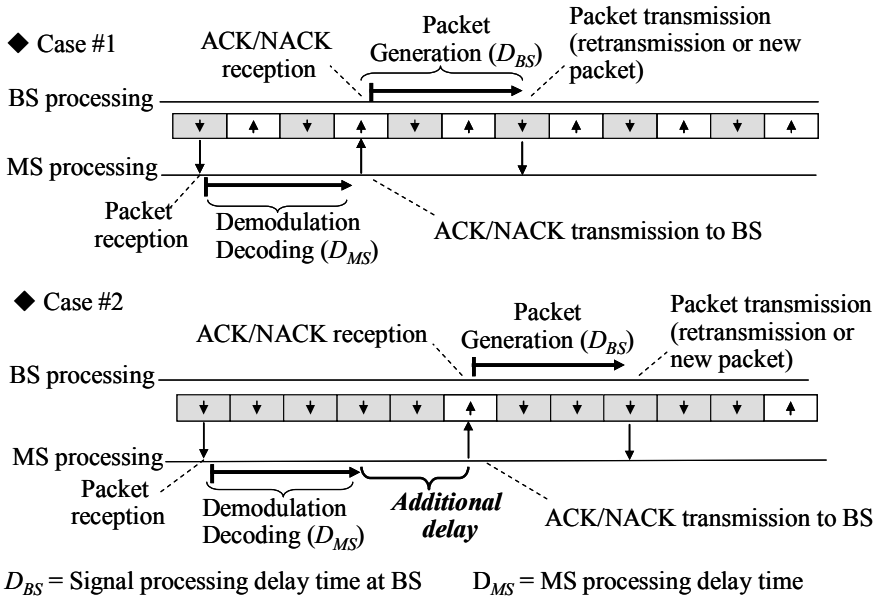

(b) HARQ control delay

Fig. 3.6 Control delay of AMC and HARQ in asymmetric TDD

Fig. 3.6 (b) shows examples of control delay scenarios in HARQ. HARQ requires a return channel to provide transmitter with the ACK/NACK status of received packet. In TDD where the availability of the return channel depends on time slot allocation, control delay in HARQ also depends on asymmetric slot assignment. On receiving the downlink packets, MS takes some time to demodulate, decode each received packet and then ACK/NACK is generated.

In this example, it is assumed that signal processing delays (D_{BS}) and (D_{MS}) in BS and MS takes three time slots, respectively. If the same delay is assumed in FDD, the total roundtrip delay to once retransmit any erroneous packet will be six time slots. In the assumed system, only one packet is transmitted in a slot. MS stores the ACK/NACK status of all received packets whose decoding processes have already been finished. When an uplink time slot is available, all the stored ACK/NACK information is assumed to be transmitted through control channel. After receiving uplink signal, BS decides whether to transmit a new packet or retransmit the packet with the oldest transmit time stamp according to ACK or NACK.

In Fig 3.6 (b), case 1 illustrates the HARQ control delay with 1:1 (downlink: uplink) slot allocation. This is a fixed delay similar to that of the round-trip delay in FDD with the assumed (D_{BS}) and (D_{MS}). However, in case 2, even though the MS has already finished decoding of the packet received in the 1st downlink slot, it still has to wait for two more time slots for the next uplink slot to transmit the ACK/NACK information back to the BS. This waiting time is an additional delay. As a result, the total time required to receive a valid packet in case 2 is longer than in case 1 when retransmission is required. Thus, in asymmetric TDD, HARQ control delay depends not only on processor speed for signal processing, but also on asymmetric slot allocation

Large AMC control delay may lead to selection of inappropriate MCS, which will result in erroneous packet reception, which in turn causes HARQ to trigger retransmission. Therefore, we define the total delay time to receive an error free packet as the time taken from initial packet transmission to the time when its ACK signal is successfully decided at the receiver. Since HARQ also works to mitigate the packet errors caused by erroneous selection of MCS in AMC, total delay performance also should be taken into account in addition to throughput performance in TDD. Asymmetric time slot allocation in this study assumes that the downlink dominates, i.e. the number of downlink slots is larger.

3.4 *Erroneous MCS Selection Probability*

To investigate the effect of different AMC control delays in asymmetric TDD, we define erroneous MCS selection probability as follows. Erroneous MCS selection is the mis-match between selected MCS and ideal MCS. Even though erroneous MCS selection may happen in both MS and BS, this study considers only that at the BS side. Selected MCS represents the MCS selected according to uplink channel measurement while ideal MCS stands for the MCS that would be selected if the actual channel condition of the downlink at the time of transmission was known.

If the SNR level on which MCS is determined lies between two thresholds ($\boldsymbol{th}_i$ and $\boldsymbol{th}_{i-1}$), such that ($\boldsymbol{th}_i > \boldsymbol{th}_{i-1}$), and the actual instantaneous SNR at the time of transmission is above $\boldsymbol{th}_i$ or under $\boldsymbol{th}_{i-1}$, an MCS level selection error occurs. This condition can be expressed by the following probability equation:

$$\sum_{i=0}^{M-1}\left(prob(th_{i-1} < x < th_i, y \le th_{i-1}) + prob(th_{i-1} < x \le th_i, y > th_i)\right), \qquad (3.1)$$

where, x, y, th, and M represents channel SNR used to determine MCS, instantaneous SNR at transmission time, SNR threshold to switch MCS, and the number of MCS levels, respectively. Furthermore, $prob(x, y)$ from (3.1) represents the joint probability of Raleigh distributed parameters x and y. (3.1) can be transformed into the closed form for all possible received SNRs, thresholds and MCS levels. In general, erroneous MCS selection probability $P_{e,sel}$ can be expressed as

$$P_{e,sel} = \sum_{i=0}^{M-1}\left(\int_{0}^{th_{i-1}}\int_{th_{i-1}}^{th_i} p_{x,y}(x,y)dxdy + \int_{th_i}^{\infty}\int_{th_{i-1}}^{th_i} p_{x,y}(x,y)dxdy\right), \qquad (3.2)$$

Furthermore, the joint probability density function of the received signal envelope, assuming a Rayleigh fading channel, sampled at two different time instants can be expressed as below [3.15],

$$p_{x,y}(x,y) = \frac{4(xy)^L e^{(-(x^2+y^2)/(\Omega(1-\rho)))}}{\Gamma(L)\Omega^{L+1}(\rho)^{(L-1)/2}(1-\rho)} * I_{L-1}\left(2xy\frac{\sqrt{\rho}}{\Omega(1-\rho)}\right) \qquad (3.3)$$

where,

x : Signal envelope at time t (measured SNR)

y : Instantaneous SNR at transmission time ($t + \tau$)

τ : Time difference between x and y

Ω: Averaged received power in each path,

ρ : Correlation coefficient,

I_{L-1} : Modified Bessel function of order L-1,

L : The number of paths.

Also,

$$\rho = J_0^2(2\pi\tau) \tag{3.4}$$

is used for land mobile channels [3.15], where, $J_0()$ stands for a zero order Bessel function of the first kind. Again,

$$\tau = f_d \, T_s * N_s * D_{AMC} \tag{3.5}$$

where f_d, T_s, N_s and D_{AMC} are maximum Doppler frequency, symbol duration, the number of symbols in a packet (slot), and AMC control delay in unit of time slots, respectively.

To simplify the use of (3.3), in simulations, we assume equal channel gain in each path so that only one Ω value needs to be calculated for all paths. For total average received SNR, Γ, with L paths, $\Omega = \Gamma/L$. The erroneous MCS selection that occurs with different TDD asymmetric slot assignments can be calculated by substituting the respective D_{AMC} into (3.5), which in turn is substituted into (3.4) and (3.3), and finally, (3.2) is solved by numerical integration for all possible SNR distribution. For example, in the case of the 1:1 format shown in Fig. 3.6 (a), the control delay in AMC is 3 time-slots for all packets. Thus, the probability calculation needs to be carried out only for $D_{AMC} = 3$ time slots. In the FDD case, taking account of the assumed control delay at both BS and MS and feedback, the D_{AMC} is two times longer than that in the 1:1 TDD case and it is constant. In the case of the 3:1 format, D_{AMC} varies between 3, 5 and 6 time slots depending on the downlink slot positions. Thus the erroneous MCS selection probability must be calculated separately for each D_{AMC} and the average must be taken to achieve the resultant selection error probability. Note that these calculations can be carried out not only for different asymmetric allocation formats but also for different channel conditions such as maximum Doppler frequency (f_d) and the number of paths (L).

Firstly, erroneous MCS selection probability when single threshold is employed to switch two MCSs in 1:1 slot allocation is shown in Fig. 3.7 with the number of path L and f_d as parameters. D_{AMC} is assumed as 3 time slots and the threshold is set at 9 dB. In flat fading, i.e. L = 1, received signal fluctuates more rapidly and large selection error variation is observed. As L increases, selection error probability distribution becomes smaller as a result of smaller variation in received SNR. Fig. 3.8 represents the erroneous MCS selection probability occurred with five MCS thresholds in 1:1 slot allocation with f_d = 40 Hz, and the number of paths L = 8. MCS levels used and the switching thresholds are as shown in Fig. 3.3. The dotted lines with solid marker represent erroneous MCS selection probability with single threshold at the SNR values of 4.4, 6.3, 9.1 dB and so on. Selection error probability with each threshold is numerically calculated by setting a threshold at one of the five SNR values. For instance, first, erroneous probability for 4.4 dB is calculated. Next, the threshold is moved to 6.3 dB and the calculation is carried out. The same procedure is repeated for all the five thresholds and erroneous MCS selection probability with each threshold is obtained. For the system with N thresholds simultaneously set, the total erroneous MCS selection probability is the same as that achieved by summing up the N different erroneous selection probabilities with individual threshold. Therefore, the variation of the total erroneous MCS selection probability curve in the system with five thresholds depends on the threshold spacing. In Fig. 3.8, the solid line with hollow markers represents total MCS selection error probability. SNRs between the most closely spaced thresholds such as, 4.4 and 6.3dB yield the highest erroneous MCS selection probabilities since MCS switching happens most frequently in these regions. The opposite can be seen in the region between the 13.2 and 9.1 dB thresholds.

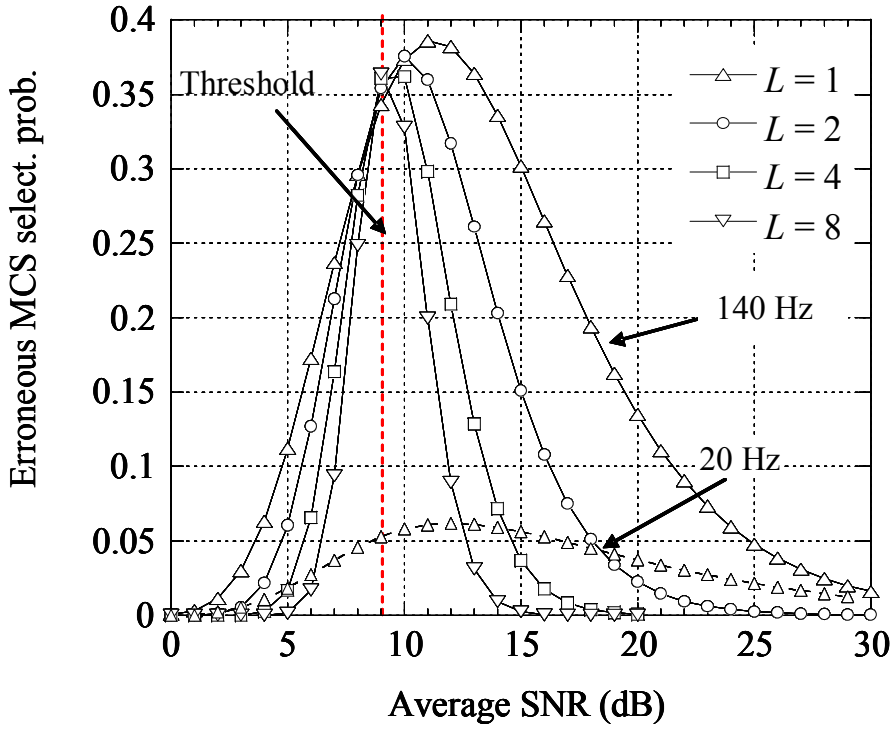

Fig. 3.7 Erroneous MCS selection probability with single threshold at 9 dB

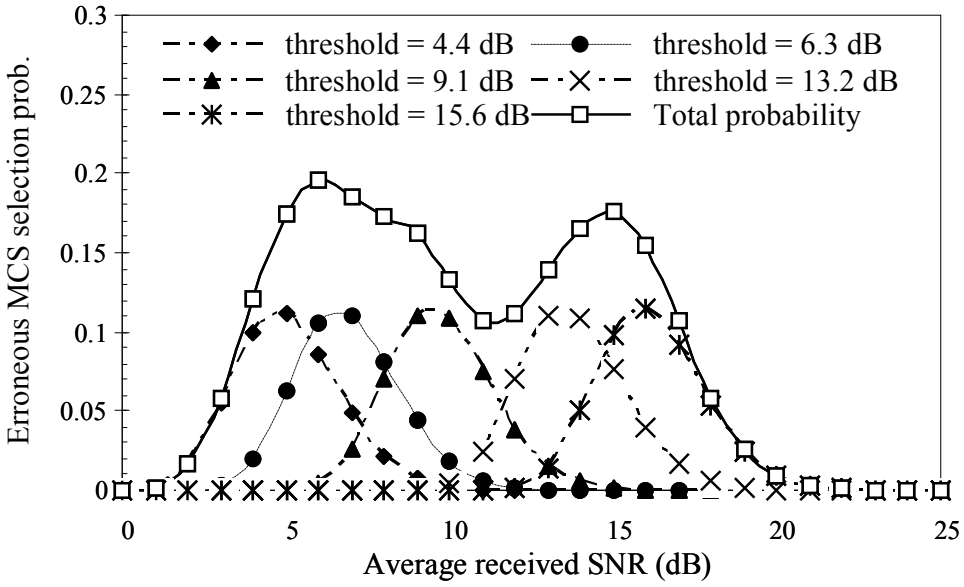

Fig. 3.8 Erroneous MCS selection with each of five thresholds and total probability

3.5 *Simulation Parameters and Channel Model*

3.5.1 Simulation Parameters

Table 3.1 Simulation parameters with asymmetric TDD

Wireless Access	MC-CDMA
Bandwidth	101.5 MHz
Number of sub-carriers	768
Sub-carrier separation	131.836 kHz
OFDM symbol duration	7.585μsec+GI 1.674μsec
Slot size (packet length)	0.5msec
Modulation	QPSK, 16QAM
Channel coding/decoding	Turbo (mother r =1/3, k =4) Max-Log-Map decoding 8 iterations
Control delay of AMC	Minimum 3 time slots for processing

Computer simulations are used to validate the theoretical approach of calculating erroneous MCS selection probability and to evaluate the throughput and delay performance of TDD systems. Only the single user case is considered. Table (3.1) lists the simulation parameters. The major radio link parameters are the same as those given in [3.13] except that only time domain spreading and single code transmissions are considered here. The thresholds to switch among six MCS levels are set at the SNRs as described in Section 3.2. Minimum control delay in AMC is 3 time slots. The actual value depends on the TDD time slot allocation. The same parameters are applied to both TDD and FDD.

3.5.2 Channel Model

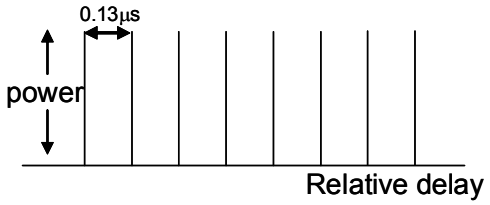

Fig. 3.9 Eight path equal gain channel model

An independent Rayleigh fading channel, depicted in Fig. 3.9, was adopted. The number of paths is 8 and each path has equal channel gain in order to match the

model assumed in our theoretical approach. R.M.S delay spread is 0.3 μsec and delay between each path is 0.13 μsec. Uplink and downlink channel conditions are assumed to be highly correlated in the TDD case, since the same frequency band is used in both links [3.1][3.6][3.7][3.8].

3.6 *Numerical Results*

This section shows the results of erroneous MCS selection for different asymmetric slot allocations in TDD; average received SNR and maximum Doppler frequency were varied. Furthermore, based on the selection error, throughput as well as delay performances will be discussed. Evaluation results of FDD in the downlink are also included as reference when needed.

3.6.1 Erroneous MCS Selection Probability in Different Asymmetric Assignments

In Fig. 3.10, erroneous MCS selection probability of symmetric slot assignment (1:1) is shown together with the results of the asymmetric slot assignments of 4:1 and 8:1 for SNR values from 0 to 20 dB; maximum Doppler frequency (f_d) is 40 Hz in all cases. Numerical results are also plotted for comparison. It is seen that erroneous MCS selection probability is higher in the formats with higher downlink slot asymmetry. This is because the correlation between the channel condition at the SNR measure time and that at the actual transmission time decreases as the number of downlink slots increases. The simulation results show close agreement with the numerical results. Here, it is seen that the maximum probability occurs at the SNRs that lie between closely spaced thresholds since more switching occurs in these regions.

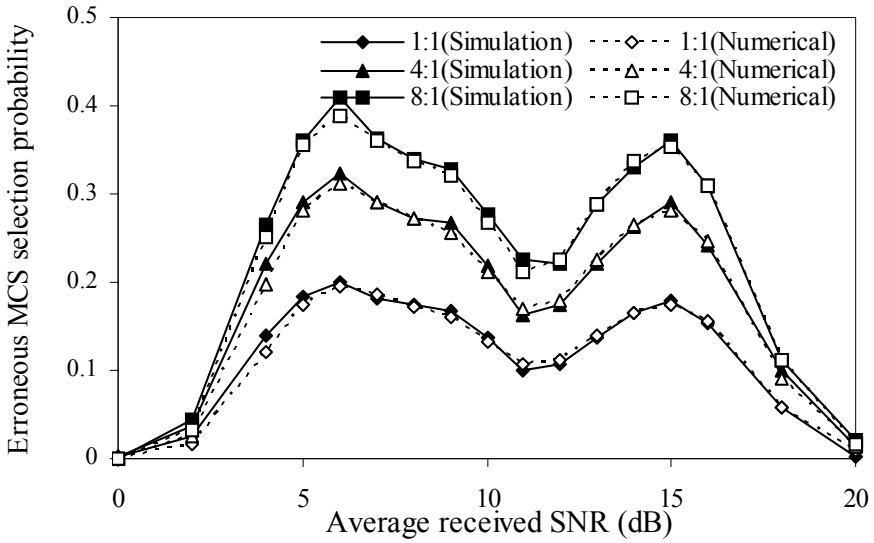

Fig. 3.10 Erroneous MCS selection probability in different TDD asymmetry

3.6.2 Total Downlink Throughput in Different TDD Asymmetry

Relative total throughput of different formats, evaluated by simulation only, is shown in Fig. 3.11. The total downlink throughput of a TDD frame consisting of N slots (uplink + downlink) with D downlink slots is calculated as: *Total downlink throughput = instantaneous throughput per slot * D/N.* Using the parameters from Table 3.1, the achievable maximum throughput should be larger than 100 Mbps when multicode ($C_{mux} > 1$) transmission is adopted as in [3.13]. However, since we focus only on relative throughput performance among different formats, only single-code transmission is used.

Throughput curves in each format are shown at two different maximum Doppler frequencies (f_d) 20 Hz and 40 Hz. Even though asymmetric slot allocations yield higher erroneous MCS selection probability, they still achieve higher relative total downlink throughput than the symmetric allocation. In fact, the 8:1 format has lower average throughput per slot than the 4:1 format; however the overall throughput in a TDD frame with 8:1 format is slightly higher. In other words, doubling the rate of asymmetry cannot be expected to double the total throughput. The 1:1 format yields similar throughput performances with maximum Doppler frequencies (f_d) of 20 Hz

and 40 Hz. The asymmetric formats, on the other hand, suffer significant throughput degradation when f_d = 40 Hz. For example at 12 dB, degradation about 0.5 Mbps can be seen with the 8:1 and 4:1 formats. This is because in 1:1 format has such low erroneous MCS selection probability that even the maximum probability with f_d = 40 Hz case is only 20 % and packet error does not occur frequently. The much higher erroneous MCS selection probabilities associated with the asymmetric formats cause more packet errors and thus the throughput degradation is significant at f_d = 40 Hz.

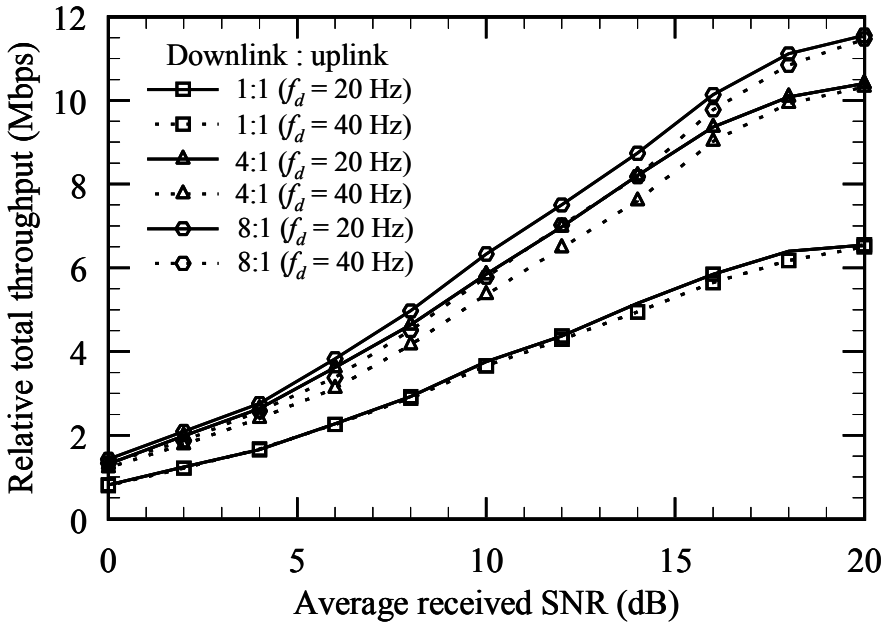

Fig. 3.11 Total downlink throughput in different TDD asymmetry

3.6.3 Average Delay in Different TDD Asymmetry

Average delay to receive error free packets in different TDD formats as a function of average received SNR is shown in Fig. 3.12; simulation results with f_d = 40 Hz. When packet error occurs, Hybrid ARQ requests retransmission and the time required to receive a valid packet increases. Delay is shown in units of time slots (each slot is 0.5 msec). Total delay time is defined as the time taken between packet transmission time and the time when ACK status of that packet is generated at the receiver. Average delay $\bar{D}$ is calculated as

$$\bar{D} = \frac{1}{N}\sum_{i} P(D_i) * D_i \tag{3.6}$$

where, D_i = delay time, $P(D_i)$ = occurrence of each delay time, i = delay index (integer multiple of slots) and N = number of packets.

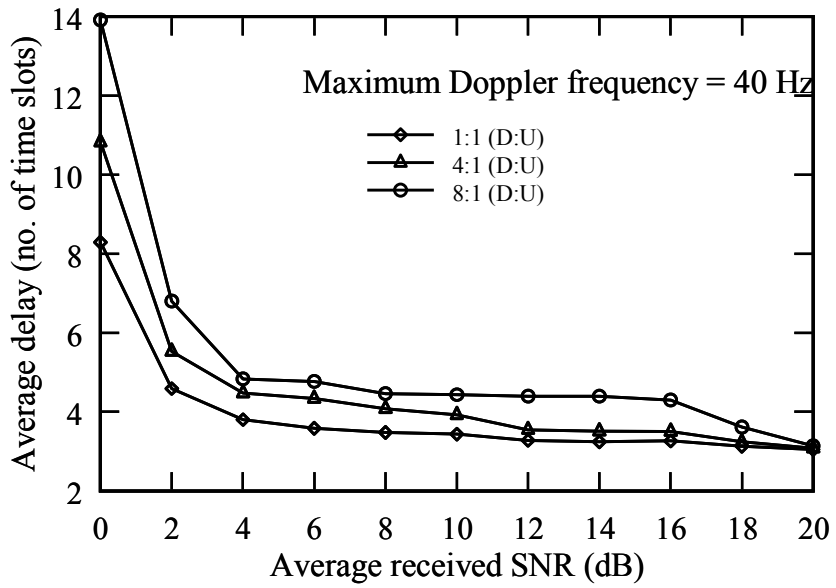

Fig. 3.12 Average delay performance in different TDD asymmetry

At very low SNR, the effect of HARQ control delay is significant since packet errors frequently occur at such SNR values even though erroneous MCS selection error is low. As discussed in Section 3.3, HARQ control delay increases with the number of continuous downlink slots. Average delay with the 4:1 format is 2 to 3 time slots and that of the 8:1 format is 4 to 6 time slots longer than that with the 1:1 format at SNR < 2 dB. At high SNR (>18 dB), all formats show the same delay performance since almost all packets are correctly received in all cases. Moreover, the minimum average delay time in all cases approaches three time slots, which is the minimum processing time assumed at the MS as discussed in Section 3.3. Since we consider only the single user case, there is no multiuser access interference (MAI). In reality, total average delay will increase with the number of users as a result of the higher packet error caused by the increased MAI.

3.6.4 Erroneous MCS Selection and Throughput Degradation with Doppler Frequency

Fig. 3.13 presents erroneous MCS selection probability as a function of f_d. The TDD plots show both numerical and simulation results. For reference, the numerical results of erroneous MCS selection probability in FDD are also included. To ensure a valid reference, we assumed that AMC control delay D_{AMC} in FDD, taking account feedback delay, is twice the minimum D_{AMC} in the symmetric TDD format. Average received SNR for all cases observed is 6 dB and f_d ranges from 10 to 200 Hz. In the asymmetric format cases 4:1 and 8:1, the erroneous MCS selection probability increases more rapidly with f_d than in the 1:1 format case. For example, with the 8:1 format, the selection error is approximately 43 % at f_d = 45 Hz while the 1:1 format shows the same error probability at about f_d =100 Hz. At high f_d values such as 200 Hz, the effect of downlink time slot duration is overwhelmed by that of f_d and SNR tracking capability is degraded in all cases regardless of the slot allocation formats. As a result, all slot allocation formats examined show high erroneous MCS selection probability at high f_d values. FDD with constant feedback delay shows higher erroneous MCS selection probability than any TDD format except 8:1. This is because, in TDD formats, some slots as shown in the example of Fig. 3.6 (a) have less AMC control delays than constant feedback delay of FDD. Better performance can be expected in either duplex, given that D_{AMC} is reduced.

At f_d = 200 Hz, erroneous MCS selection probability in all cases is seen to converge to 0.63~0.64.This can be explained as follows. In a time varying channel, channel coherence time (T_0) is defined as the time duration over which the channel's response to sinusoids yields a correlation between these sinusoids of at least 0.5. It follows that the relation between T_0 and f_d can be approximated as $T_0 = 0.424/f_d$ [3.16]. At f_d = 200 Hz, T_0 becomes approximately 2 msec. With the system parameters assumed in this paper, the minimum AMC control delay of 3 time slots (1.5 ms) plus packet transmission time becomes approximately T_0 for the channel in which f_d = 200Hz. Thus SNR tracking capability is dramatically degraded when $f_d \geq$ 200 Hz.

Suppose AMC employs only one threshold to switch two MCSs, and the averaged received SNR is near the threshold, erroneous MCS selection probability in fast varying channel will converge on 0.5 as SNR tracking capability degrades. However, for a system with two thresholds, i.e. three MCSs employed, that evenly divide the possible received SNR region in a very rapidly varying channel, for any MCS_k, $k = \{1, 2, 3\}$, the probability that the instantaneous received SNR will fall in any certain MCS region will be 1/3 and the probability of selecting the wrong MCS at any instant will be approximately 2/3. Without loss of generality, this analogy can be applied to explain why MCS false selection probability in all the cases shown in Fig. 3.13 approaches 0.63. Note that the width of the SNR region between two thresholds also governs the MCS false selection probability if the thresholds are not evenly spaced.

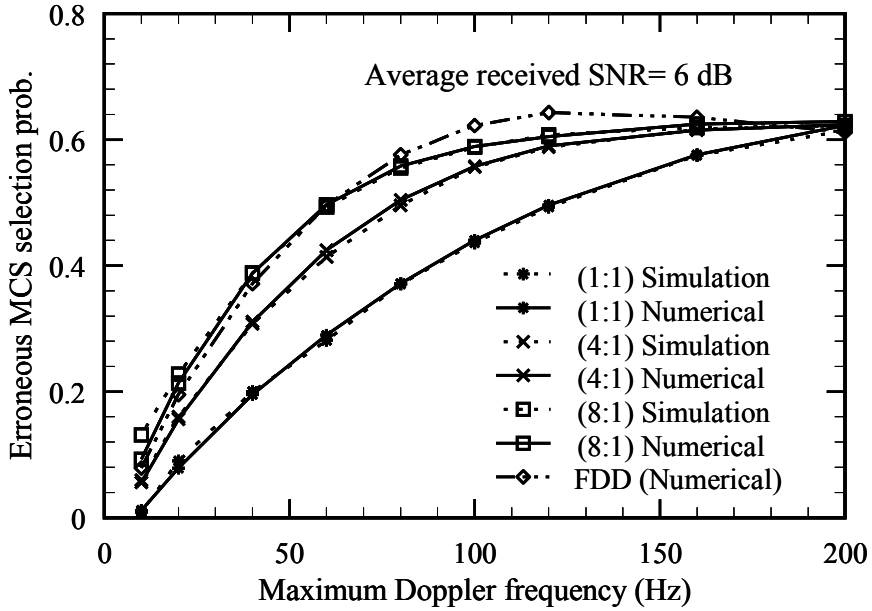

Fig. 3.13 Erroneous MCS selection probability as a function of maximum Doppler frequency

The immediate consequence of MCS selection error is instantaneous throughput (in each slot) degradation. Fig. 3.14 shows the simulated result of throughput degradation as a function of maximum Doppler; the averaged received SNR = 6 dB. The throughput in each asymmetric allocation format at each f_d is normalized by its

respective throughput at the lowest f_d (here 10 Hz) to better illustrate the degradation. The same is also done for the FDD case. Again, note that throughput here is average through per slot while that discussed in Section 3.6.2 is the total downlink throughput in a TDD frame with N downlink slots. It is seen that the throughput of the asymmetric formats degrades more rapidly at relatively low f_d values. For example, the throughput of the 8:1 suffers a degradation of about 12 % when f_d = 40 Hz while the 1:1 format shows the same degradation when f_d = 100 Hz.

It can be seen that throughput degradation in Fig. 3.14 corresponds to the erroneous MCS selection probability in Fig. 3.13. From Fig. 3.14, the differences in throughput degradation among the three TDD slot formats can be seen at f_d values around 50~80 Hz where the differences in erroneous MCS selection probability of all formats are significant. At higher f_d values (150 Hz to 200 Hz), as erroneous MCS selection probability is high in all cases, the throughput degradations are almost the same; the throughput degradation is about 20 % at f_d = 200 Hz. This can be explained as follows. Up to f_d = 200 Hz, the MS receiver can compensate the channel fading since the channel condition is essentially constant within one slot (packet). For instance, to achieve the constant average block error rate (BLER) of 10^{-1} with each MCS, the required average received SNR is almost constant until maximum Doppler frequency of about 200 Hz [3.13]. The required SNR increases dramatically when f_d exceeds 300 Hz because the channel condition changes within the packet due to the fast fading leading to imperfect channel compensation at the MS side. Therefore, we can conclude that the throughput degradation shown in Fig. 3.14 is due to erroneous MCS selection at the BS side. Since erroneous MCS selection probabilities in all cases approach to the same saturation point when $f_d \approx 200$ Hz, their throughput degradation converges to 20 %. A further degradation in throughput due to channel compensation errors at the MS side can be expected when f_d becomes large enough so that the channel inside packet (slot) is no longer close to static.

TDD formats such as 4:1 and 1:1 show less throughput degradation than FDD since they have lower erroneous MCS selection probability. Therefore, we can see

that even though asymmetric TDD frame format causes different AMC control delays that cause different probability of MCS false selection in each format, its throughput performance shows satisfactory result compared to that of reference FDD so long as asymmetry in TDD is not extreme.

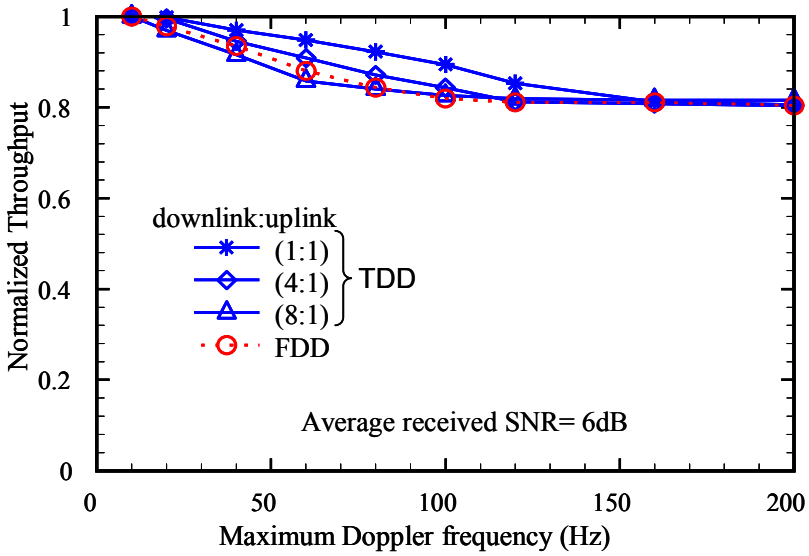

Fig. 3.14 Normalized throughput degradation as a function of Doppler frequency

3.6.5 Average Delay as a Function of Doppler frequency

The average delay to receive error free packets as a function of maximum Doppler frequency is presented in Fig. 3.15. Only simulation results were used with averaged received SNR = 6 dB. The calculations of average delay and delay units are the same as those mentioned in previous section. At low f_d values, erroneous packet reception rarely occurs in all formats due to the low erroneous MCS selection probability and so the delay performance differences among the formats are small.

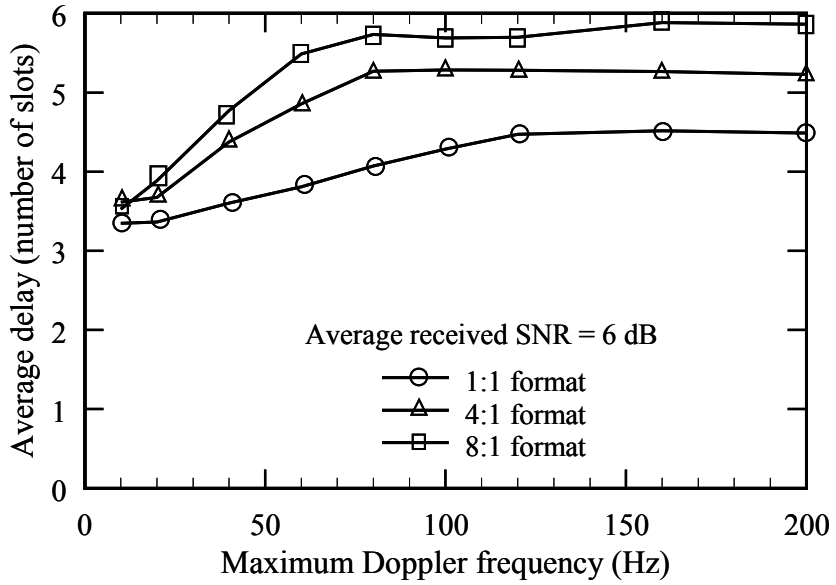

Fig.3.15 Average delay with different TDD asymmetry as a function of Doppler frequency

As f_d increases, the delay of all formats increases due to the increase in erroneous MCS selection probability because selection error causes erroneous packet reception and retransmission. However, the average delay increases more rapidly in the formats with higher asymmetry as maximum Doppler frequency increases, corresponding to their higher erroneous MCS selection probabilities. Finally, at very high f_d values, erroneous MCS selection probability is high and the differences in average delay among the three formats are mostly due to their HARQ control delays, which increases with the increased number of continuous downlink slots as discussed in Section 3.3.

3.7 *Conclusion*

The throughput and delay performance of TDD systems influenced by different control delay components and different asymmetric slot allocations were evaluated. AMC control delay and HARQ control delay are dependent on the TDD time slot structure used. This study has presented an analytical approach to calculate erroneous MCS selection probability. Throughput and delay performance of a TDD system that

uses AMC and HARQ can be explained with regard to erroneous MCS selection probability. Average delay to receive a valid packet increases with the number of continuous downlink slots due to the increase in HARQ control delay. Instantaneous throughputs of asymmetric formats in TDD degrade more rapidly as the maximum Doppler frequency increases than that of symmetric allocation. However, the throughput results show that TDD systems with open loop channel estimation for AMC and a moderate degree of asymmetry can give good throughput performance compared to their FDD counterparts.

References

[3.1] Prabhakar Chitrapu, *Wideband TDD–WCDMA for the unpaired spectrum*, John Wiley & Sons Ltd, 2004.

[3.2] R. Esmailzadeh and M. Nakagawa, *TDD-CDMA for wireless communications*, Artech House, 2003.

[3.3] Mobile WiMAX Part I: A technical overview and performance evaluation, WiMAX Forum, Apr. 2006.

[3.4] S. Parkvall and D. Astely, "The evolution of LTE towards IMT-advanced," Journal of Commun., vol. 4, no. 3, pp. 146-154, Apr. 2009.

[3.5] J.M.C. Brito and I.S. Bonatti, "Thresholds levels for adaptive modulation with channel coding in the wireless ATM networks," 5th IEEE Int'l Conf. on High Speed Networks and Multimedia Communications (HSNMC) , pp. 187-191, July 2002.

[3.6] O. Kato, K. Miya, K. Homma, T. Kitade, M. Hayashi, and M. Watanabe, "Experimental performance results of coherent wideband DS-CDMA with TDD scheme," IEICE Trans. Commun., vol.E81-B, no.7, pp.1337-1344, July 1998.

[3.7] K. Miya, O. Kato, K. Homma, T. Kitade, M. Hayashi, and T. Ue, "Wideband CDMA systems in TDD-mode operation for IMT-2000," IEICE Trans. Commun., vol.E81-B, no.7, pp.1317-1316, July 1998.

[3.8] D.G. Jeong and M.J. Kim, "Effects of channel estimation error in MC-CDMA/TDD systems," Proc. 51st IEEE VTC 2000, vol.3, pp.1773-1777, May 2000.

[3.9] 3GPP, 3G TR25.858, "Physical layer aspects of UTRA high speed downlink packet access".

[3.10] N. Miki, H. Atarashi, K. Higuchi, S. Abeta, and M. Sawahashi, "Experimental evaluation on effect of hybrid ARQ with packet combining in forward link for VSF-OFCDM broadband wireless access," Proc. 14th IEEE PIMRC 2003, vol.1, pp. 360-365, Sept. 2003.

[3.11] M. Dottling, J. Michel, and B. Raaf, "Hybrid ARQ and adaptive modulation and coding schemes for high speed downlink packet access," Proc. 13th IEEE PIMRC, vol.3, pp. 1073-1077, Sept. 2002.

[3.12] N. Miki, H. Atarashi, S. Abeta, and M. Sawahashi, "Comparison of throughput employing Hybrid ARQ packet combining in forward link of OFCDM broadband packet wireless access," IEICE Trans. commun., vol.E88-B, no.2, pp.594-603, Feb. 2005.

[3.13] Y. Kishiyama, N. Maeda, K. Higuchi, H. Atarashi, and M. Sawahashi, "Experiments on throughput performance above 100-Mbps in forward link for

VSF-OFCDM broadband wireless access," 58th IEEE VTC 2003-fall, vol.3, pp.1863-1868, Oct. 2003.

[3.14] H. Atarashi, N. Maeda, S. Abeta, and M. Sawahashi, "Broadband packet wireless access based on VSF-OFCDM and MC/DS-CDMA," Proc.13th IEEE PIMRC 2002, pp.992-997, Sept. 2002.

[3.15] C.D.Iskander and P.T.Mathiopoulos, "Analytical envelope correlation and spectrum of maximal-ratio combined fading signals," IEEE Trans. Vehicular Tech., vol.54, no.1, pp.399-404, Jan.2005.

[3.16] Greenwood, D. and L. Hanzo, *Characterization of mobile radio channels*, Mobile Radio Communications, Pentech Press, London, 1994.

Chapter 4

A Novel Cooperative ARQ with Distributed Relay Selection for Multi-hop Relay Systems

4.1 *Background*

It has been envisioned that multi-hop relaying mode will become an integral part in the future wireless communications. As discussed in the previous section, the primary goal of relaying mode is extension of communication coverage by reducing path loss and shadowing effect [4.1]. Further, relay systems can mitigate small scale fading effectively by means of diversity gain through distributed relays transmitting the same information in a cooperative manner. The simplest relay cooperation scheme that achieves a full diversity is the repetition-based cooperation [4.2] in which each relay transmits in its orthogonal sub-channel, in time or frequency. The achievable spectral efficiency in repetition based cooperation is $1/(M+1)$, given M relays are cooperating. Distributed space-time code (STC) relay cooperation can improve spectral efficiency to 0.5 by allowing simultaneous transmission of relays using orthogonal space-time codes. However, distributed STC cannot guarantee full rate and full diversity for an arbitrary number of cooperating relays due to limitation in STC design issue [4.2]. In addition, STC demands distributed relays to have symbol level synchronization to coherently combine symbols from the cooperating relays. Distributed transmit beamforming [4.3][4.4] is another option to allow simultaneous transmission of multiple relays for the cooperative diversity. With distributed transmit beamforming, the transmit nodes at different locations must synchronize in frequency and phase of transmit carrier [4.3]. Hence, synchronization

is a key challenging issue for both distributed STC and distributed transmit beamforming particularly when the cooperating nodes are mobile.

Recently, the term cooperative automatic repeat query (Cooperative ARQ) [4.5][4.6] has been widely used in relay communications. Cooperative ARQ is an ARQ scheme applied to multihop relay networks to exploit cooperative diversity. Reference [4.5] presents STC based cooperative hybrid ARQ protocols. [4.5] assumes a topology in which source and destination can directly communicate. Firstly, source broadcasts its signal to the destination and the relays. If the destination fails to receive the source transmission correctly, the relays and the source retransmit the signal through STC cooperation. STC cooperated retransmission is carried out until the destination receives the signal correctly, with more relays cooperating after each retransmission as they become available to cooperate as a result of repeatedly decoding the retransmitted signal. However, as discussed earlier, STC code design issue imposes restriction on the number of cooperation relays so as to achieve full diversity while maintaining a full rate.

In [4.6], a selection based cooperative ARQ is presented assuming a simple three node topology, including source, relay and destination. Firstly source transmits to the destination and the relay, and then selection is carried out between the source and the relay when the initial transmission fails. However, detail procedure of selection has not been addressed. In [4.7], analytical expressions for outage probability and capacity have been derived for selective relaying and cooperative diversity assuming a two-hop multi-relay system with no direct link between source and destination. Similar analysis can also be found in [4.8]. Despite its ability to achieve full diversity order, centralized relay selection degrades spectral efficiency due to the requirement of time division orthogonal pilot channel for each relay. Using pilot signals transmitted from each relay, destination may select the best relay and notify of the selection back to the relays. In [4.9], transmit time-offset based distributed relay selection technique is presented. In that technique, none of the nodes takes leading role to decide the best relay but each relay assigns itself a transmit time-

offset, i.e. a timer, which is inversely proportional to the instantaneous channel quality. Based on transmit time-offset values calculated from channel quality, relays compete for transmission. During contention period, each relay counts down the timer till it elapses to zero, at which point relay transmission starts. Obviously, the relay with the best channel quality will have the smallest timer value and thus, it will transmit first among all the relays. As it transmits, the other relays hear the transmission and stop competition for transmission. As a result, selection effect is achieved without requiring for the destination to collect the channel information of each relay to decide the best relay.

This study considers a two-hop relay system, as in [4.7], which consists of N relays. Fig. 4.1 depicts the assumed system model. The source is located beyond the coverage of the destination. Communication between the source and the relay is established through the relays. The relays may be designated ones that have access point functionality or mobile terminals. In every relay transmission, we employ a distributed relay selection technique similar to that of [4.9] to achieve full diversity order. The source uses one time slot to broadcast the signal to the relays and the best relay uses one time slot to forward the signal to the destination. Thus, at least two time slots are used to complete communication link between source and the destination. If retransmission is needed, relay uses one more slot to retransmit; in that case, the number of time slots used becomes three slots. Assuming that the relay system under consideration supports real time traffic with a strict delay constraint, the number of retransmissions is limited to one. The relays are not necessarily to be located close to the source. The relays employ decode and forward (DF) to avoid noise amplification and error propagation associated with amplify and forward (AF). AF is not appropriate for the assumed relay topology since the relays cannot ensure if they have received the signal correctly. AF may be advantageous if source-relay channel is good.

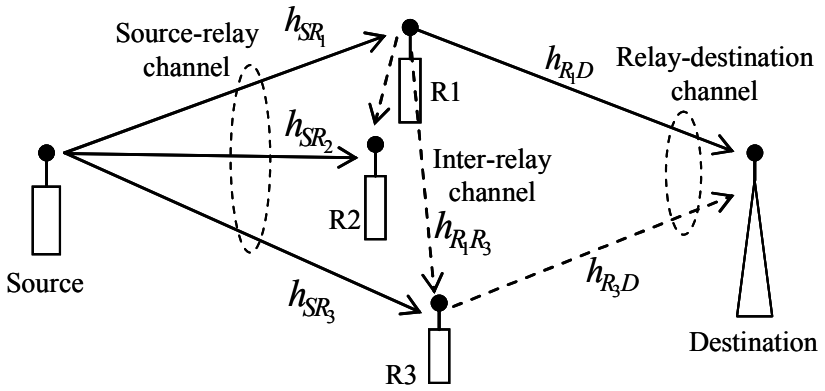

Fig.4.1 Two-hop relay system model

Although relay selection can achieve diversity order equal to the number of cooperating relays, the actual number of relays that can participate in the selection depends on source-relay channels. Due to instantaneous deep fading in the source-relay channels, some relays may not successfully receive the signal transmitted by the source at some instances. It causes a decrease in achievable selection diversity. While a relay has poor instantaneous source-relay channel (h_{SR}), its relay-destination channel (h_{RD}) may be good because the channel in one side is independent from that in the other side. If we can make use of such relay to transmit to the destination, performance improvement can be expected. Thus, we consider exploiting the broadcast nature of wireless channel for the erroneous relays to listen to the transmission of other relay. Upon receiving the signal from the source, the relays whose cyclic redundancy check (CRC) results show correct reception contend for transmission in the distributed selection. As the best relay transmits, the erroneous relays listen to the signal to combine with their erroneous signals and decode again; we refer to such listening other relay's transmission and exploiting to achieve diversity as inter-relay opportunistic listening (*OL*). Thanks to the spatial diversity obtained by *OL*, the erroneous relays may become error-free and available to be selected for subsequent retransmission, if requested. As a result, higher selection diversity order can be expected in subsequent retransmission.

However, a new selection protocol for the distributed relay selection is needed as the conventional selection protocol [4.9] cannot take full advantage on the increased relay availability offered by *OL*. In the conventional protocol, each relay determines its instantaneous channel quality by taking the minimum value between source-relay and relay-destination channel gains. The transmit time-offset is calculated using that channel quality. In our system, there may be instances that a relay has the poorest source-relay channel while its relay-destination channel is the best. By taking the minimum between the source-relay and relay-destination channel gains as the channel quality in the conventional protocol, the source-relay channel gain is used in computing transmit time-offset. Due to the reciprocal relationship with the channel quality, its transmit time-offset will be the largest among the relays. As a result, that relay will never have chance to transmit even if it is error-free owing to the *OL*.

In our cooperative ARQ, influence of the source-relay channels over relay availability in selection decreases due to exploiting inter-relay channels. Hence, this study proposes a new selection protocol suitable for our relay system by taking relay-destination channel only into account to compute transmit time-offset. We make sure that each relay has updated knowledge on its relay-destination channel using common pilot signal broadcasted by the destination periodically within the channel coherent time. Having calculated their transmit time-offsets based on their channel qualities in advanced, the relays that become error-free after *OL* will also automatically participate in the distributed relay selection for retransmission. Our proposed selection protocol can take full advantage on the increased selection diversity offered by *OL*. The contribution of this study has two key points. First, a new cooperative ARQ that employs a distributed relay selection and *OL* is proposed. Secondly, a new selection protocol is proposed for the distributed relay selection of our cooperative ARQ. Theoretical error rate performance expressions for the proposed system are derived. Performance of the proposed system is verified in terms of packet error rate (PER) by both simulations and theoretical calculations.

Section 4.2 describes a description of the assumed relay system and our cooperative ARQ. Section 4.3 describes the relay selection protocol for the proposed system. Then, theoretical error rate performance analysis of the system is provided in Section 4.4. Section 4.5 presents the numerical results. Section 4.6 discusses the possible areas of systems where the proposed cooperative ARQ is applicable. Finally Section 4.7 draws conclusion.

4.2 *System Description*

The operational procedure of the relay system under consideration is depicted in Fig. 4.2 using three steps. Firstly, as the source is transmitting, the relays listen to the source and prepare to transmit in the next slot. Since relays' reception and transmission are taken place in time division, the same frequency band is used. In the assumed system, relay selection is incorporated in every relay transmission to achieve diversity order equal to the number of available relays at each time. The distributed relay selection employed is similar to that of [4.9] in using transmit time-offset. Firstly, let use define a quantity representing channel quality in any of source-relay or relay-destination or source-relay-destination channel of each relay as a_i. Assuming each relay R_i, $i \in \{1,...,N\}$, has knowledge on its channel quality a_i, the transmit time-offset is calculated as $\tau_i = \frac{\lambda}{a_i}$, where λ is a constant having unit of time and a_i is a scalar. The best relay is the one which has $\max\{a_i\}$, i.e. $\min\{\tau_i\}$, thus, it will transmit first among all the relays. If λ is small, relay selection takes small delay; however, the system becomes more sensitive to the relay synchronization errors including inter-relay propagation delays. In that case, probability of relay transmission collision increases. If λ is large, the probability of collision reduces while distributed relay selection takes longer time to decide the best relay. Therefore, the speed of relay selection and transmission collision is a tradeoff in determining λ. Interested readers are referred to [4.9] for the analysis of collision probability as a function of λ. For simplicity, it is assumed that only one packet occupies a transmission slot. The duration of time slot T_{slot} assigned to the relays is larger than the data packet duration

T_{pkt} to provide contention time in the distributed relay selection. The maximum allowable time-offset (τ_{max}) will then be $\tau_{max} \leq T_{slot} - T_{pkt}$.

The transmission flow of the assumed system is as following. In the 1st slot, the source broadcasts signal to the relays. Upon reception from the source, each relay decodes the signal and checks if the received signal has errors using CRC. If none of the relays transmits to the destination till the time elapsed from the beginning of the 2nd slot is larger than τ_{max}, the source retransmits the same packet. Note that ACK or NACK is not necessary in source-relay channel since the source can determine if any relay receives correctly as it detects transmission of a relay during contention period. Suppose N_1 relays, such that $N_1 \leq N$, correctly receive the signal from the source. Without loss of generality, these N_1 relays are indexed starting from one as $i \in \{1,...,N_1\}$. N_1 relays compete for the transmission by counting down their transmit time-offsets from the beginning of the 2nd time slot. The index of the best relay for the initial relay transmission is

$$k = \arg\max_i \{a_i\} \Leftrightarrow \tau_k = \min\{\tau_i\}, i \in \{1,...,N_1\} \quad (4.1)$$

As relay R_k transmits, $N–N_1$ erroneous relays opportunistically listen to the transmission to combine the transmit packet of R_k with their erroneous packets and decode again. Simple Chase combining (CC) [4.10] is employed in combining the packets. Forward error correction (FEC) is not considered in this study. Thanks to the spatial diversity offered by *OL*, some of $N–N_1$ erroneous relays may successfully decode their Chase-combined packets. Then the number of relays whose CRC results show correct reception may increase to N_2, where $N_1 \leq N_2 \leq N$, at the end of the 2nd slot. If the destination successfully receives R_k's transmission, the relaying completes in the 2nd slot. It is assumed that ARQ feedback channel is assigned after data transmission channel as shown in Fig. 4.2. If the destination fails to correctly receive the initial relay transmission, retransmission is requested at the relays by notifying via feedback channel. For retransmission in the 3rd slot, N_2 relays are available to compete for the retransmission. As can be seen, relay availability for retransmission

increases thanks to *OL*. If simple distributed selection scheme without *OL* is used, the selection diversity order will be the same (N_1) in both initial transmission and retransmission. It should be noted that, unlike existing standard such as IEEE 802.11 [4.11] where only ACK is used to notify correct reception to the transmitter, ARQ feedback in this study uses both ACK and NACK. This is because, in our system, there may be events that ACK packet cannot reach successfully, i.e. packet loss, to some relays due to instantaneous deep fading. If ACK only is used, the relays that do not receive ACK may assume that the destination fails to receive correctly and attempt retransmission. To avoid such situation, we use both ACK and NACK. The relays that receive ACK/NACK can be regarded as having usable channel qualities and they will contend for retransmission. The relays that do not receive any of ACK and NACK are convinced that their instantaneous channel is too poor to transmit; and they will stay idle without doing attempts to retransmit.

4.3 *Relay Selection Protocol for the Proposed System*

In this section, the difference between the conventional selection protocol and the proposed one for the assumed cooperative ARQ scheme is described. According to the selection protocol employed the distributed relay selection of [4.9], the end-to-end channel quality of each relay R_i is determined from the source-relay h_{SR_i} and relay-destination h_{R_iD} channels as

$$a_i = \min\{\left|h_{SR_i}\right|^2, \left|h_{R_iD}\right|^2\} \tag{4.2}$$

Given the a_i of each relay from (4.2), the best relay for initial relay transmission is given by (4.1). The drawback of the conventional selection protocol in our cooperative ARQ is explained using Fig. 4.2. Fig. 4.2 includes a snapshot example showing instantaneous channel ranks of each relay and their CRC results, OK or NG. As seen in Fig. 4.2, the channel quality rank in source-relay channel is $\left|h_{SR_2}\right| > \left|h_{SR_1}\right| > \left|h_{SR_3}\right|$ and that in relay-destination channel is $\left|h_{SR_3}\right| > \left|h_{SR_2}\right| > \left|h_{SR_1}\right|$. R_3 has the poorest source-relay channel and its received signal from the source has errors

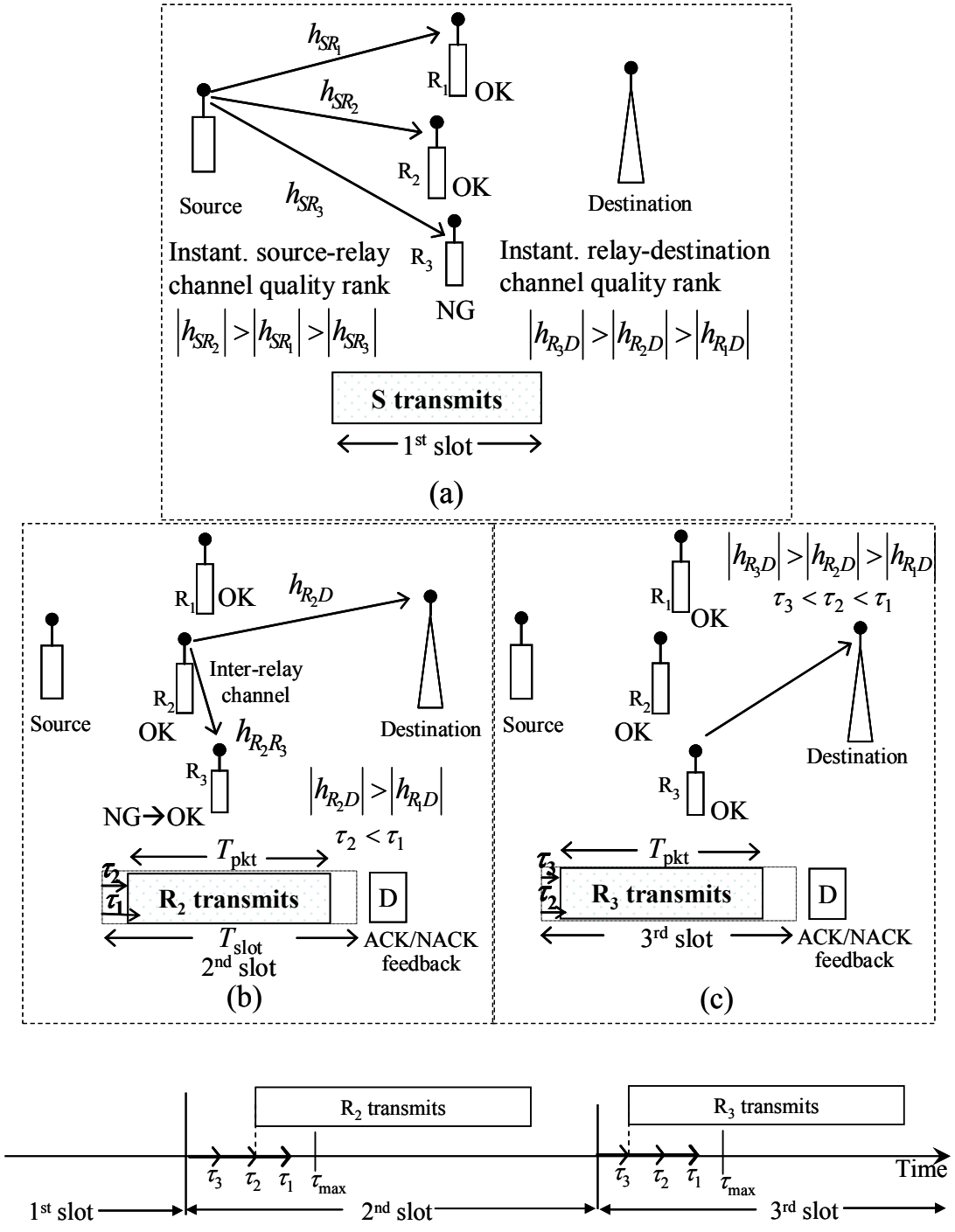

Fig. 4.2 Operational procedure of the proposed cooperative ARQ and access timeline

(CRC: *NG*) while its relay-destination channel is the best, with $\left|h_{SR_3}\right| < \left|h_{R_3D}\right|$. R_1 and R_2 successfully receive the signal from the source (CRC: OKs) and they compete for the transmission in the 2nd slot. If $a_2 > a_1$, R_2 will transmit first since $\tau_2 < \tau_1$ according to (4.1). As R_2 transmits, R_1 stops attempt to transmit whereas R_3 listens to the R_2's transmission to combine with its erroneous received packet and decode again. At this time, R_3 successfully decodes its signal (CRC: NG→OK) thanks to the spatial diversity resulted from exploiting R_2's transmission. Now R_3 becomes ready to participate in the distributed selection in the 3rd slot if retransmission is requested by the destination. However, since $\min\{\left|h_{SR_3}\right|^2, \left|h_{R_3D}\right|^2\}$ is taken as end-to-end channel quality according to the conventional selection protocol, τ_3 will be the largest. As a result, R_3 does not have chance to transmit although it has the best relay-destination channel condition. It clearly shows that the conventional selection protocol cannot take full advantage on increased relay availability in our cooperative ARQ.

In the proposed cooperative ARQ, as a result of exploiting inter-relay channels, relay availability dependency over the source-relay channels decreases in subsequent retransmission. Thus, in our selection protocol, only relay-destination channel is taken into account to compute transmit time-offset. In the proposed selection protocol, for the transmission in the 2nd slot, each relay R_i, $i \in \{1,...,N_1\}$, determines its channel quality as

$$a_i = \left|h_{R_iD}\right|^2, i \in \{1,..., N_1\}. \tag{4.3}$$

With a_i from (4.3), R_i determines τ_i and the index of the best relay is given by (4.1). After *OL* to the transmission of the best relay (R_k), the number of relays whose CRC results show correct reception becomes N_2. Again, without loss of generality, N_2–N_1 newly available relays are indexed starting from N_1+1 as $\{N_1+1,..., N_2\}$. In a slowly varying channel environment, the channel conditions in initial transmission and retransmission slots may be almost the same. Hence, the channel rank of the relays may also be the same in initial relay transmission and retransmission times.

Thus, only R_k and the N_2-N_1 newly available relays need to compete in the distributed relay selection when retransmission is requested. For retransmission, each relay R_j, $j \in \{k, N_1+1, ..., N_2\}$, determines its channel quality as in (4.3).Then, the index of the best relay for retransmission is given by

$$l = \arg\max_j \{a_j\} \Leftrightarrow \tau_l = \min\{\tau_j\}, j \in \{k, N_1+1, ..., N_2\}. \quad (4.4)$$

From the example in Fig. 4.2, R_3 becomes error-free thanks to *OL* and competes with R_2, which is the best relay in initial transmission, for the transmission in the 3rd slot. Since R_3 has better relay-destination channel than that of R_2, R_3 will transmit in the 3rd slot according to (4.4). By Chase-combining of the initial packet from R_2 and the retransmitted packet from R_3, the destination achieves diversity gain, which otherwise may not be available with conventional selection protocol.

4.3.1 Overheads in the Proposed System

In a relay system that uses distributed relay selection, necessary channel information can be basically categorized into two: 1) instantaneous channel information for coherent detection of the received signals, 2) the periodic channel gain information for distributed relay selection. The instantaneous channel information for coherent detection can be estimated from the pilot symbols or preambles attached to the data packet. For the channel information used in relay selection, the conventional selection protocol of [4.9] uses periodic control handshaking packets used in medium access control (MAC) protocols. It is assumed in [4.9] that the each relay extracts information on h_{SR_i} and h_{R_iD} from ready-to-send (RTS) packet from the source and clear-to-send (CTS) packet from the destination respectively.

On the other hand, our proposed selection protocol uses only relay-destination channel information. Owing to channel reciprocity in time-division-duplex (TDD), each relay can estimate h_{R_iD} from the pilots broadcasted by the destination at a regular interval smaller than the channel coherent time. The general format of time slot and

packet structure assumed is shown in Fig. 4.3. In a practical system, multiple packets may be transmitted in a slot. However, in our evaluations, we simply assume that only one packet is transmitted in a time slot. If we assume τ_{max} =10 % of T_{slot}, a packet will have duration T_{pkt} = 0.9 T_{slot}. Again, assuming a packet has 100 data symbols (100·m bits, where m = 1, 2 4 for BPSK, QPSK and 16QAM, respectively) and 10 % preambles with respect to data, symbol duration T_s will have a relationship with maximum time-offset as $\tau_{max} \approx 12 T_s$.

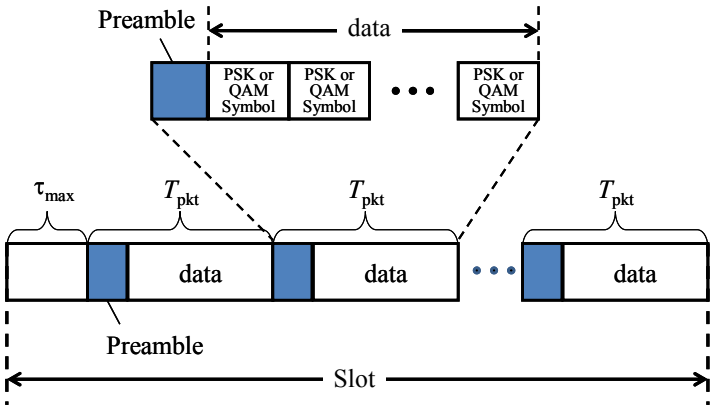

Fig. 4.3 Time slot and packet structure

4.4 *Error Rate Analysis*

In this section, the error-rate analysis of the system under consideration is presented on case by case basis. For the sake of simplicity, the theoretical analysis is limited to BPSK data modulation. With BPSK, only single threshold needs to be considered in deriving the error probability of initial transmission with ARQ. With QAM modulations, multiple thresholds must be taken into account in derivation of error probability. The simulated results with QPSK and QAM data modulations are also provided.

Firstly, the notations are defined. We denote the source-relay channels, relay-destination channels, and inter-relay channels as h_{SR_i}, h_{R_iD}, and $h_{R_iR_j}$ respectively; the corresponding instantaneous *SNR*s as $\gamma_{uv} = |h_{uv}|^2 \cdot (E_S/N_0)$, the averaged *SNR*s

as $\bar{\gamma}_{uv} = E[|h_{uv}|^2] \cdot (E_S / N_0)$, respectively with $u \in \{S, R_i\}$, $v \in \{R_i, D\}$, $i=\{1,\ldots,N\}$ and $E[.]$ denote the ensemble average. E_S/N_0 is the signal energy per bit-to-additive white Gaussian noise (AWGN) spectrum density ratio (SNR). In this study, we focus only on the cooperative diversity rather than the diversities from frequency selective fading and multiple-input-multiple-output (MIMO) channels. Thus, we simply assume flat fading and single omnidirectional antenna at each node. Moreover, we do not stick to a specific standard, air interface wireless access scheme and parameters in this study since the proposed cooperative ARQ is generally applicable to any standard and wireless access scheme. Also, it is assumed in the analysis that the channels do not change during initial transmission and retransmission times. The number of bits N_b transmitted by a packet is given by $N_b = 100 \cdot m$ bits, where m represents modulation scheme.

4.4.1 Element Error Rates

Having received the signal from the source in the 1st slot, the possible CRC results at relays can be classified into three cases.

Case 1) All relays correctly receive the signal.

Case 2) None of the relays correctly receive the signal.

Case 3) Some relays correctly receive the signal while some do not.

Depending on each of above three cases, the achievable cooperative diversity is different. For instance, in addition to the inherent selection diversity, some SNR improvement is achieved at retransmission time. The amount of SNR improvement also depends on the selected relay in retransmission. Thus, overall error rate performance is a function of cooperative diversities achievable in each case of relay errors. We characterize the error rates with different cooperative diversities as element error rates of the system. In the following, as preliminary to the derivation of expressions for end-to-end error performance in each case, we first give the expressions for element error rates.

(a) Error Probability at Each Relay

After receiving from the source, the average bit error rate (BER) at each R_i, assuming BPSK modulation in a flat Rayleigh fading channel, is given by [4.12]

$$P_{b,1}\left(\overline{\gamma}_{SR_i}\right) = \int_0^{\infty} \frac{1}{2} erfc\left(\sqrt{\gamma_{SR_i}}\right) f_{\gamma_{SR_i}}\left(\gamma_{SR_i}\right) d\gamma_{SR_i} . \tag{4.5}$$

where $f_\gamma(\gamma)$ denotes the chi-square distributed probability density function (PDF) of received SNR and *erfc*(.) is the complementary error function. Assuming a block fading, channel is static inside a packet allowing PER at each relay to be expressed as

$$P_{p,1}(\overline{\gamma}_{SR_i}) = 1-(1-P_{b,1}(\overline{\gamma}_{SR_i}))^{N_b} . \tag{4.6}$$

(b) N-branch Selection Diversity

If all N relays successfully receive the signal from the source, the selected relay transmits to the destination, achieving N-branch selection diversity. In [4.15], average bit error probability for N-branch selection diversity is described for a Nakagami-m distributed fading channel. Rayleigh distributed fading can be achieved from Nakagami fading by setting the fading figure m as one. Hence, average BER of selection diversity can be described,

$$P_{b,SEL} = \sum_{i=1}^{N} \int_0^{\infty} \tfrac{1}{2} erfc(\gamma_i) f_{\gamma_i}(\gamma_i) \prod_{j=1, j\neq i}^{N} F_{\gamma_j}(\gamma_i) d(\gamma_i) . \tag{4.7}$$

From (4.7), $F_{\gamma_{R_jD}}\left(\gamma_{R_iD}\right)$ is the probability that j^{th} relay's relay-destination channel SNR is lower than that of i^{th} relay and is deduced as

$$F_{\gamma_{R_jD}}\left(\gamma_{R_iD}\right) = \int_0^{\gamma_{R_iD}} f_{\gamma_{R_jD}}(\gamma_{R_jD}) d\gamma_{R_jD} = 1-\exp\left(-\gamma_{R_iD}/\overline{\gamma}_{R_jD}\right) \tag{4.8}$$

where

$$f_\gamma(\gamma) = \tfrac{1}{\overline{\gamma}} \exp(\tfrac{-\gamma}{\overline{\gamma}}) . \tag{4.9}$$

Following Eq. (4.7), the average PER at the destination with *N*-branch selection diversity in Rayleigh fading (m = 1) can be expressed as

$$P_{p,\mathrm{SEL}} = \sum_{i=1}^{N} \int_{0}^{\infty} (1-(1-P_{b,1}(\gamma_{R_iD}))^{N_b} f_{\gamma_{R_iD}}\left(\gamma_{R_iD}\right) \prod_{j=1, j\neq i}^{N} F_{\gamma_{R_jD}}(\gamma_{R_iD}) d\gamma_{R_iD} . \qquad (4.10)$$

(c) Error Probability with ARQ at Each Relay

Since relay system needs to decide maximum allowable contention time $\tau_{\max}$ in advance before forming cooperation group with the relays, $\tau_{\max}$ can be known to each relay as well as source. When none of the relays successfully receives the signal, the source retransmits the same signal when the elapsed time reaches $\tau_{\max}$ in the 2nd slot. In this case, the error probability with ARQ at each relay is the error probability at retransmission conditioned on that of initial transmission. With BPSK data modulation, the probability that a bit error occurs during initial transmission time is given by

$$\mathrm{Pr}_e\left(h_{SR_i}\right) = erfc\left(\left|\mathrm{Re}(h_{SR_i})\right| \Big/ \sqrt{2\sigma^2}\right) \qquad (4.11)$$

where $2\sigma^2$ is the variance of the noise. In terms of packet error, the error probability in the initial transmission can be expressed as,

$$\mathrm{Pr}_p(h_{SR_i}) = 1-\left(1-\mathrm{Pr}_e(h_{SR_i})\right)^{N_b} \qquad (4.12)$$

Assuming a slow channel, the channel is invariant during retransmission time resulting in the SNR of the Chase-combined received signal to be twice (3dB improvement) as that of the initial received signal. Then, the average PER with ARQ at each relay is the packet error probability with $\mathrm{SNR} = 2\gamma_{\mathrm{SR_i}}$ at the retransmission time conditioned on error probability in initial transmission $\mathrm{Pr}_p(h_{SR_i})$ as,

$$P_{p,\mathrm{ARQ}_{SR_i}} = \int_{0}^{\infty} \left(1-\left\{1-\left(\mathrm{Pr}_p(h_{SR_i})\right) P_{b,1}(2\gamma_{SR_i})\right\}^{N_b}\right) f_{\gamma_{SR_i}}\left(\gamma_{SR_i}\right) d\gamma_{SR_i} \qquad (4.13)$$

Similarly, if the same relay transmits to the destination in both initial transmission and retransmission, the PER at the destination, denoted as $P_{p,\mathrm{ARQ}_{R_iD}}$, is also given by (4.13) by substituting the corresponding h_{R_iD} and γ_{R_iD}.

(d) Error Probability with Selection and ARQ

If all *N* relays successfully receive the signal from the source in the 1st slot, the selected relay transmits to the destination. When the destination fails to receive the initial transmission correctly, the same relay retransmits since the channel quality rank of the relays does not change. Thus, in addition to the selection diversity, 3 dB SNR improvement is achieved at retransmission time. Following the *N*-branch selection diversity in (4.10) and ARQ in (4.13), the average PER at the destination can be deduced as

$$P_{p,\text{SEL-ARQ}}=\sum_{i=1}^{N}\int_0^{\infty}\left(1-\left\{1-\left(\Pr_p(h_{R_iD})\right)P_{b,1}(2\gamma_{R_iD})\right\}^{N_b}\right)f_{\gamma_{R_iD}}(\gamma_{R_iD})\prod_{j=1,j\neq i}^{N}F_{\gamma_{R_jD}}(\gamma_{R_iD})d\gamma_{R_iD} \tag{4.14}$$

(e) Diversity of Cooperative ARQ Using Different Relays

In our cooperative ARQ, the relay selected for retransmission may be different from that transmitted in initial transmission. When different relay is selected, two-branch diversity is achieved at the destination with effective SNR $\gamma_{R_iD,R_jD}=\gamma_{R_iD}+\gamma_{R_jD}$ [4.13], where $i\neq j$. Similarly, the effective SNR after *OL* at an initially erroneous R_l is $\gamma_{OL,R_l}=\gamma_{SR_l}+\gamma_{R_lR_k}$, where R_k is the selected relay whose transmission is captured by R_l in the 2nd slot. The average PER with 2-branch diversity at the destination and that at the opportunistically listening relay are denoted as $P_{p,2}(\overline{\gamma}_{R_iD,R_jD})$ and $P_{p,2}(\overline{\gamma}_{OL,R_l})$, respectively.

4.4.2 End-to-End Packet Error Rate (PER)

Based on the element error rates, the error rate expressions for each case of the relay errors are derived in this subsection. For an arbitrary number of relays, the number and the set of available relays (N_1, N_2) in selection is an indeterministic value. Then, error probability calculation will have to be carried out for all the possible combinations of relays. Thus, for simplicity in theoretical presentations, $N = 2$ is used in the theoretical analysis.

Case 1) All *N* Relays' CRC: OKs

The end-to-end packet error probability of this case is the PER given by selection and ARQ in (4.14) conditioned on the probability that all N relays correctly receive the signal from the source.

$$P_p^{(c1)} = \prod_{i=1}^{N} \left(1 - P_{p,1}(\overline{\gamma}_{SR_i})\right) \times P_{p,\text{SEL-ARQ}} \tag{4.15}$$

Case 2) All *N* Relays' CRC: NGs

When none of the relays successfully receives the signal from the source, the source retransmits in the 2nd slot. The occurrence probability of case 2 is $\prod_{i=1}^{N} P_{p,1}(\overline{\gamma}_{SR_i})$. Upon receiving the retransmitted packet, there are three cases of relay errors.

Case 2.1) some relays ($N_m \le N$) become error-free: in this case, the relay with the best h_{RD} transmits in the 3rd time slot, achieving selection-diversity of order N_m. In this analysis, $N_m = 2$ since $N = 2$. Note that, the selection diversity achieved in this case is conditioned on N_m relays becoming error-free at the retransmission. Hence, the conditional error probability in this case is

$$P_p^{(c2.1)} = \left(\prod_{i=1}^{N_{re}} \left(1 - P_{p,\text{ARQ}_{SR_i}}\right) \right) \cdot P_{p,\text{SEL}} \tag{4.16}$$

Case 2.2) only one relay becomes error-free: the error-free relay transmits in the 3rd time slot. The conditional error probability of this case is given by

$$P_p^{(c2.2)} = \sum_{i,j=1}^{N} \left\{ \left(1 - P_{p,\mathrm{ARQ}_{SR_i}}\right) \cdot P_{p,\mathrm{ARQ}_{SR_j}} \cdot P_{p,1}\left(\bar{\gamma}_{R_iD}\right) \right\}, \; i,j = \{1,2\}, \forall i \neq j \; . \tag{4.17}$$

Case 2.3) all relays keep on having errors: the packet is discarded and a new packet transmission will be initiated. The PER probability that all the relays keep on having errors after the retransmission is

$$P_p^{(c2.3)} = \prod_{i=1}^{N} P_{p,\mathrm{ARQ}_{SR_i}} \tag{4.18}$$

Since the occurrence probability of case 2 is the a priori probability for each sub-case, the total end-to-end PER of case 2 is

$$P_p^{(c2)} = \prod_{i=1}^{N} P_{p,1}(\bar{\gamma}_{SR_i}) \left\{ P_p^{(c2.1)} + P_p^{(c2.2)} + P_p^{(c2.3)} \right\} \tag{4.19}$$

Case 3) Some Relays' CRC: OKs

In this case, there are $N_1 < N$ relays that can participate in the distributed relay selection. Opportunistic listening (*OL*) is carried out in this particular case. Among N_1 relays that have correctly received the signal from the source, the relay with the best relay-destination channel transmits to the destination, achieving selection diversity of order = N_1. As the best relay transmits, the erroneous relays carry out *OL* and decode their received signals again. With $N = 2$, $N_1 = 1$.

When none of the N–N_1 erroneous relays become error-free after *OL*, the number of error-free relays available to be selected remains the same (N_1). Then, if retransmission is needed, the number of relays available in the distributed selection is also N_1. This means the same relay is selected for retransmission since the channel rank does not change. The end-to-end PER when the erroneous relay keeps having errors can be expressed as

$$P_p^{(c3.1)} = \sum_{i,j=1}^{2} \left\{ \left(P_{p,1}\left(\bar{\gamma}_{SR_j}\right) \cdot P_{p,2}\left(\bar{\gamma}_{OL,R_j}\right) \right) \cdot \left(\left(1 - P_{p,1}\left(\bar{\gamma}_{SR_i}\right)\right) \cdot P_{p,\mathrm{ARQ}_{R_iD}} \right) \right\} \; i,j = \{1,2\}, \forall i \neq j \tag{4.20}$$

where, $P_{p,2}(\bar{\gamma}_{OL,R_j})$ is the error probability of *OL* at the erroneous relay R_j, with the effective SNR being $\gamma_{OL,R_j} = \gamma_{SR_j} + \gamma_{R_iR_j}$.

On the other hand, when N–N_1 erroneous relays become error-free after *OL*, relay availability increases to N_2, where $N_1 < N_2 = N = 2$. If the destination fails to receive initial relay signal correctly, N_2 relays contend for transmission in retransmission time. Depending on which relay transmits, i.e. the selected relay, the destination achieves either 2-branch diversity or 3 dB improvement in *SNR*. Given R_i transmitted in the 2nd slot, the destination achieves $P_{p,2}(\bar{\gamma}_{R_iD,R_jD})$ conditioned on selection diversity when R_j transmits in the 3rd slot or $P_{p,\mathrm{ARQ}_{R_iD}}$ conditioned on selection diversity when R_i retransmits. This can be expressed as

$$P_p^{(2\gamma,2\mathrm{div})} = \sum_{i=1}^{2}\left\{\int_0^\infty P_{p,\mathrm{ARQ}_{R_iD}} f_{\gamma_{R_iD}}\left(\gamma_{R_iD}\right) F_{\gamma_{R_jD}}\left(\gamma_{R_iD}\right) d\gamma_{R_iD} + \int_0^\infty\int_0^\infty P_{p,2}(\gamma_{R_iD,R_jD}) f_{\gamma_{R_jD}}\left(\gamma_{R_jD}\right) F_{\gamma_{R_iD}}\left(\gamma_{R_jD}\right) d\gamma_{R_iD}\, d\gamma_{R_jD}\right\} \qquad i,j=\{1,2\}, \forall i \neq j \tag{4.21}$$

Then, the end-to-end PER when erroneous relay becomes error-free can be expressed as,

$$P_p^{(c3.2)} = \sum_{i,j=1}^{2}\left\{\left(1-P_{p,1}\left(\bar{\gamma}_{SR_i}\right)\right) P_{p,1}\left(\bar{\gamma}_{SR_j}\right)\left(1-P_p\left(\bar{\gamma}_{OL,R_j}\right)\right) P_p^{(2\gamma,2div)}\right\} \quad i,j=\{1,2\}, \forall i \neq j \tag{4.22}$$

Finally, the overall average PER of case 3 is the summation of Eqs. (4.20) and (4.22),

$$P_p^{(c3)} = P_p^{(c3.1)} + P_p^{(c3.2)} \tag{4.23}$$

Since each case of relay error events are mutually exclusive, the end-to-end PER of the cooperative ARQ with selection and inter-relay *OL* is the summation of the error probabilities of each case,

$$P_p = P_p^{(c1)} + P_p^{(c2)} + P_p^{(c3)} \tag{4.24}$$

In a relay system that uses distributed relay selection only without *OL*, the number of available relays will be the same in both initial relay transmission and retransmission time. In such system, the end-to-end PERs of case 1 and case 2 are the same as given by Eqs. (4.15)-(4.19). As for case 3, the end-to-end PER is given by (4.20) without conditional probability $P_{p,2}(\bar{\gamma}_{OL,R_i})$ by *OL* at the erroneous relay. Performance evaluations also include the cooperative ARQ that uses distributed selection only as a reference to compare with the proposed system.

4.5 *Numerical Results*

The transmit power of each relay node is the same. To incorporate the effect of path loss in channel fading h_{uv}, the variance of h_{uv} is calculated as $(d_{uv}/d_0)^{-\alpha}$, where d_{uv} is the distance between S-R_i or R_i-D, (u,v)$\in\{S, R_i, D\}$, $i=\{1,\ldots,N\}$and d_0 is the reference distance which is 1. Simulations assume a block Rayleigh fading model in which each channel is invariant within three time slots duration. Each channel changes continuously and slowly in next three time slots duration. Perfect channel knowledge is available at each receiving node. As for the channel information required for the selection procedure, is perfectly estimated at intervals well within the channel coherent time. The relay nodes perfectly decode the ACK/NACK feedback packets from the destination. Table 4.1 lists the assumed parameters.

Table 4.1 Simulation assumptions for cooperative ARQ

Path loss exponent, α	3.5
Number of retransmission	1
Modulations	BPSK, QPSK, 16QAM
Number of symbols/packet	100
Slot length ,T_{slot}	10 ms
Maximum time-offset τ_{max}	1 ms
Control factor, λ	200 μs

Collision occurs owing to the uncertainty interval that consists of propagation delay and transmit/receive switch delay in which two or more relays' τ_i's expire to zero simultaneously [4.9]. It was shown in [4.9] collision probability is well below

0.6 % with $\lambda = 200$ μs. In simulations, real channel gain instead of a quantized value is used in determining channel quality a_i of each relay. In addition, propagation delay and transmit-receive switch delay are not taken into account. Thus, in the assumed environment, collision does not occur. With the chosen parameters, the possible maximum overhead is only 10 %. In practice, since likelihood of all the relay nodes' to fall in deep fade simultaneously is very low, most relay transmission happens at τ_k well within $\tau_{\max}$, shortening the contention time.

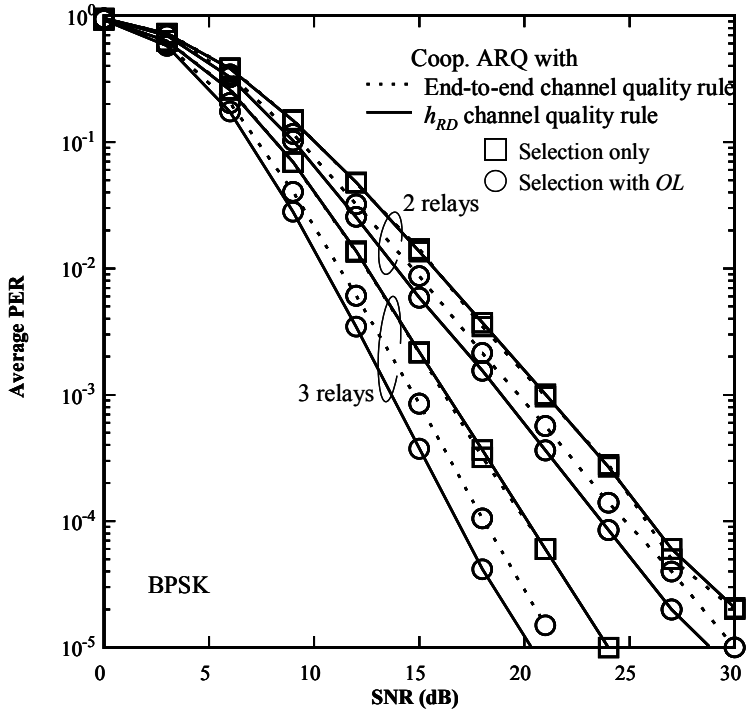

Fig.4.4 Performance difference of selection protocols (simulation only)

4.5.1 Effect of Selection Protocols

Firstly, we investigate the effect of selection protocols on the performance of the cooperative ARQ with distributed relay selection and *OL*. We compare the error rate performances of two selection rules: (a) conventional selection protocol of [4.9] that uses end-to-end channel quality given by Eq. (4.2) and (b) proposed selection protocol using Eqs. (4.3) and (4.4). Assuming all the channels have equal average

power, distances d_{uv}'s are set as one. Figure 4.4 plots the simulated PER performances of cooperative ARQ with selection only and that with selection and *OL* using BPSK in both cases. With both selection protocols, it is seen that the cooperative ARQ with selection and *OL* always outperforms cooperative ARQ with selection only. With cooperative ARQ that uses selection only, both selection protocols provide the same performance. This is because, in the case without *OL*, the relay availability does not change in retransmission time. Thus, the proposed selection protocol also does not have chance to exploit increased relay availability. With selection and *OL*, PER performance with conventional selection protocol is poorer than that of proposed selection protocol. Thus, as we discussed in Sec. 4.1, the conventional selection protocol is not optimal for our relay system where relay availability dependency over source-relay channels decreases in retransmission. From now on, we use our proposed selection protocol in the following evaluations.

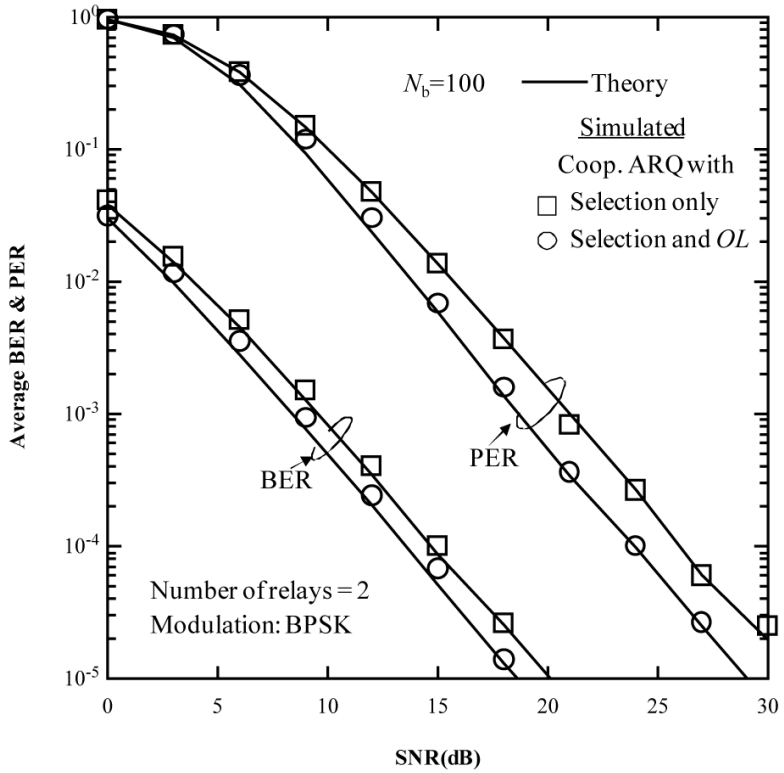

Fig. 4.5 BER and PER comparison: theory and simulation.

4.5.2 Theoretical and Simulated Results

(a) Error Performance with Two Relays

In this section, the theoretical error rate performance expressions derived in Section 4.3 are verified by computer simulations. For comparison with the theoretical results, BPSK modulation is assumed and $N = 2$. All the channels involved are flat Rayleigh fading with equal average power. Figure 4.5 plots both BER and PER performances. As a reference comparison, the performance of cooperative ARQ with selection only is also plotted. As can be seen, the theoretical results agree with the simulated results, proving the validity of the expressions for error performance of the relay system under consideration. The result shows that, in equal power Rayleigh fading channels, cooperative ARQ with relay selection and *OL* can achieve performance gain in term of PER about 2 dB over cooperative ARQ with selection only.

(b) CDF of Normalized Throughput with Different Relay Positions

Obviously, the performance of the system with *OL* depends on the inter-relay channel condition. In order to evaluate the performance with various inter-relay channel conditions, positions of (R_1, R_2) are randomly distributed using a model shown in Fig. 4.6. In that model, the source is located at an edge and the destination at the opposite end. R_1 is on the left side and R_2 is on the right side. Their positions in their respective areas change randomly at each time. As the positions of R_1, R_2 change, the distances $d_{uv} \in (d_{SR_i}, d_{R_iD}, d_{R_1R_2})$ also change resulting in unequal power channels. Consequently, inter-relay channel condition also changes at each time. The effect of shadowing loss is also taken into account and the standard deviation of normally distributed shadowing loss coefficient, η, is 6.5 dB. The distance between the source and the destination d_{SD} is kept as reference distance and remains the same for every set of R_1, R_2 locations. Since the positions of R_1, R_2 vary at each time, the received SNRs at each relay and at the destination also vary. The received SNR with d_{uv}=1 is

kept as the reference SNR (SNR_{ref}). From SNR_{ref} , the actual received SNR, SNR_{uv}, at the relays or at the destination can be calculated as,

$$SNR_{uv} = SNR_{ref} \cdot \left(\frac{d_{uv}}{d_{SD}} \right)^{-\alpha} \cdot 10^{\frac{\eta_{uv}}{10}},\ u, v \in \{S, R_i, D\}, i = \{1, 2\}. \tag{4.25}$$

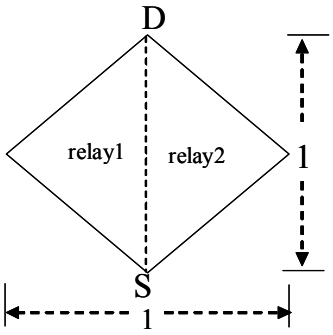

Fig. 4.6 Model for distribution of various relay positions

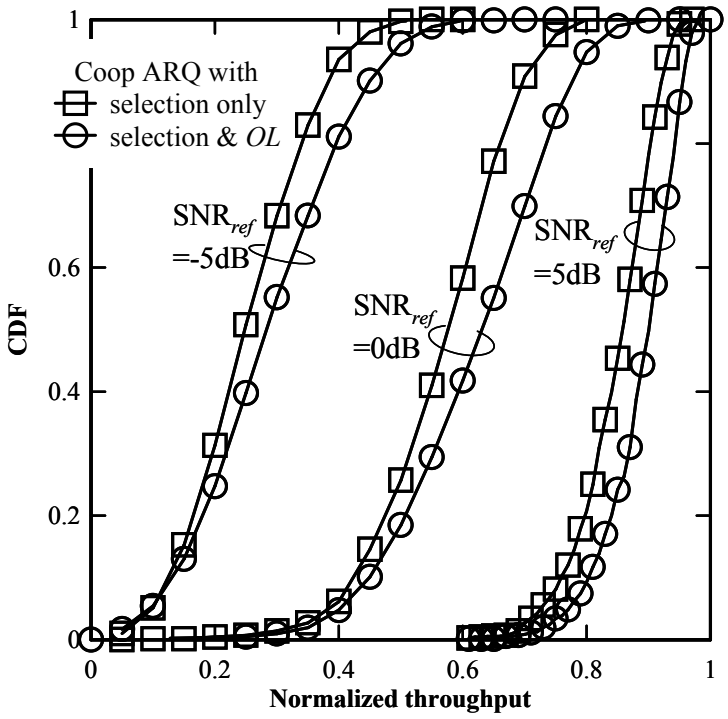

Fig. 4.7 CDF of normalized throughput performance (Simulation and theory)

In this evaluation, normalized throughput is used as the performance criterion. Normalized throughput is defined as the percentage of the packets correctly received at the destination. Substituting SNR_{uv} in respective PER expressions given by Eqs. (4.15)-(4.24), the end-to-end packet error P_p is achieved. From P_p at each SNR_{ref}, normalized throughput is given by

$$Thr(SNR_{ref}) = \left(1 - P_p(SNR_{ref})\right). \tag{4.26}$$

Figure 4.7 plots cumulative distribution function (CDF) of throughput performance with randomly distributed different (R_1, R_2) locations. Moreover, performances with different SNR_{ref} = –5, 0, 5 dB are also plotted to show performance variation with SNR_{ref}. The results show that even with various inter-relay distances, the cooperative ARQ with selection and *OL* always outperforms cooperative ARQ with selection only. For instance, at SNR_{ref} =0 dB, while 80 % of the relay position distributions achieve throughput about 0.66 with selection only, the same percentage of the relay position distributions achieve throughput about 0.73 with selection and *OL*. When SNR_{ref} is so small, the probability that both relays do not successfully receive from the source is high, consequently the probability of conducting *OL* is small. Therefore, performance gain at SNR_{ref} = –5dB is slightly small compared to SNR_{ref} = 0 dB.

As SNR_{ref} increases, the probability that any one of the relay nodes successfully receives the signal from the source increases. As a result, the probability of conducting *OL* becomes high. When SNR_{ref} is large enough so that the probability of both relays to correctly receive from the source is high, the probability of conducting *OL* reduces. Therefore, the performance difference becomes smaller at SNR_{ref} = 5 dB.

(c) PER Performance with Higher Level Modulations

In this section, PERs of proposed cooperative ARQ are evaluated using higher level modulations by simulations. The channel is assumed as the same channel used in Fig. 4.5. Maximum number of retransmission is also the same. Figure 4.8 (a) plots

the PER with the number of relays $N = 2$ and Fig. 4.8 (b) plots the PER with $N = 3$. It is seen that for all the modulations, BPSK in Fig. 4.4 and QPSK and 16QAM in Fig. 4.8, as the number of relays increases, the performance gain with cooperative ARQ with selection & *OL* increases. This is because improvement in selection diversity order at retransmission increases as N increases. With 16QAM, the improvement is relatively small compared to lower level modulations because more SNR is required to correct errors in amplitude modulated symbols. Although performance gain with $N = 3$ is larger than that with $N = 2$, performance gain may be saturated as N becomes very large, because there may be sufficiently large number of relays available to be selected in the 2nd slot and the diversity improvement in the 3rd slot may become less significant.

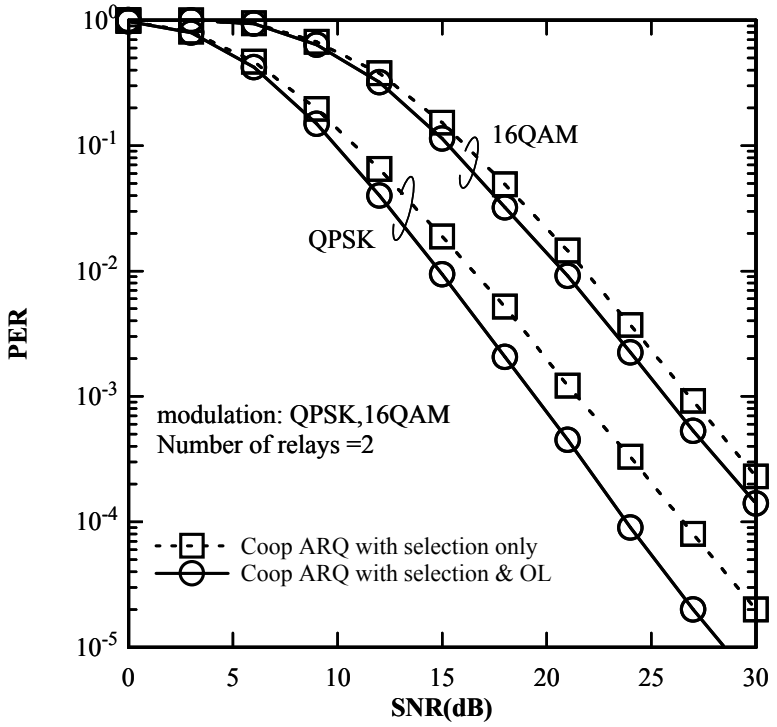

Fig. 4.8 (a) PER with higher modulations, $N = 2$ (simulation only)

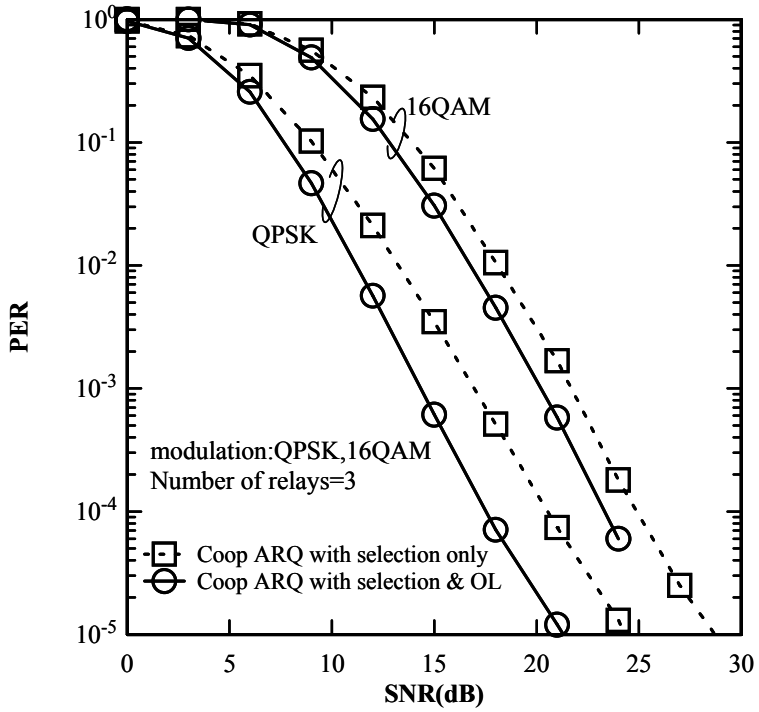

Fig. 4.8 (b) PER with higher modulations, $N = 3$ (simulation only)

(d) Average End-to-End Delay

Although PER quantify packet arrival rate and throughput performance, it is also necessary to quantify the required end-to-end delay for each packet when ARQ is concerned. In cooperative ARQ, not only SNR but also the number of relays and achievable diversity structure in cooperation also influence the required delay. Average End-to-End delay incurred is investigated keeping the number of relays as a parameter. Regardless of fail or success in decoding a packet, the delay may incur due to retransmission attempts. Following the assumptions in the previous literature for ARQ [4.16], ACK/NACK feedback delay including demodulation and CRC decoding processing time is assumed to take one time slot. Thus, in the case the destination successfully receives relay transmission in the 2nd slot, the total time taken until ACK/NACK decision will be three time slots.

The average delay is expressed in unit of time slot, thus, it includes the delay time due to distributed selection. So far, we have limited the maximum number of

relay retransmissions R_{Tx} to one. With R_{Tx} =1, average delays of the system using selection only and that using selection and *OL* may be almost the same since the diversity gain from the proposed system is achieved only at retransmission time. Thus, in order to show delay performance improvement due to increased diversity in the proposed system, the R_{Tx} *i*s set as R_{Tx} = 2. The maximum number of source retransmission S_{Tx} is one. Thus, including S_{Tx}, R_{Tx} and the time required for CRC result feedback, the maximum allowable End-to-End delay is eight time slots.

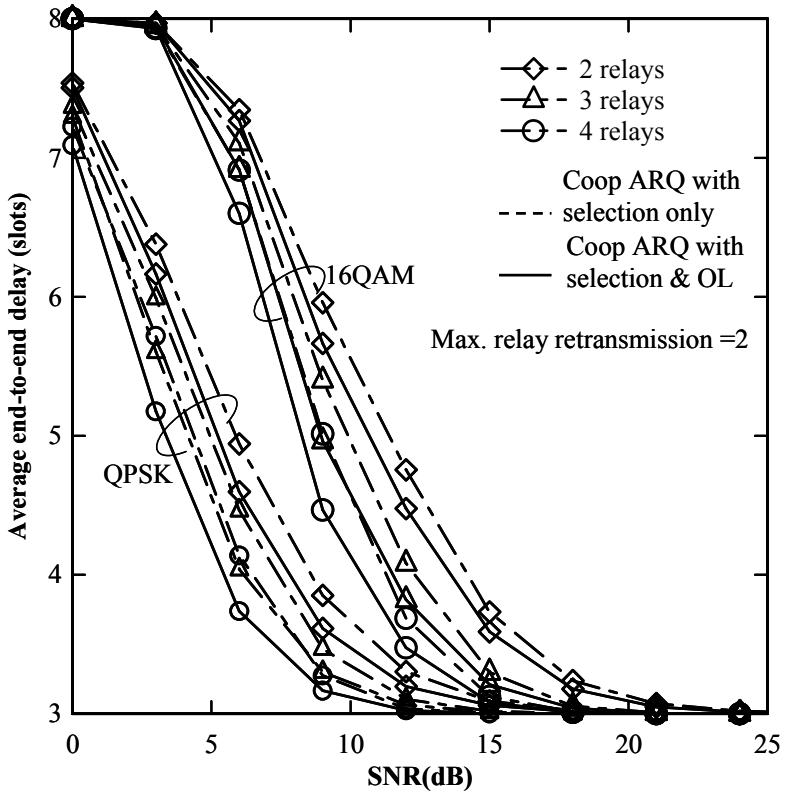

Fig. 4.9 Average End-to-End delay performance (simulation only)

The same channel model as in previous sections is assumed, where channel is static within three time slots duration and varies slowly in next three time-slots duration. Fig. 4.9 plots the average delay incurred for a packet as a function of SNR. The results show that, in all the cases, cooperative ARQ with selection & *OL* incur less delay compared to that with selection only with both QPSK and 16QAM

modulations. The delay improvement of cooperative ARQ with selection & *OL* is about $T_{slot}/4$ with $N = 2$ and $T_{slot}/2$ with $N = 4$ at SNR around 10 dB. Moreover, as the number of relays N increases, the delay significantly decreases in both cases. For instance, at a given SNR, $N = 3$ incurs about $T_{slot}/2$ less delay than N=2. The same can be seen between $N = 3$ and $N = 4$. With QPSK, relay retransmissions are almost not necessary at SNRs ≥ 15 dB; with 16QAM almost no retransmissions are required at SNR ≥ 20dB.

4.6 *Application Areas of Proposed Cooperative ARQ*

The proposed cooperative ARQ may be readily incorporated in the existing cellular networks, wireless LAN and MAN networks since necessary features such as carrier sense and ARQ are already available in those networks. In addition, the proposed scheme can be incorporated in a hybrid wireless sensor network [4.18-4.20], which is attracting attention recently. The term hybrid stems from the integration of sensing/monitoring networks with heterogeneous devices that have capability of mobility and access to large scale networks such as existing cellular networks, wireless LAN and MAN networks.

Recent advancements in the integration of sensors and radio communication in mobile terminals that can operate on the existing wireless networks have increasingly motivated for the possibility of deploying mobile enabled large scale wireless sensor networks [4.18]. Traditionally, distributed stationary wireless sensing/monitoring nodes directly transmit the sensed/monitored information via radio link to the destination where data is accumulated and computing is carried out. The basic idea is that information from sensor is collected by mobile terminals nearby which serves as data carriers to further forward the information [4.19]. The motivation of such hybrid mobile sensor networks is to send the information gathered by sensor more efficiently and reliably to end users while expanding coverage by collaborating with wide area mobile networks. Fig. 4.10 illustrates the concept of a general wide area hybrid mobile wireless sensor networks.

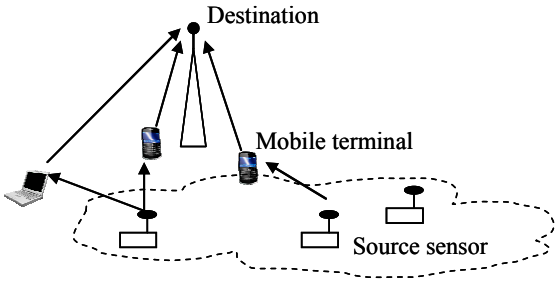

Fig. 4.10 Concept of hybrid mobile wireless sensor network

In hybrid wireless sensor networks, sensors may be traditionally resource limited and low power, however, the relays may be more powerful and computationally efficient heterogeneous devices which are connected to the large scale cellular or MAN networks. Since the main part of proposed cooperative ARQ is operated in relay nodes, no significant overhead or burden occurs on the overlaying sensor network. Thus, the proposed protocol is suitable for hybrid mobile wireless sensor network. Moreover, potential relay selection to form cooperation group should take remaining battery life of the relays into account so that life time of the relays is conserved.

4.7 *Conclusion*

In this chapter, a novel cooperative ARQ scheme was presented for a general distributed multihop relay network. The proposed protocol allows minimal cooperation of relay while enabling the distributed relays to cooperate in ARQ autonomously. With the proposed relay system, achievable selection diversity order is increased in subsequent retransmissions. It was also shown that the proposed selection protocol can make full use of the increased selection candidates. The results show that the proposed cooperative ARQ improve PER performance significantly. In equal average power independent and identically distributed (i.i.d) channels, environment, the improvement in terms of PER of the proposed protocol over that does not exploit inter-relay opportunistic listening was about 2 dB in two relay case.

As the number of relays increases, the improvement becomes larger since the diversity order during retransmission increases.

References

[4.1] P. Herhold, E. Zimmerman, and G. Fettweis, "Relaying and cooperation-a system perspective," in Proc. of 31st IST Summit'04, Lyon, France, 27-30 June 2004.

[4.2] J. N. Laneman and G. W. Wornell, "Distributed space-time-coded protocols for exploiting cooperative diversity in wireless networks," IEEE Trans. Inf. Theory, vol.49, no.10, pp.2415-2425, Oct. 2003.

[4.3] R. Mudumbai, G. Barriac, and U. Madhow, "On the feasibility of distributed beamforming in wireless networks," IEEE Trans. Wireless Commun., vol.4, no.4, pp.1-10, Apr. 2007.

[4.4] S.A. Fares, F. Adachi, and E. Kudoh, "A Novel Cooperative Relaying Network Scheme with Inter-Relay Data Exchange," IEICE Trans. on Comm.,vol.E92-B, no.5, pp.1786-1795, May 2009.

[4.5] I. Stanojev, O. Simeone, Y. Bar-Ness, and C. You, "Performance of multi-relay collaborative hybrid-ARQ protocols over fading channels," IEEE Commun. Letter, vol.10, no.7, pp.522-524, July 2006.

[4.6] G. Yu, Z. Zhang, and P. Qiu, "Cooperative ARQ in wireless networks: Protocols description and performance analysis," in Proc. of IEEE ICC 2006, vol.8, pp.3608-3614, Istanbul, Turkey, June 2006.

[4.7] A. Adinoyi, Y. Fan, H. Yanikomeroglu, H. Poor, and F. Al-Shaalan, "Performance of selection relaying and cooperative diversity," IEEE Trans. On Wireless Commun., vol. 8, pp. 5790-5795, Dec. 2009.

[4.8] K. Woradit, et al., "Outage behavior of selective relaying schemes," IEE Trans. On Wireless Commun. vol. 8, no. 8, pp. 3890-3895, Aug. 2009.

[4.9] B. Aggelos, K. Ashish, P. R David, and L. Andrew, "A simple cooperative diversity method based on network path selection," IEEE JSAC, vol.24, no.3, pp.659-672, Mar. 2006.

[4.10] D. Chase, "Code combining - A maximum-likelihood decoding approach for combining an arbitrary number of packets," IEEE Trans. Commun., vol.33, no.5, pp.385-393, May 1985.

[4.11] IEEE 802.11 WG, IEEE standard for wireless LAN Medium Access Control (MAC) and Physical Layer (PHY) specifications, ANSI/IEEE Std 802.11, 1999 Edition.

[4.12] R. Janaswamy, *Radiowave Propagation and Smart Antennas for Wireless Communications*, Kluwer Academic Publishers, 2000.

[4.13] J.G. Proakis, *Digital Communications*. McGraw-Hill, 4th Ed., 2001.

[4.14] A. Nosratinia, T.E. Hunter, and A. Hedayat, “Cooperative communication in wireless networks,” IEEE Communications Magazine, vol.42, no.10, pp. 74-80, Oct. 2004.

[4.15] A. Annamalai, “Micro-Diversity reception of spread-spectrum signals on Nakagami fading channels,” IEEE Trans. Commun., vol.47, no.11, pp.1747-1756, Nov. 1999.

[4.16] D. Wang, C. Chong, F. Watanabe, H. Minn, and N. Al-Dhahir, “Opportunistic cooperative ARQ transmission scheme in cellular networks,” in Proc. of IEEE ICC 2008, pp. 4802-4808, Beijing, China, May 2008.

[4.17] A. Abrardo and C. Maraffon, “Analytical evaluation of transmit selection diversity for wireless channels with multiple receive antennas,” in Proc. IEEE ICC 2003, vol. 5, pp. 3200-3204.

[4.18] L. Zheng and D. Tse, “Diversity and multiplexing: A fundamental tradeoff in multiple antenna channels,” IEEE Trans. Inf. Theory, vol. 49, no. 5, pp. 1073-1096, May 2003.

[4.19] J. Ma, C. Chen, and J. P. Salomaa, “mWSN for large scale mobile sensing,” Special Issue on Sensor networks and applications, Journal of Signal Processing Systems, vol. 51, no. 2, pp. 195-206, 2008.

[4.20] P. P. Jayaraman, A. Zaslavsky, and J. Delsing, “Sensor data collection using heterogeneous mobile devices,” IEEE Int’l Conf. on Pervasive Services, pp. 161-164, 15-20, July 2007.

[4.21] S. Krčo, D. Cleary, and D. Parker, “Enabling ubiquitous sensor networking over mobile networks through peer-to-peer overlay networking,” Comput. Commun. vol. 28, no. 13, pp. 1586-1601, Aug. 2005.

Chapter 5

Overall Conclusions

In this dissertation, issues related to asymmetric traffic requirement, data rate adaption, coverage extension, diversity techniques to mitigate fast channel variations have been addressed for the future generation wireless communications.

Chapter 1 described evolution of wireless communications in each generation, requirements and possible solutions for current and future systems. Highlighting the needs of the future systems, motivation and contribution of this study were provided.

In Chapter 2, comprehensive descriptions of the key technologies used in this study were provided. In particular, AMC, HARQ, asymmetric TDD and multihop cooperative relaying were discussed.

Chapter 3 highlighted control delays in AMC and HARQ operation in different asymmetric TDD slot formats. In particular, this study laid out a theoretical frame work to evaluate the effect of control delay in AMC. In multiuser environment, users may be roaming with different mobility. Although a user may be in a close range from the base station or access point, its perceived channel may be fluctuating fast according to the relative movement in the channel. Effect of erroneous selection of MCS is more significant in case of higher level modulations as 16QAM, 64QAM. Thus, rate adaption should be carefully carried out by taking selection error probability of a user into account. Also, information on average delay incurred in HARQ for a given channel fading rate is useful in user scheduling. Thus, analytical frame work provided in Chapter 3 to calculate probability of erroneous MCS

selection and evaluation of delay incurred in HARQ may be instrumental in rate adaptation and multiuser scheduling in future generation wireless systems.

Chapter 4 proposed a novel cooperative ARQ protocol suitable for any distributed network ranging from large scale cellular, wireless LAN or MAN to hybrid wireless sensor network. The proposed protocol considered a distributed relay selection that exploits overhearing from inter-relay channels. The cooperating relays have autonomy in deciding whether to serve as relays by contending for transmission, based on their own CRC results. As a result of exploiting listening to inter-relay channels, the influence of source-relay channels over the availability of relays to be selected is decreased. This allows the relays to take into account relay-destination channel only in contending for transmission. For each retransmission, diversity order increases as more relays become available to transmit after erroneous received signals become error-free thanks to the spatial diversity provided by the inter-relay opportunistic listening. The results showed a significant performance improvement can be achieved with the proposed protocol. A straightforward theoretical framework was provided to derive end-to-end PER of the systems for a two relay case. The PER improvement with the proposed protocol using BPSK in equal average power channels is from about 2 dB with two relays to 4 dB with three relays over the cooperative ARQ protocol using conventional selection.